uOttawa

L'Université canadienne
Canada's university

Evaluation of Adaptation Options to Flood Risk in a Probabilistic Framework

by

Saeideh Kheradmand

Thesis submitted to the University of Ottawa
in partial Fulfillment of the requirements for the
degree of Doctor of Philosophy

Department of Civil Engineering
Faculty of Engineering
University of Ottawa

© Saeideh Kheradmand, Ottawa, Canada, 2021

Abstract

Probabilistic risk assessment (PRA) has been used in various engineering and technological fields to assist regulatory agencies, and decision-makers to assess and reduce the risks inherent in complex systems. PRA allows decision-makers to make risk-informed choices rather than simply relying on traditional deterministic flood analyses (e.g., a Probable Maximum Flood) and therefore supports good engineering design practice. Type and quantity of available data is often a key factor in PRA at an early stage for determining the best methodology. However, implementation of PRA becomes difficult and challenging since probability distributions need to be derived to describe the variable states. Flood protection is one of the rare fields in civil engineering where probability is extensively used to describe uncertainty and where the concept of failure risk is explicitly part of the design. The concept of return period is taught in all civil engineering classes throughout the world, and most cities in the developed world have developed flood risk maps where the limits of the 50-year or 100-year flood are shown. While this approach is useful, it has several limitations:

- It is based on a single flow value while all flow ranges contribute to the risk;
- It is not linked to the actual economic damage of floods;
- So far, flood risk maps only account for river water levels. It has been demonstrated that intense rainfall causes significant property damages in West Africa.

This study aimed to explore the possibility of developing and implementing a probabilistic flood risk estimation framework where all flow ranges are accounted for: 1) The probability of flood occurrence and the probabilistic distribution of hydraulic parameters, and 2) The probability of damages are spatially calculated in order for the decision-makers to take optimal adaptation decisions (e.g., flood protection dike design, recommendations for new buildings, etc.). In this study the challenges of inferring the probability distribution of different physical flood parameters in a context of sparse data, of linking their parameters to flood damages, and finally the translation of the estimation risk into decision were explored. The effect of the choice of the one-dimensional

(1-D) or two-dimensional (2-D) hydraulic models on the estimated flood risk and ultimately on the adaptation decisions was investigated.

A first case study on the city of Niamey (Niger, West Africa), was performed using readily available data and 1-D and 2-D HEC-RAS (Hydrologic Engineering Center-River Analysis System) models. Adaptation options to flood risk in Niamey area were examined by looking at two main variables: a) Buildings' material (CAS: Informal constructions – a mixture of sundried clay and straw, also known as Banco, BAN: Mud walls, DUR: Concrete walls, and SDU: Mud walls covered by mortar); and b) Dike height within a scenario-based framework, where numerical modelling was undertaken to quantify the inundated area. The 1-D and 2-D hydraulic models, HEC-RAS, were tested on a 160 km reach of the Niger River. Using the numerical modelling, water levels within the inundated areas have been identified. The extent of residential areas as well as exposed assets (polygons and building material) associated with each scenario have been evaluated. 1000 probabilistic flood maps were generated and considered in the estimation of the total loss. Benefits and costs of different adaptation options were then compared for residential land-use class in order to implement flood risk maps in the city of Niamey. Results show the individual as well as the combined impact of the two abovementioned variables in flood risk estimation in Niamey region. Dike heights ranged from 180.5 m to 184 m, at a 0.5 m interval, and buildings' material were considered to be of 0% to 100% of each type, respectively. The results enable decision-makers as well as the regulators to have a quantitative tool for choosing the best preventive measures to alleviate the adverse impacts arising from flood.

Also, because of the lack of detailed information on the exposed infrastructure elements in the study area, a feasible yet fast and precise method of extracting buildings from high-resolution aerial images was investigated using an Artificial Intelligence (AI) method – Deep Learning (DL). The applied deep learning method showed promising results with high accuracy rate for the area of interest in this study and was able to successfully identify two introduced classes of Building and Background (non-building).

The findings contend that although the proposed structural adaptation options, as a resisting to environment approach, are applied to the area of interest and considered to be technically feasible, other non-structural measures, which have long-term effect of risk mitigation, should be taken into consideration, especially for highly hazard-prone areas. The results of this study would significantly help in loss estimation to the buildings due to the yearly floods in the region of interest, Niamey, Niger. However, since the buildings are of various type of material, having an accurate building database has a great importance in assessing the expected level of damage in the inundated areas, especially to the critical buildings (hospitals, schools, research labs, etc.) in the area.

Acknowledgements

First, I would like to express my sincere and deep gratitude to my supervisor, Professor Ousmane Seidou, for his constant support and guidance during the course of the program. I would also like to thank Professor Ioan Nistor and Professor Majid Mohammadian for their encouragements and support; the invaluable suggestions and comments received from them, and other committee members, Professor Abhijit Sarkar and Professor Philippe Gachon are highly appreciated. I also thank Professor Bahram Daneshfar for his guidance in improving this research.

I would like to thank the Niamey office of the United Nations Development Program and the International Development Research Centre, the Agrhymet Regional Centre of Niamey, and the Dispositif National de Préevention et de Gestion des Crises Alimentaires for funding and supporting the data collection for this research.

I would like to extend my warmest appreciation and love to my family, specifically my parents, for their life-long dedication and support; I am endlessly grateful for their constant encouragement and kindness. Last but not least, I would like to thank my friends (Mohammad, Mostafa, Yarzar, Katie, Ata, Hanifeh, and Parna) for their support throughout the difficult parts of my academic career.

Table of Contents

List of Figures

List of Tables

List of abbreviations and acronyms

1-D	One-Dimensional
2-D	Two-Dimensional
ACOE	United States Army Corps of Engineers
Adam	Adaptive Moment estimation
AI	Artificial Intelligence
ANN	Artificial Neural Networks
ADRC	Asian Disaster Reduction Center
BAN	Mud walls
BG	Background
BUI	Building
CAPRA	Central American Probabilistic Risk Assessment
CAS	Informal constructions-a mixture of sundried clay and straw, also known as Banco
CFA	West African Franc
CI	Confidence Interval
CNN	Convolutional Neural Network
CORINE	Coordination of Information on the Environment
DL	Deep Learning
DSM	Digital Surface Model
DTM	Digital Terrain Model
DUR	Concrete walls
EA	Environmental Agency
EM-DAT	Emergency Events Database
ESA	European Space Agency
FAO	Food and Agriculture Organization of the United Nations
GEV	Generalized Extreme Value

GDP	Gross Domestic Product
GIS	Geographical Information System
GloFAS	Global Flood Awareness System
GLOG	Generalized Logistic
GPAR	Generalized Pareto
GPS	Global Positional Systems
HANZE	Historical Analysis of Natural Hazards in Europe
HEC	Hydrologic Engineering Center
HEC-RAS	Hydrologic Engineering Center-River Analysis System
HMT	Hit-or-Miss Transformation
IDW	Inverse Distance Weighting
IPCC	Intergovernmental Panel on Climate Change
KS	Kolmogorov-Smirnov
LN2	Lognormal
LN3	Lognormal 3-parameter
MDR	Mean Damage Ratio
ML	Machine Learning
MLC	Maximum Likelihood Classification
MODIS	Moderate Resolution Imaging Spectroradiometer
OECD	Organisation for Economic Co-operation and Development
P-III	Pearson III
PGRC-DU	Projet de Gestion des Risques de Catastrophes et de Développement Urbain-Disaster Risk Management and Urban Development Project
PRA	Probabilistic Risk Assessment
RMSE	Root Mean Squared Error
SDU	Mud walls covered by mortar
SRTM	Shuttle Radar Topography Mission
TIN	Triangular Interpolation Networks
TL	Transfer Learning
UNDRR	United Nations Office for Disaster Risk Reduction
UNISDR	United Nations International Strategy for Disaster Reduction

USACE	U.S. Army Corps of Engineers
USEPA	U.S. Environmental Protection Agency
USGS	United States Geological Survey
WAM	West African Monsoon
WB	Word Bank
WMO	World Meteorological Organization
WSE	Water Surface Elevation

List of symbols

A	Cross-section area
AAL_b	Average annual loss in the study area before dike retrofitting and building conversion
AAL_a	Average annual loss in the study area after dike retrofitting and building conversion
C_d	Cost of dike retrofitting
C_{br}	Cost of building conversion
d_j	Distance between any two building of the same material
D	Investment return length in years
D_i	Sum of inverse squared distance of a building with material of type i to all other buildings with the same type of material
$D_{xx,xy}$	Dispersion terms
$f\_mat(h)$	Loss fraction
g	Gravitational acceleration
h	Water depth
H	Water surface elevation
i	Type of building material
M	Number of classes
n	Exponent value
$P(i \mid \omega)$	Probability that a pixel with feature vector ω belongs to class i
$P(i)$	Probability that class i occurs in the study area
$P(\omega \vert i)$	Likelihood function
$P(\omega)$	Probability that ω is observed
P_i	Probability of a building having type i material
$p(mat)$	Probability for the building to be of a given material

q	Source/sink term
Q	Flow discharge
S_f	Friction slope
S_0	Channel bed slope
t	Adaptive Moment estimation
$T_{xx,xy}$	Depth average turbulent shear stresses
u	Cross-sectional averaged velocity in x-direction
v	Velocity component in y-direction
$value\_m_{mat}^2$	Monetary value per square meter of the area based on the type of the building material
x	Input of the next layer
x, y	Cartesian coordinates
z	Surface elevation
θ	Net mass input
Ω	Coriolis parameter
$\tau_{bx,by}$	Bed shear stress
$\tau_{wx,wy}$	Wind shear stress

Chapter 1

Introduction

1.1 Problem definition

Flood, a natural hazard, could affect our environment and, in most of vulnerable areas of the world, may cause damages including loss of human life; damage to property, business premises, and crop; interruption to transportation and utility services; and other damages arisen from economic activity disruption. The number of people who could be affected by flood is reported to be more than all the other natural hazards together (Asian Disaster Reduction Center, 2011); one reason could be the increasing trend of flooding over the last 30 years (Freer et al., 2013). According to Emergency Events Database (EM-DAT) records over the 50-year period (from 1970 to 2019), weather, climate and water hazards accounted for 50% of all disasters, 45% of all reported deaths and 74% of all reported economic losses, where the most common of the weather-, climate, water-related disaster types recorded were floods (WMO, 2021). Moreover, floods, which last for several days, endanger affected people to exposure to water borne and vector borne diseases, which could lead to death. At some regions along the river, sediment deposits could significantly reduce the flood passage capacity of the river (Japan International Cooperation Agency, 2003), which in turn causes more water to enter the floodplain and more area to be inundated, in case of flooding.

Two main categories of flood damages are identified as tangible and intangible damages. Tangible flood damages could be estimated and expressed in monetary value and are further classified as direct (caused by direct contact of floodwater) and indirect types. Both direct and indirect damages are subdivided into primary and secondary damages (Dutta et al., 2003). In this study, direct-tangible losses are being considered. Flood could also displace a large amount of debris along its way, which may cause channel instability and reduce the flood conveyance capacity of channels (National Research Council, 1996).

Risk and uncertainty are defined as the measures of deviation from "normal", where risk is the quantifiable (by the calculation of probabilities) portion of the unexpected (UNDRR, 2019). Intergovernmental Panel on Climate Change (IPCC) defines risk as the resultant of the interaction of social and environmental processes, of the combination of physical hazards and the vulnerabilities of exposed elements (Cardona et al., 2012). Flood risk analysis, which includes flood hazard mapping, hydraulic structure design, urban drainage system planning, and reservoir management, is a method to quantify flood frequency and its damage. Overall, as the Environmental Agency's Strategy for Flood-Risk Management states (Environmental Agency, 2003), flood risk estimation is to evaluate the probability that the safety standard would be exceeded. Flood risk assessments consists of the following main components: a) Flood hazard; b) Exposure; and c) Vulnerability.

Flood hazard (e.g., depth, velocity, discharge, occurrence, intensity, duration and frequency of high water levels and discharges), is defined by the probability and magnitude of flooding. Flood hazard assessment estimates the probabilities of different magnitudes of damaging flood conditions, such as the depth and duration of inundation and flow velocity. Different parameters including meteorological, hydrological, hydraulic, and topographic properties of the watershed, channels, and floodplains at and upstream of the location of interest, affect the magnitudes for the various probabilities (National Research Council 2015). When flood hazards cause damages to assets, the value of the assets as well as the relationship between the flood hazard and damage to the assets, are examined by exposure and vulnerability analysis. The results of such analysis may be represented with inundation depth–damage functions for the structures. Depth-damage curves (also known as stage-damage curves) are commonly used to determine direct flood damage, i.e., to estimate the flood damage that would occur at specific water depths per asset (Huizinga et al., 2017).

Recent approaches in flood risk assessment, which are called probabilistic or risk-based strategies, enable a more precise assessment of the risk by using probabilistic tools and aimed at reducing the costs of over or under design, whereas the main objective of the classical strategies was to increase the level of flood protection (Doorn, 2014). Probabilistic Risk Assessment (PRA) requires an extensive data set and more realistic (less conservative) assumptions (USEPA, 2014). Despite the better results of risk assessment using probabilistic approach, complex and specific mathematical calculations in this approach, make it more challenging to use. Moreover, probabilistic approach is generally harder to implement and is computationally more intensive (USEPA, 2021). Typically, a large amount of data is required to characterize properly the distribution of the input parameters; however, this kind of data is not always available for all inputs.

The probabilistic approach, in flood risk assessment, has been subject to increasing popularity amongst researchers in recent years as it accommodates for the specification of uncertainty (Apel et al., 2006, 2008; Purvis et al., 2008; Di Baldassarre et al., 2009b, 2010; Neal et al., 2013; Dyck and Willems, 2013; Ganguli and Reddy, 2013; Dale et al., 2014; Jalayer et al., 2014; Alfanso et al., 2016; Shortridge et al., 2017; Tang et al., 2018; Garrote et al., 2021). Describing flood risk in a probabilistic framework could help better propose management and mitigation measures, as well as assessing such measures. Several continental- and global-scale flood and drought forecasting systems have been reported to be successful in producing more accurate predictions at longer lead times than before. For example, Global Flood Awareness System (GloFAS), which is a Medium-Range Weather Forecasting system of the European Centre, has been producing global probabilistic forecasts of river discharge up to 30 days ahead, since 2018 (Guimarães Nobre, 2019).

The focus in this study is adaptation to the associated direct tangible losses to residential land-use classes as a result of flooding. These involve efforts to modify and strengthen the environment subjected to flooding, which are presented in subsequent chapters. Through proposing some adaptation options, the main goal of this research is to develop a probabilistic framework in order to evaluate impact of the proposed adaptation options to flood risk in Niamey, the area of interest. It also aims to help decision-makers to contribute to improvements in the ability of Niamey community to better respond in the scenario of any disastrous flooding event. Also, the present study aims to analyze the impact of the proposed adaptation options in order to lessen the effect of the hazard and accordingly reduce the risk of flood in the study area to a significant extent.

1.2 Research needs

Flood risk analysis based on the traditional T-year event (deterministic approach), where T is the threshold return period, is used to assess disaster impacts of a given hazard scenario and do not account for the full range of possible flood; therefore, provide an incomplete representation of the risk. Since deterministic models do not reflect the impact of a range of scenarios (Thompson and Frazier, 2014), it is not easy to relate the damages of a single flood to the cost of infrastructure for instance. In a probabilistic framework, possible scenarios, their likelihood, and associate impacts are being considered. Probabilistic methods are used to obtain more refined estimates of hazard frequencies and damages; however, probabilistic methods are characterized by inherent uncertainties (because of incorporating the concept of randomness), partly related to the natural randomness of hazards, and partly because of our incomplete understanding and measurement of the hazards, exposure, and vulnerability under consideration (OECD, 2012).

One challenge in the application of probabilistic framework is the availability of data and knowledge to generate the joint probability distributions. It is therefore legitimate to ask if it is applicable in practical cases, especially in developing countries. This thesis explores the possibility of implementing probabilistic risk assessment with very limited data in a region that has not been studied in much detail to the best knowledge of the authors.

Storms and floods are in the top 10 disasters that led to the largest economic losses from the 1970s to the 2010s, with US$ 521 billion and US$ 115 billion, accordingly. Moreover, for the same period, a sevenfold increase has been reported for economic losses due to weather, climate and water extremes (WMO, 2021). Increases in loss levels during the recent decades made the researchers, as well as stakeholders and decision-makers to work harder in order to find mitigation and management measures to mainly prevent the occurrence of such extreme events, and in the areas which the occurrence could not be prevented, to diminish the loss levels as much as possible. Amongst the various investigated constructional and non-constructional methods, to this end, floodplain delineation using Geographical Information System (GIS) and various numerical models, has been considered an efficient non-constructional method, which helps decision-makers and stakeholders to better understand the risk and hazard of various extreme events in the potentially affected areas (Knebl et al., 2005; Yang et al., 2006; Haq et al., 2012; Jalayer et al., 2014; Nut and Plermkamon, 2015; Samela et al., 2018; Ben Khalfallah and Saidi, 2018).

Delineation of flood inundated areas and river floodway is an important parameter in taking an action on sustainable flood prediction, protection, and mitigation. Moreover, the need for flood risk evaluation and assessment is more recognized in flood-prone and vulnerable regions since the loss level in affected areas is directly proportional to the level of vulnerability and exposure of the area. Growing vulnerability to floods could be related to various economic, social, cultural, political, and environmental drivers.

In addition to flood frequency and its intensity, understanding the flood flow behavior in the floodplain should also be considered as a prerequisite for determining consequences of the phenomenon in the affected areas and for planning and implementing efficient adaptation and risk management approaches. Moreover, detailed studies are needed at various places in order to develop the regional and national damage functions which are the basis of further flood prediction and loss assessments models.

In the first phase of this study, one-dimensional simulation of the Niger River, within the study area, was performed using 1-D HEC-RAS model. Accordingly, the one-dimensional analysis of the results was used in economic loss estimation of the possible damages induced by floods under different scenarios. In the second phase, and since the study area does not have detailed information on the exposed infrastructure elements to accurately estimate economic losses associated with flooding, an artificial intelligence method was applied to extract buildings from high-resolution aerial images. In the last phase, and in order to provide more realistic results, the Niger River was simulated by a 2-D model, HEC-RAS, to better analyze the flow in lateral and horizontal directions. Comparing one-dimensional (1-D) and two-dimensional (2-D) models would help decision-makers with limited resources choose the best tool to perform their flood analysis.

1.3 Research Objectives

In most cities in developing countries, drivers like poor governance and spontaneous development due to rapid growth and urbanization, cause an increase in the communities' vulnerability. Moreover, due to the climate change effects, impacts from natural disasters are on the rise (WMO, 2021) and low-income countries, with far less adaptation capabilities, are suffering the most (Levy and Patz, 2015; De Silva and Kawasaki, 2018). In the case of the study area in the current research, Niamey, several other causal factors of vulnerability played a role in diminishing resilience and capacity to cope with and adapt to the extreme events. Examples of such factors include: the lack of proper runoff collection systems, the use of low-strength constructional material in the residential areas which are mainly located in the vicinity of the Niger River, the lack of any type of early warning system, and the lack of enough disaster recovery and rehabilitation time due to yearly flooding in the region. Therefore, the existing flood control measures may not perform as expected, in the future. Finding the right approach to increase the community resilience, requires more strategizing and planning and taking several factors into account, especially for poor communities. Moreover, given that resources are limited, the budget depends on the estimation of the cost of, and the expected benefit from the approaches taken.

The main objective of the current study is to assess the applicability of probabilistic flood risk assessment (based on economical, social, and environmental characteristics of the study area) in a data-scarce environment, demonstrate its usefulness for decision-makers in designing any risk-based flood-related mitigation and management measures, and perform cost-benefit analysis of implementing such measures.

The secondary objectives are the following:

- Demonstrate the feasibility of probabilistic risk assessment using readily available data sets and easy to set-up models (HEC-RAS 1-D and Google Map imagery) with taking into account relative flooding scenarios.
- Develop a simple probabilistic approach to attribute building material based on limited survey data, and demonstrate distribution of the direct monetary flood damage to the buildings in the study area.
- Investigate the use of machine learning algorithms for exposure identification from aerial images.
- Quantitatively assess the benefits of flood adaptation measures.
- Propose a general methodology that the decision-makers can use to select adaptation options in a context of uncertainty.

1.4 Research Scope

This research was performed with the main objective of investigating the application of probabilistic flood risk assessment, and developing the risk profile for Niamey, Niger, through hydrodynamic 1-D and 2-D simulations. Due to data constraints for the flood risk elements (hazard, exposure, vulnerability) in the area, evaluation of the risk assessment in this study has some inherent limitations:

- Due to the lack of information on past losses, vulnerability curves for the study area were generated using a number of assumptions based on expert judgement, known typical construction types in the study, and field surveys.

- In the current study, loss estimation due to flood, was limited to direct tangible losses to residential building land-use class only. Neither human casualties nor any other land-use classes (agricultural, etc.) were considered in the analysis. Moreover, when assessing damage to the buildings, critical buildings (such as hospitals and schools) were not classified separately.
- In the absence of an accurate building database for the study area, a probabilistic approach (Inverse Distance Weighting interpolation technique – IDW) was applied to identify the material of the buildings based on the limited survey data. Four common type of building construction material were used in this method.
- The arial images used in building detection with artificial intelligence method, were taken in 2014 which do not represent the most recent terrain changes in the region.
- The 1000 flow used in the simulations are anterior to 2014 and may not be representative of the current flood regime in the area, since the extreme events occurred in 2017, 2019 and 2020 were not used in the statistical analysis.
- Considering the variations in hydrological conditions, e.g., climate change projections was not in the scope of this study; therefore, using a combined hydrological and hydraulic model is being suggested to incorporate such variations and to achieve more realistic results.

1.5 Contribution and novelty of research

This research assesses the feasibility of probabilistic risk assessment in a context of scarce data. The main contribution and novelty of the research could be summarized as follows:

- It is demonstrated that limited data availability is not a valid reason for not using probabilistic risk assessment. For instance, a probabilistic approach was developed to attribute building material based on limited survey data.
- The study contributes to a better integration of uncertainty in infrastructure planning by helping decision-makers analyze the impact of the decisions on the risk profile (i.e., information on the hazard such as flood zone location and base flood elevation; potential damage cost; and potential mitigation options).
- Using readily available data and developing a novel methodology to derive flood risk profile in a developing nation.

- Exploring various ways (less or more labor intensive) of deriving the risk profile; the use of 1-D versus 2-D hydrological models is explored in this regard.
- Implementing a quantitative analysis of flood risk and adaptation options for the first time.
- Developing easy to understand products to help decision-makers make better (and more objective) decisions.

The following journal and conference papers are the outcomes of the current research:

- Kheradmand, S., Seidou, O., Konte, D., and Barmou Batourec, M.B., 2018. Evaluation of adaptation options to flood risk in a probabilistic framework. Journal of Hydrology: Regional Studies, 19, 1-16. <http://dx.doi.org/10.1016/j.ejrh.2018.07.001>. (Thesis: Chapter 2)
- Kheradmand, S., and Seidou, O., 2021. Building Extraction from Aerial Imagery and Digital Elevation Model using Artificial Intelligence – Deep Learning, International Conference on Climate Nexus Perspectives: toward innovative, resilient and sustainable solutions for natural resources and biodiversity management - I2CNP 2021, Higher School of Technology of Khenifra, Sultan Moulay Slimane University in Morocco, June 2021 (Thesis: Chapter 3)
- Kheradmand, S., Seidou, O., Konte, D., and Barmou Batourec, M.B., 2021. Flood vulnerability derivation using Artificial intelligence and limited ground truth: a case study of the city of Niamey, Niger, West Africa. *Draft to submit to Journal of African Earth Sciences* (Thesis: Chapter 4)
- Kheradmand, S., and Seidou, O., 2021. Assessment of two flood mitigation options for the city of Niamey. *Draft to submit to Journal of African Earth Sciences* (Thesis: Chapter 5)

1.6 Organization of the thesis

The thesis is structured as follows:

Chapter 1 identifies the research problem as well as the research needs, the scope, objectives, and important contributions.

Chapter 2 aims to explore the possibility of implementing a probabilistic framework for flood risk estimation for the city of Niamey (Niger, West Africa). A probabilistic set of flood maps were generated by forcing a HEC-RAS model with a stochastically generated ensemble of flood peaks representing the river regime at Niamey. Loss curves were derived from expert judgment, and various adaptation options to flood risk were examined by considering two main variables: a) buildings' material; b) dike height within a scenario-based framework. Floods with return periods of 2-, 10-, 20-, 50-, 100-, 200-, 500-, and 1000-yr were considered in estimating total loss, and benefits and costs of different adaptation options were compared.

Chapter 3 investigates a feasible yet fast and precise method of extracting buildings from high-resolution aerial images. To achieve this goal, the possibility of applying an automated and a semi-automated building detection techniques was explored. Therefore, an artificial intelligence (AI) – Deep Learning (DL) method, and Maximum Likelihood Classification (MLC) method were used to extract building polygons from high-resolution images of flood-prone areas in the city of Niamey, Niger. Details on the input data, methodology, and the results are explained in this chapter.

Chapter 4 presents a developed methodology to generate loss exceedance curves and using imperfect data. Using the results of AI method (chapter 3) and given that the geographical information in the ground survey data is too imprecise to associate a collected point to a building polygon, Inverse Distance Weighting (IDW) method with various exponents was used to evaluate the probability of each building in the floodplain to belong into one of these four categories: Mud walls (BAN); Concrete walls (DUR); Mud walls covered by mortar (SDU), Informal constructions – a mixture of sundried clay and straw, also known as Banco (CAS). The probabilistic information on building material were then used to derive loss exceedance curves for the city of Niamey.

Chapter 5 explores the assessment of the proposed flood mitigation adaptation options for right riverbank of the Niger River. According to the results achieved in the previous chapters, exponent value of 2 was used in inverse distance weighting method to estimate the type of material for the buildings (which were previously extracted with deep learning method), in the study area. Subsequently, loss exceedance curves were generated for right riverbank and loss to the residential buildings were estimated as a function of dike crest height.

Chapter 6 provides the summary and conclusions of the research, as well as suggestions for future work.

Chapter 2

Evaluation of adaptation options to flood risk in a probabilistic framework[1]

2.1 Introduction

For millennia, coastal and riverside areas have been received priority for human habitation by major part of world population. Main advantages of living at such areas include having access to low-cost marine transportation and rich environmental resources (United Nations. 2017), which lead to the growth in population in such flood-prone areas. Accordingly, the exposure and thus vulnerability for both human population and natural system would increase due to low environment adaptive capacity in the world's coastal regions, especially in developing countries (Levy and Patz, 2015). Therefore, floodplain management has been received a significant attention within the past decades, thanks to the ever-developing tools that enable proper analysis of river systems. Nowadays, a hydraulic analysis is often required by federal, state/provincial, and local regulations prior to any development or construction in a floodplain in order to predict the effects of such activities on the floodplain. However, hand computations to calculate water surface profiles were time-consuming and often required spending days or weeks to complete a water surface profile analysis for a reach of river. Therefore, researchers have developed various computer models to aid engineers in accurate floodplain modelling and management. Modelling helps in estimating the water surface elevations during selected flood events and the effect of potential flood levels on the community. The choice of the model depends on the application purpose, level of accuracy required, and computational efficiency demands (Schumann, 2011).

[1] Kheradmand, S., Seidou, O., Konte, D., and Barmou Batourec, M.B., 2018. Evaluation of adaptation options to flood risk in a probabilistic framework. Journal of Hydrology: Regional Studies, 19, 1-16. <https://doi.org/10.1016/j.ejrh.2018.07.001>.

Computer programs, which are being used to simulate the general hydraulic procedures, vary from simple uniform-flow assumptions to multidimensional models.

Flood analysis have been done using various approaches such as: Analysis based on in-situ observation (Hagen and Lu, 2011), using remote sensing data (Chormanski et al., 2011; Haq et al., 2012), and numerical models for cases which in-situ flood observation and remote sensing data are not available (Di Baldassarre et al., 2009a; Ruiz-Bellet et al., 2015; Schober et al., 2015). Numerical modeling which could be done by one-dimensional (1-D) or two-dimensional (2-D) models, enable flood simulating under different scenarios. Hydrodynamic models which include one-dimensional (1-D), two-dimensional (2-D), and three-dimensional (3-D) models, solve equations derived from applying physical laws to fluid motion in order to simulate and replicate water movement. Some typical hydrodynamic models, which have been used for modelling flood inundation, include TUFLOW (Şen and Kahya, 2017; Morsy et al.; 2018), SOBEK (Musa et al., 2015; Suman and Akther, 2016; Chang et al., 2018), MIKE11/MIKE HYDRO River (Singh et al., 2020; Kocsis et al., 2020), Telemac-MASCARET (Horritt and Bates, 2002; Tadesse and Fröhle, 2020), InfoWorks RS (Prinos, 2008; Othman et al., 2013), and HEC-RAS (Knebl et al., 2005; Quiroga et al., 2016; Ongdas et al., 2020). Amongst them, Hydrologic Engineering Center-River Analysis System (HEC-RAS) model is one of the most widely used programs for floodplain modelling which has been continuously improved since its initial release (Version 1.0) in 1995. There are a significant number of studies (using 1-D, 2-D or a combination of them) to model floodplain, being conducted annually across the globe.

This chapter presents the results of implementing a probabilistic approach in deriving risk profile for the city of Niamey, Niger, West Africa. First, numerical modelling was performed, using HEC-RAS 1-D model, in order to simulate the flood inundation and map the areas at risk, under specific scenarios. To this end, floods with return periods of 2- to 1000-yr were considered to generate a probabilistic set of flood maps; the results were used to develop loss exceedance curves. Next, the output of HEC-RAS model was used in delineating potentially flooded areas and, subsequently, extracting the exposure in the area. In the end, direct tangible damage to the buildings in the study area were estimated using the generated flood maps and developed depth-damage curves. Various adaptation options were examined, when quantifying the dame to the buildings, by considering two variables of: a) Buildings' material; and b) Dike height. Flood exposure assessment and depth-damage curves were limited to residential land–use class only. Abovementioned steps are described in more detail in the following sections.

2.2 Deterministic and probabilistic risk assessment

Flood risk analysis could be performed using two main approaches: deterministic, and probabilistic approaches (Apel et al., 2004). Deterministic approaches, where the impact of a single risk scenario is being considered, are used to assess disaster impacts of a given hazard scenario. However, when using probabilistic methods with possible scenarios, more refined estimates of damages and hazard frequencies are obtained (OECD, 2012). Historical losses can explain the past; however, they do not necessarily provide a good guide to the future since most disasters that could happen have not happened yet (UNISDR, 2013). Probabilistic risk assessment resolves this problem, posed by the limits of historical data, through simulating future disasters, which, based on scientific evidence, are likely to occur (UNISDR, 2015). Therefore, probabilistic flood risk assessment is the subject of various recent projects and has been considered by many others. As an example, Dyck and Willems (2013), developed a probabilistic flood risk assessment methodology to estimate the recurrence rate of flood losses to a geographically distributed properties in the large areas where limited information is available. They presented the results of the application of their methodology to river flood loss from residential buildings in Belgium. While considering all the major sources of uncertainty that introduce variation on the flood losses, the methodology simplifies the necessary calculations considerably and estimates the model parameters either directly from general topographic information and historical observations, or on the basis of simulated model results.

In another study, Apel et al. (2006), developed complex, spatially distributed models representing the relevant meteorological, hydrological, hydraulic, geo-technical, and socio-economic processes. A simple probabilistic model, consists of modules each representing one process of the flood disaster chain, complemented these complex deterministic models in order to assess flood risk. The simple stochastic approach allows a large number of simulations runs in a Monte Carlo framework thus providing the basis for a probabilistic risk assessment. Apel et al. (2006) applied the proposed model to quantify flood risk including an estimation of flood damage for an example area at the river Rhine. They also investigated the effect of upstream levee breaches on the flood risk at the lower reaches. Based on the satisfactory results, they suggested that their proposed model concept to be used for the integrated assessment of flood risks in flood prone areas, as well as cost-benefit assessment and risk-based design of flood protection measures and as a decision support tool for flood management.

2.3 Exposure quantification and analysis

Exposure represents the economic and social values that are likely to be affected by floods. It includes people; livelihoods; environmental services and resources; infrastructure; or economic, social and cultural assets in places that could be adversely affected. Several methods have been used to analyze and quantify the exposure (elements at risk in flood-prone areas, e.g., households or communities) which is considered the main driver of observed increase in flood damages (Hallegatte et al., 2013; IPCC, 2012; de Moel et al., 2011). Exposure can be quantified by the number or the value of elements at risk. Röthlisberger et al. (2017) considered two types of exposure indicators: the density of exposed assets (exposed number of assets per km^2) and the share of exposed assets (share of exposed assets compared to the total number of assets in a specific region) in their study. They applied different aggregation and normalization methods on object-specific information about the building stock and flood hazards map with the case study of Switzerland. They investigated the impact of the aggregation scheme on resultant differences to help decision-makers in risk management. According to their findings, more information is provided by spatial cluster analysis for the prioritization of flood protection measures than simple maps of spatially aggregated data represented in quantiles. Paprotny et al. (2018) presented the Historical Analysis of Natural Hazards in Europe (HANZE) database which contains maps of exposures in 37 countries at various resolutions, and a database of past disasters. The exposure information consists of high-resolution gridded data with information on land use, population, production, and wealth. Geographic Information System (GIS) is commonly used to intersect land-use data with inundation data to extract the exposed objects in floodplain. Using flood hazard data, land-use information, asset data, and hazard maps can be analyzed in a GIS system to quantify the assets at risk (Figure 2.1).

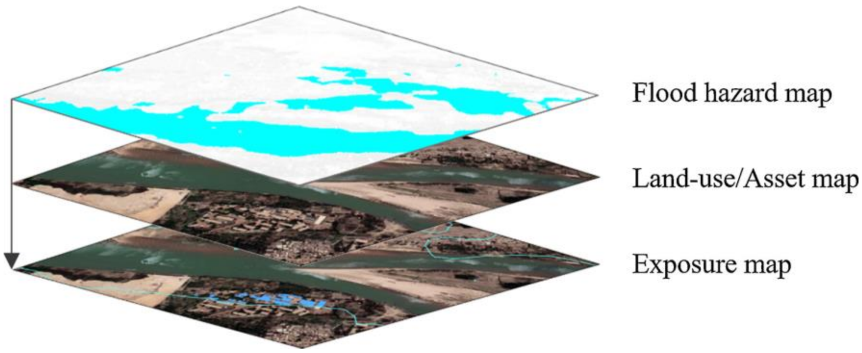

Figure 2.1. Quantifying the exposure through combining hazard maps and asset map using Geographic Information System (GIS).

Accordingly, asset values, which depend on the type of the elements at risk (tangible and intangible), have to be estimated for all the exposed value. However, not many studies on risk assessment have explained explicit approaches for the estimation of assets. One reason could be that many risk analyses do not use any quantitative indicators, or that absolute damage functions are used for damage modelling. Moreover, when land-use data are used to identify the affected sectors, monetary values are not given. Some examples of approaches for the estimation of exposure data are shown in Table 2.1 (Merz et al., 2010). Size of the study area, the available input data, and the required level of accuracy of the risk assessment are the important factors affecting the detail of asset estimation.

Table 2.1. Examples of approaches for the estimation of exposure data. CORINE stands for Coordination of Information on the Environment (Merz et al., 2010).

Models (references)	Country	Approach	Scale	Sectors
Unit Values [€/m^2] derived from stock data MURL (2000), Grunthal et al. (2006)	Germany (North Rhine-Westphalia, Cologne)	Gross stock of fixed assets in combination with land use data (land register ATKIS)	Meso	All, except for residential sector (distinction in immobile (e.g., buildings) and mobile (e.g., machinery, inventory) asset values

Table 2.1. *Cont.*

Models (references)	Country	Approach	Scale	Sectors
Mean insured value MURL (2000) Grunthal et al. (2006)	Germany (North Rhine-Westphalia, Cologne)	Total asset per community is estimated by multiplying the number of buildings with their mean insurance value; transformation to a unit value [€/m^2] by relating the sum to the total settlement area	Meso	Residential sector (distinction in immobile (e.g., buildings) and mobile (e.g., machinery, inventory) asset values)
Rhine-Atlas (ICPR, 2001)	Rhine Valley (France, Germany, Netherlands, Switzerland)	Modified approach of MURL (2000) in combination with CORINE land cover data; transfer from Germany to other countries by matching coefficients derived from gross domestic products	Meso to macro	All sectors (distinction in immobile and mobile asset values)
Standardised building construction costs with dasymetric mapping Kleist et al. (2006), Thieken et al. (2006)	Germany	Combination of standardized construction costs for residential buildings in Germany with census data about the building stock and the living area per community resulting in the total as well as the per-capita replacement costs for residential buildings, differentiated by type, for all communities in Germany. A spatially-distributed inventory was provided by dasymetric mapping adapted from Gallego and Peedell (2001) based on CORINE land cover data.	Meso	Residential sector (building asset values)

Table 2.1. *Cont.*

Models (references)	Country	Approach	Scale	Sectors
Branch-specific assets with dasymetric mapping Seifert et al. (2010)	Germany	Derivation of branch-specific asset values for three sizes of production sites and 60 economic activities based on stock data; municipal values were further disaggregated with the help of CORINE land cover data and a mapping approach modified from Mennis (2003).	Meso	60 commercial and industrial sectors (mobile and immobile; gross/net values)
HAZUS-MH (FEMA, 2003; Scawthorn et al., 2006)	USA	Building asset values were estimated by multiplying the total floor size of a building occupancy in a census block, which reflects to a certain degree the type of economic activity and was assumed to be uniform, with the building replacement costs per square foot in this census block. Depreciated values are derived from data about building costs and consider the age and the condition of the structure. Contents asset values are estimated as a fixed percentage of the building asset value.	Meso	Commercial and industrial sector (16 different building occupancies)
Unit economic values combined with aerial photographs (Dutta et al., 2003)	Japan	To assess the monetary values for property and inventory of non-residential objects, the number of non-residential objects, the number of workers per type was multiplied by unit prices per worker and type. The values of residential buildings were estimated by the product of the unit area with the structure value per unit area and the content value per unit area, respectively. Calculations are done on ward-level; for further spatial disaggregation the floor area per grid cell was determined considering land cover type, building ratios and floor area fractions derived from aerial photographs	Micro	Residential sector and eight non-residential types of economic activity (mining; construction; production; electricity/gas/water; wholesale and retail sale; finance and insurance; real estate; services)

Table 2.1. *Cont.*

Models (references)	Country	Approach	Scale	Sectors
Constructio n cost ratios Blong (2003b)	Australia	Construction costs (replacement costs) per square meter of different building types as published by the Australian authorities are related to construction costs of a medium-sized family house (cost ratios). Differences in the building size (floor area) are considered by a replacement ratio (RR = [(Cost Ratio × Floor area)/Floor area of a medium-sized family house]. Replacement ratios are used in the damage model, which calculates damage as house equivalents. Monetary damage is achieved by multiplying the house equivalents by the costs of a medium-sized family house.	Micro	All building types

Several researchers have demonstrated the capability of geo-information techniques (Adega, 2009; Mayomi et al., 2013; Nkeki et al., 2013; Fuchs et al., 2017). Fuchs et al. (2017) presented a spatially explicit, object-based temporal assessment of elements at risk to mountain hazards in Austria and Switzerland. In their study, they used two different data sets to assess flood hazard exposure: information on flood hazards; and data on residential buildings inventory. They first combined available hazard maps with nationwide flood modeling results to obtain spatial information on flood hazards, and later the hazard information was overlaid with building inventory data in the Geographic Information System. In a research by Daffi et al. (2014), flood inundation maps were overlaid on the settlement map of the study area in order to obtain the exposure map and view those that will be affected by flood. Likewise, the land uses that would be inundated by the flood were achieved by overlaying the flood inundation maps on the Landsat land-use classified maps. Abah (2013) also used ArcView GIS package to digitize a topographic map and through GIS overlay and manipulative functions, he mapped flood risk zones in Makurdi Town, Nigeria.

Mayomi et al. (2013) used GIS and Global Positional Systems (GPS) measurements in their study to identify the settlements that are within the floodplain by integrating the mapped settlements and the terrain model of the area. Adelekan (2009) and Oyinloye et al. (2013), used both quantitative and qualitative methods by using GIS coupled with analyzed data acquired from questionnaires and interviews to better understand the susceptibility level of the people and properties in the study area. Whereas, in small scale studies, such as the case in the study by Rogelis et al. (2014), exposure analysis could be done without applying the advanced technologies. In their study, data from Census, the municipal cadaster and field visits were used to classify the buildings located in the area of study according to construction type, estimate the value for each exposed element and identify the population exposed. Risk assessment in their study addressed 4.8 km reach of the Caldera River located in the Municipality of Boquete in Panama.

In the current study and in order to quantify the exposure (here residential buildings), the output of the HEC-RAS model, describing flood-prone areas (hazard maps), was imported to Google Earth software. Potential floodplain polygons, which identify the buildings in the flood-prone areas, were then digitized in Google Earth (Figure 2.2). For this purpose, visual interpretation was applied to the Google Earth images in order to identify the number of properties (buildings) at risk of flooding. It should be mentioned that in the current study, one main land-use class of residential was considered. Subsequently, the digitized buildings' polygons (shown in red polygons in Figure 2.2) were exported to ArcMAP to calculate the total area of potentially affected region. Buildings are considered exposed if the polygons are partially or completely within the flood-prone area according to the flood hazard maps. After all processing steps, our dataset includes 2600 potentially flooded buildings with a total area of 170,193.30 m^2.

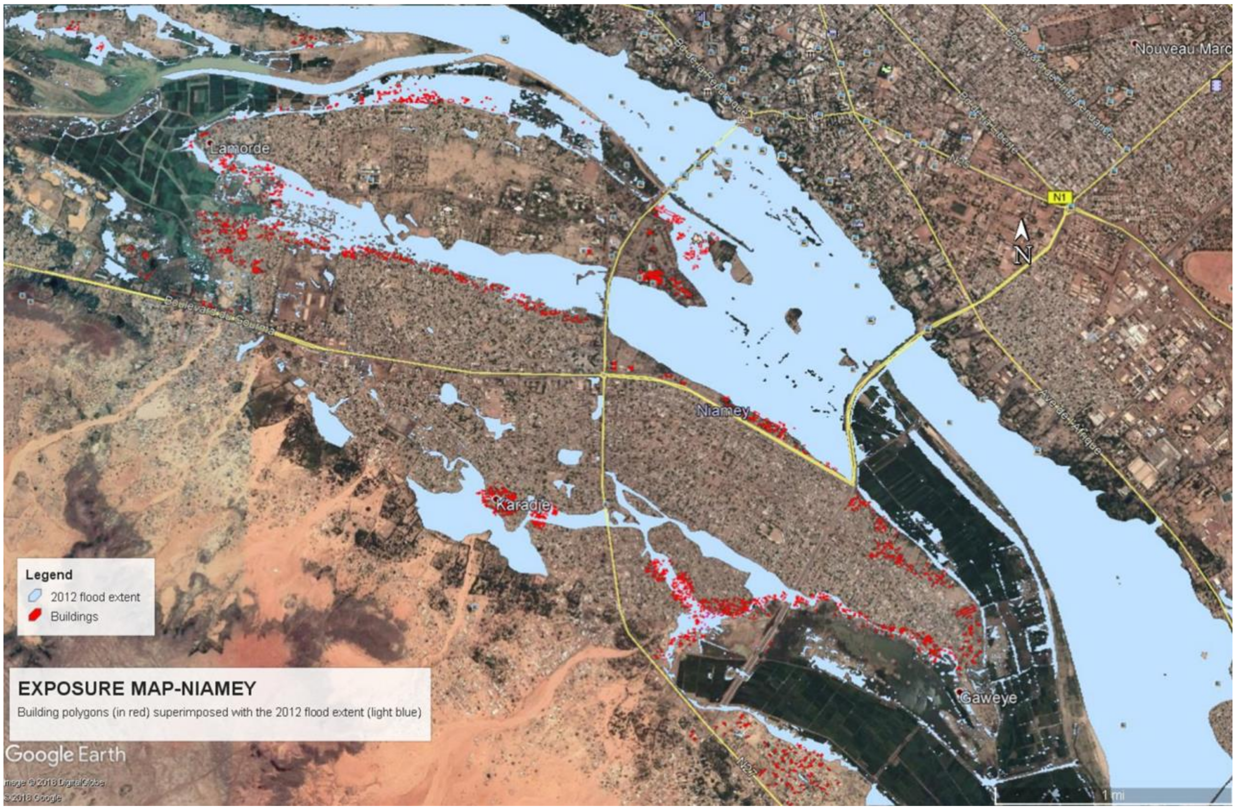

Figure 2.2. Localization of the digitized buildings in Niamey.

2.4 Study area – Regional features

Niger river, the third-longest river in Africa and the principal river of western Africa, extends about 4,200 km (2,600 mi) (Mabogunje, 2014) with a total basin area of 2,117,700 km^2 (817,600 mi^2) (Gleick, 2000). However, less than half of the basin is considered to be active drainage area (Kerres, 2010). Niger River traverses four countries (Guinea, Mali, Niger, and Nigeria) and discharges through the Niger Delta into the Atlantic Ocean; the River discharge is 192 km^3/y (Raux et al., 2011). Niger River basin covers 44.5% of Niger, which equals to 24.8% of the basin total area (FAO, 1997). The Niger River floods yearly during the rainy season – May through October. Floods in July, 2015, has been reported to affect more than 135,000 people in seven central and southern regions in the area including Agadez, Dosso, Maradi, Niamey, Tillabéry, Tahoua and Zinder. The floods also left 7,450 displaced people and destroyed 5,019 buildings (OCHA, July 2015; OCHA, Sep. 2015). Floods between 13 and 14 June, 2017, due to heavy rain, caused severe damage in several parts of the country, with Nimaey and Tillabéri the most severely affected. According to the reports, 14 people have died, a total of 456 households have been affected, and 395 homes have collapsed as a result of the floods and heavy rain (OCHA, June 2017; Floodlist in Africa, NEWS, 2017). Since 2010, significant damages including damages to property and loss of life among people in the vicinity of the river have been reported in Niamey, the region of interest in this study (Descroix et al., 2012; Sighomnou, 2011; Sighomnou et al., 2013; ACTED and OXFAM report, 2012). However, to the best knowledge of the authors, no detailed studies on the amount of losses in the study area neither any research on evaluation of any adaptation options for the region have been performed or reported so far. Lack of any early warning system in the area of interest in this study makes the region more vulnerable and prone to potential risks caused by flooding. Early warning systems enable individuals, communities and organizations, in potentially affected areas, to prepare and to act appropriately and in sufficient time to reduce the possibility of harm or loss. In high hazard-prone areas, such as the area in this study, where complete avoidance of losses is not feasible, the mitigation measures such as public awareness, corrective disaster risk management etc., should be considered (Tompkins, 2005); this approach requires a thorough flood risk assessment which is one of the fundamental steps in any flood mitigation and management program.

Niamey, the largest city of Niger, is also the most populated one with a population of estimated of 1 to 1.5 million inhabitants, which are mainly located along both sides of the Niger River, hence are prone to flooding. Niamey is located between latitudes 13.29° N and longitude 2.09° E in Niger, Africa. The area has a mean elevation below 227 m above sea level. The city subjects to severe inundations that may inundate up to 150,000 km^2, affect thousands of people, and cause human-economic losses as high as millions of U.S. dollars. The type of houses prominent in each settlement is generally reflective of the perceived level of vulnerability of occupants. The current available buildings' materials in Niamey are informal straw walls (a mixture of sundried clay and straw also known as Banco), mud walls, concrete walls, and mud walls covered by mortar. There are also some temporary houses, which are inappropriate in terms of resiliency towards flood. Nonetheless, preference of this house type is possibly due to the facts that its buildings' materials are cheaper, and most of the inhabitants are seasonal settlers who are reluctant to invest in the construction of more durable houses. Figure 2.3 shows the study area, Niamey, which covers 160 kilometers of Niger River.

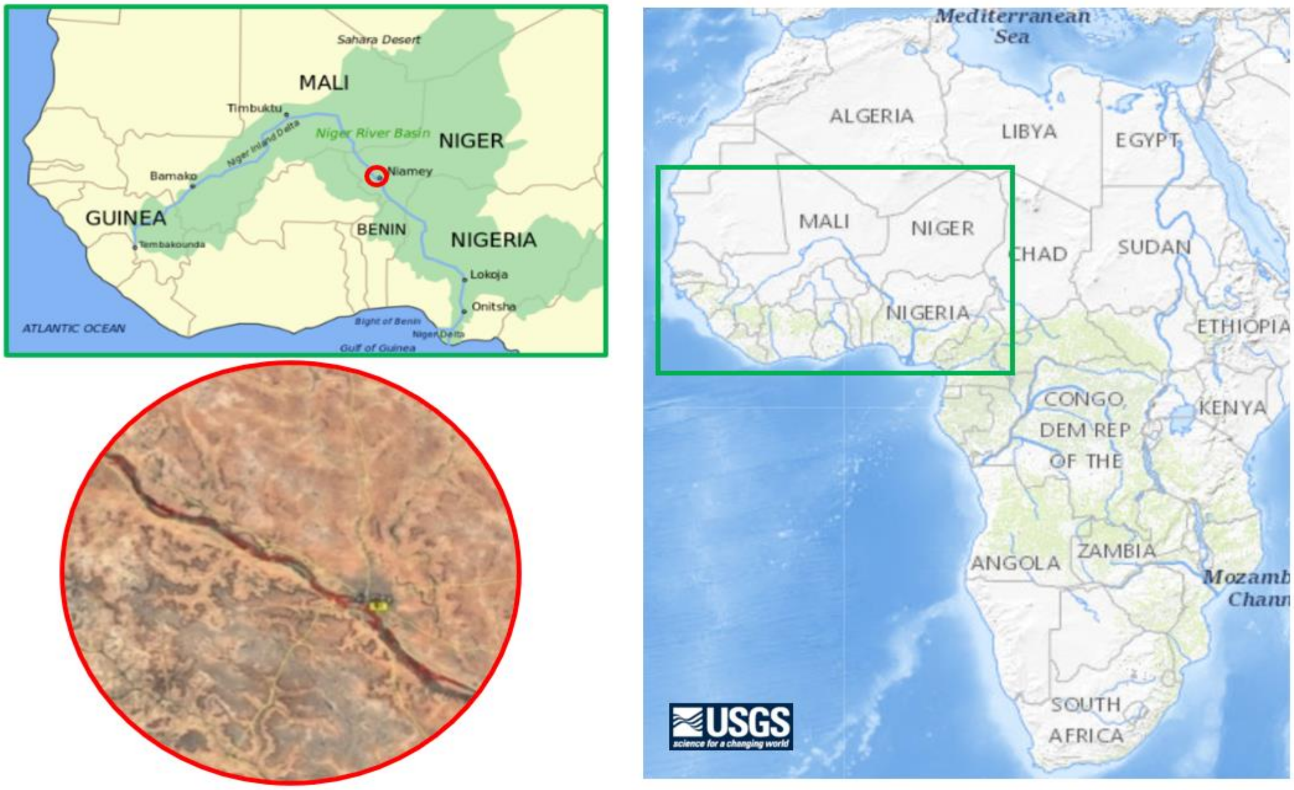

Figure 2.3. Niger River basin (United States Geological Survey (USGS). The red line indicates the section of the River simulated in this study.

Niger River is part of the daily life of the city of Niamey, capital of the Republic of Niger. Part of the city was built in the riverbed of a dead branch of the Niger River and is protected from floods by a system of dikes with crest heights of approximately 181 m. While the dikes are very effective during most years, they failed in August 2012 after heavy precipitation events upstream of the city (Figure 2.4). Peak flow in 2012 (2492 m^3/s), in Niamey, was reported to be the highest peak since the beginning of the records in 1929 (Sighomnou et al., 2013). The subsequent flash flood claimed the lives of 10 people and affected a total of 6535 households. The economic losses were estimated to be about 4.3 billion West African Franc – CFA (6 million USD), a significant amount of money given that Niger is one of the poorest countries in the world.

Figure 2.4. Location of flood protection dikes (red lines) in Niamey, and extent of the 2012 flood (in blue).

2.5 General methodology

In this section, the objective was introducing the best possible option to control and manage the flood losses according to the least construction costs and minimum risk for the studied area, Niamey in Niger, and aimed to contribute to a better preparedness and a better operational risk management for flash floods in the study region. The improvements shall help reducing fatalities and economic damage, caused by this kind of natural hazard and making the effects of flooding negligible. The proposed methodology is a strategy encompassing hazard, exposure, and vulnerability components of flood risk.

As it is shown in the flowchart in Figure 2.5, the first step is input data collection and analysis. For this purpose, flow data were received from the existing observed data at one hydrometric station at Niamey region, for the 1980-2014 period. Moreover, in order to represent the stream channel and floodplain as a series of cross-sections to the hydraulic model (HEC-RAS) bathymetric measurements along the Niger River, within the study area, were performed. Accordingly, geometry file that contains physical parameters describing the cross-sections was created using the measured data. Figure 2.12 shows the existing observed data which were received from one hydrometric station at Niamey collectively for four decades from 1980 to 2014. The second step, after receiving the data from the existing hydrometric station, is calculating extreme flows. One method to do so, which has been used in this study, is using statistical distribution function. In the current study, extreme flowrates for floods with various return periods ranging from 2- to 1000-yr were calculated using statistical distribution function method. For this purpose, eight randomly chosen distribution functions (Generalized Extreme Value – GEV; Pearson III – P-III; Lognormal 3-parameter – LN3; Lognormal – LN2; Generalized Logistic – GLOG; Gumbel – EV1; and Generalized Pareto – GPAR) were used and the best function which fitted the best to the observed data was chosen based on graphical observation and Kolmogorov-Smirnov test (KS test). The calculated extreme flow rates for various floods with different return periods (Table 2.3) were then given to the hydraulic model, HEC-RAS, in order to determine water level associated with each return period. After calculating water level and converting them to the floodplain associated with each return period produced (Figure 2.14a, and b), potential floodplain polygons were digitized in Google Earth and exported to ArcMAP in order to calculate the area of potentially affected regions. One main land-use class of residential was considered in this study. At the last step and in order to estimate the possible economic losses induced if such floods happen in the defined area, total loss were calculated based on vulnerability functions, damage criteria for residential land-use class, and the proposed adaptation options which are further explained in section 2.10. Total potential loss is presented in Tables 2.5 to 2.8 for flood with return period of 1000-yr and various type and percentage of buildings' material. Depending on the degree of monetization and the degree of physical contact of the hazard, flood damage can be classified into four categories of direct tangible, indirect tangible, direct intangible, and indirect intangible (Dutta et al., 2003). In the current study, damage estimation is restricted to direct tangible loss of available land-use classes. Sequences of the abovementioned steps are shown in a flowchart in Figure 2.5 and results are presented in section 2.11.

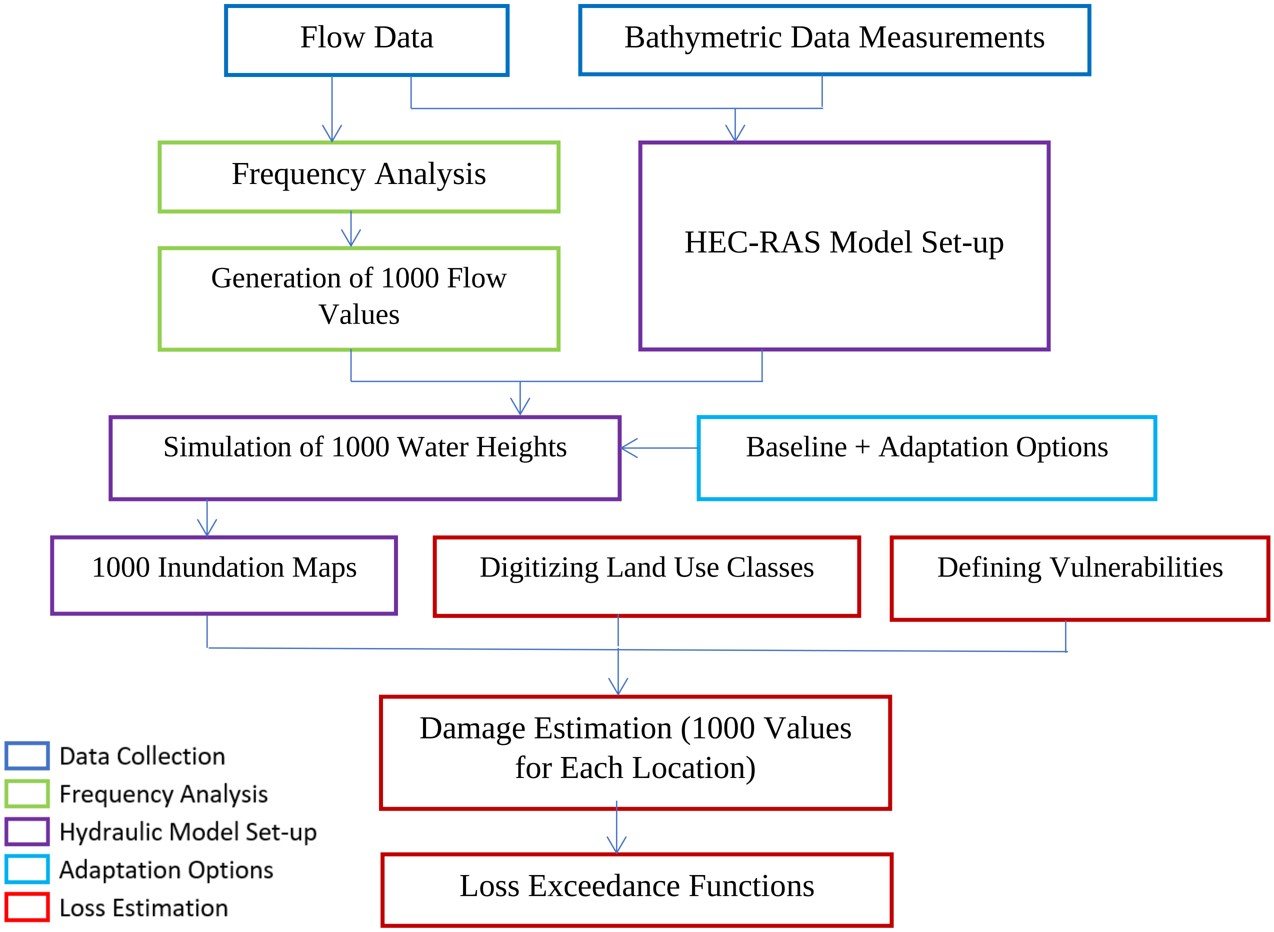

Figure 2.5. Schematic illustrating the probabilistic flood risk estimation process.

The peak discharge values for the Niger River watershed, within the study area, for 2-, 10-, 20-, 50-, 100-, 200-, 500-, and 1000-yr flood were calculated using statistical methods. The results and the details have been presented in section 2.11. Deciding the best statistical distribution function was based on best-curve of observed data received from Niamey station. The chosen *n*-values for channel and floodplain were estimated based on bed material, as well as vegetation type to better represent the physical system and adjust the flood-wave progression over the floodplain. Total number of 988 surveyed channel cross sections were spaced to model transitions between wide and narrow cross sections and represent change in shape and direction of the river.

2.6 Flood risk assessment

Riverine floods have been inevitable during the past decades. Some of the reasons include the increase in population especially at the areas close to the rivers, lack of proper run-off collection systems, and mismanagement both in constructions as well as exploitation of the land mainly in more vulnerable regions on sides of the rivers. Riverine floods lead to severe direct and indirect economic and non-economic losses in the affected areas. Therefore, the importance of flood risk management in order to diminish the losses has been increased significantly.

According to United Nations International Strategy for Disaster Reduction – UNISDR (2009) 'risk' is the combination of the probability of an event and its negative consequences; i.e. frequency of the hazard and intensity of the resulted effect determine the risk. It is essential to identify risk components in order to have a better assessment and management. World Meteorological Organization (WMO, 2006) defines the risks to be composed of three elements of hazard, exposure, and vulnerability. Hence, a thorough assessment of risk requires that an evaluation of each component in a given area be carried out. In the context of this study, the hazard is defined as flood magnitude, which is defined by probability of occurrence, and the exposure describes environment in the hazard zone.

2.7 Probabilistic risk estimation

Probabilistic risk assessment is performed to quantify risk and identify the parameters, which could have the most impact on safety; so that the designs could be improved by reducing vulnerabilities discovered through probabilistic risk assessment. Research should be directed at improving our understanding of the process in a way that is directly relevant for practical application.

2.8 Numerical modelling and hazard mapping

2.8.1 HEC-RAS 1-D modelling

HEC-RAS, one of the most popular hydraulic models, simulate one-dimensional steady and unsteady state flow through the river channel. The software is free and developed by the U.S. Army Corps of Engineers, USACE, (United States, US Army Corps of Engineers). The application of HEC-RAS software has been reported to be successful in flood studies (Knebl et al., 2005; Lian et al., 2013; Mohammadi et al., 2014). This chapter presents the application of HEC-RAS 1-D to develop a hydrodynamic model of the study area and to determine the extent of floodplain inundation in response to various floods with different return periods. The model was used for each dike elevation and forced with 1000 random flow values, taken from the probabilistic distribution of annual maximum discharge values in Niamey. This resulted in 1000 water level maps (one map for each flow value), which were each converted into flood loss values, using the previously developed loss functions (the process is summarized in Figure 2.5, earlier in section 2.5).

In one-dimensional models, flow is treated along the centre line of the river channel and floodplain as only in the longitudinal direction, which is the simplest representation of floodplain flow. Equations for 1-D models can be derived by considering mass and momentum conservation between adjacent cross-sections, which yield the well-known one-dimensional Saint-Venant equations:

Conservation of mass: $$\frac{\partial Q}{\partial x} + \frac{\partial A}{\partial t} = 0 \tag{2.1}$$

Conservation of momentum: $$\frac{1}{A}\frac{\partial Q}{\partial t} + \frac{1}{A}\frac{\partial(\frac{Q^2}{A})}{\partial t} + g\frac{\partial h}{\partial x} - g(S_0 - S_f) = 0 \tag{2.2}$$

Where Q is the flow discharge ($Q = uA$, u is the cross-sectional averaged velocity and A is the cross-section area), t represents time, g is the gravitational acceleration, h is the water depth, S_f is the friction slope, and S_0 is the channel bed slope. Numerical techniques are used to solve equations (2.1) and (2.2) and obtain estimates of flow discharge (Q) and water depth (h) for every cross-section at each time step.

In order to model the flooded area under specific scenario, the hydraulic model has to know about the properties of the respective catchment such as cross-section geometry (bathymetric measurements) and characteristics, bridge and culvert information, steady or unsteady flow data. For this purpose, geometric, hydrological, and hydraulic data of the Niger River was introduced to HEC-RAS in order to estimate flood level for several return periods ranging from 2- to 1000-yr, and prepare floodplain zoning for each return period. The peak flow data from flow measurement stations in Niamey, for the period of 1980 to 2014, were given to the hydrodynamic model, HEC-RAS, in order to compute water-surface elevations and develop flood inundation areas along the study area for the flood discharges. The steps are as follows. First, Digital terrain model (DTM) of the Niger River system was built under HEC-GeoRAS environment in the ArcInfo Triangular Interpolation Networks (TIN) format and imported to the model as an input file. The digital terrain model with 90 m resolution was used to set-up the 1-D model. The geometry file containing the

RAS layers and line themes were then created using field measured cross-sections and in-line (weir) and lateral (dikes) structures' information. It should be noted that two nodes, as well as adequate number of cross-sections cut lines, were specified in this model. Figure 2.6 shows the path at which bathymetric measurements along the Niger River, within the study area, were performed using special instruments. Total number of 988 surveyed channel cross-sections were spaced to model transitions between wide and narrow cross-sections and represent change in shape and direction of the river. The Manning's roughness values used for main channel and right- and left-bank were 0.035 and 0.11, respectively. For each dike elevation, flow values taken from the probabilistic distribution of annual maximum discharge values in Niamey were used at upstream flow boundary condition, and normal depth was used for downstream condition with measuring the average slope of channel at the downstream section. Figures 2.7 (a and b) and 2.8 (a and b) show the modelled area and an example of river cross section, respectively. Examples of the results of the model, which are mainly the water surface profile of the river, are shown in the following sections and were used in defining the hazard zones and supporting the hazard mapping.

Figure 2.6. The path of the Niger River in the study area for measuring bathymetric data.

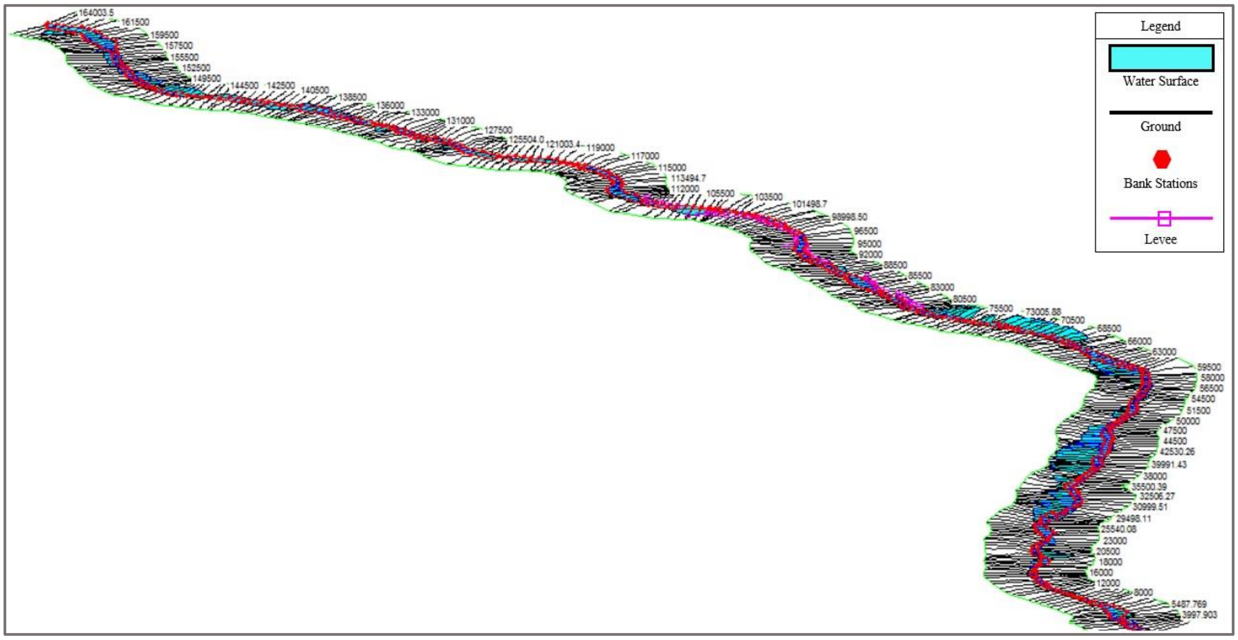

(a)

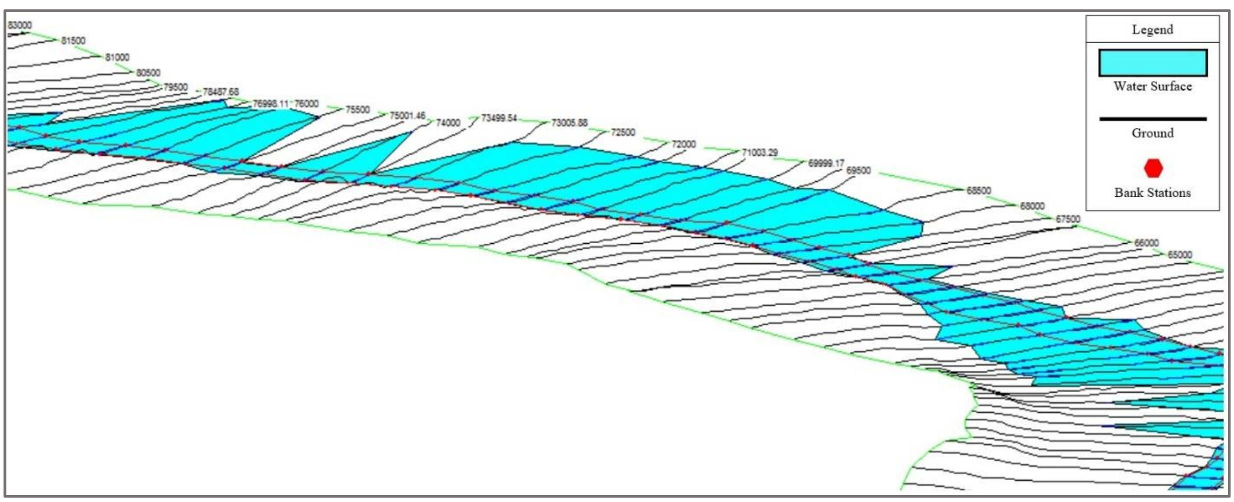

(b)

Figure 2.7. (a) and (b): Introduced geometry of the study area to HEC-RAS model.

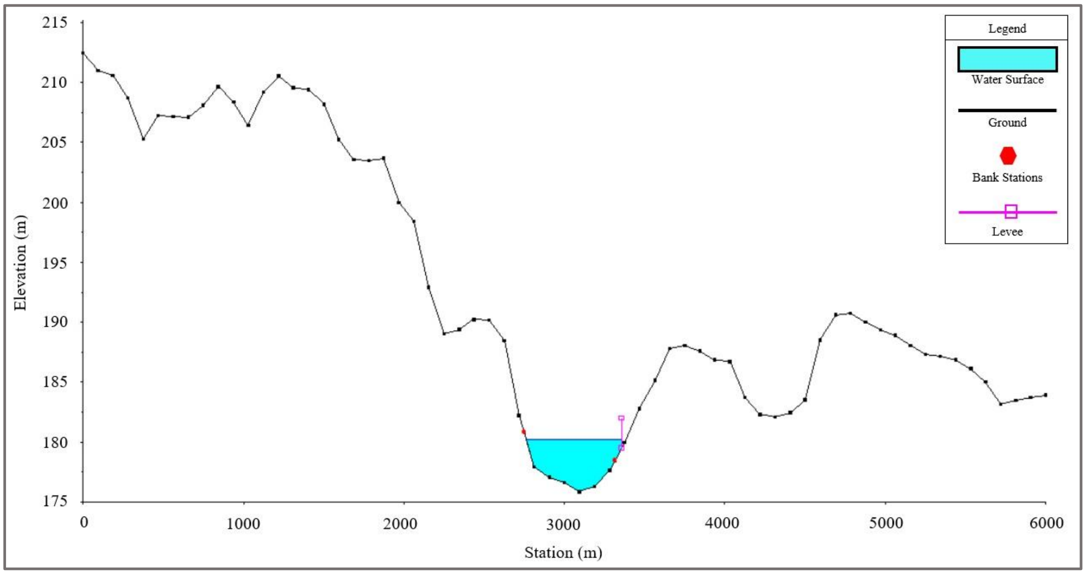

(a)

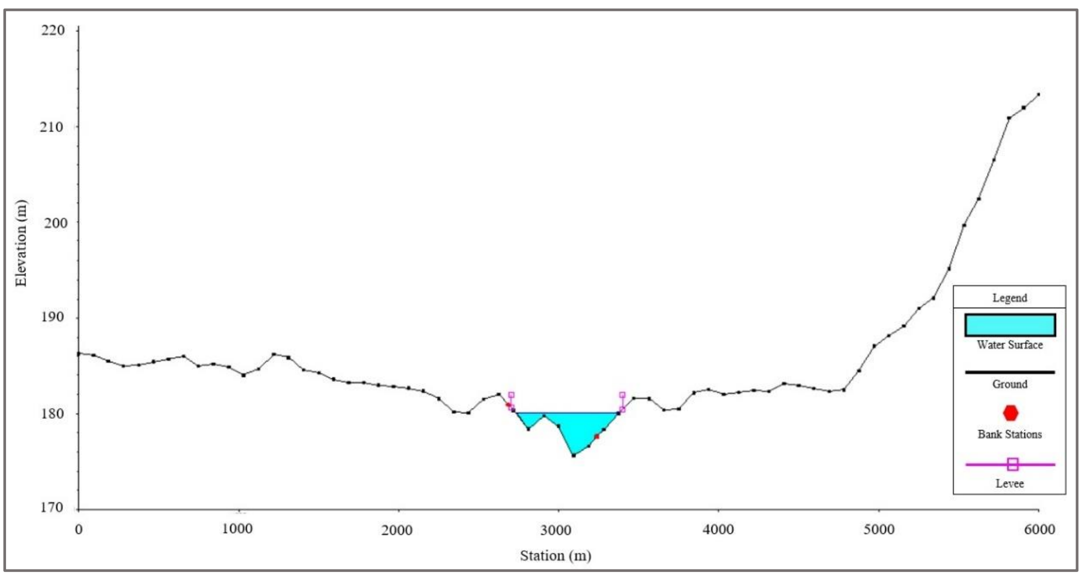

(b)

Figure 2.8. (a) and (b): Two cross sections along the Niger River.

At the last step, geometry data, flow data, and boundary conditions were given to the model in order to perform simulations and obtain water-surface profile and velocity data. The developed HEC-RAS model was calibrated to reproduce the last rating curve over the period 2009–2014 using the available observed elevation data for Niamey and bathymetry data for the Niger River. As illustrated in Figure 2.9, it was found that the calibrated model over the period 2009–2014 almost perfectly reproduced the last rating curve over the indicated period. The Root Mean Squared Error (RMSE) was calculated to ensure the agreement between the modeled and the observed values: RMSE = 0.196. As shown in Figure 2.9. the two curves match well, confirming that the calibration process was satisfactory.

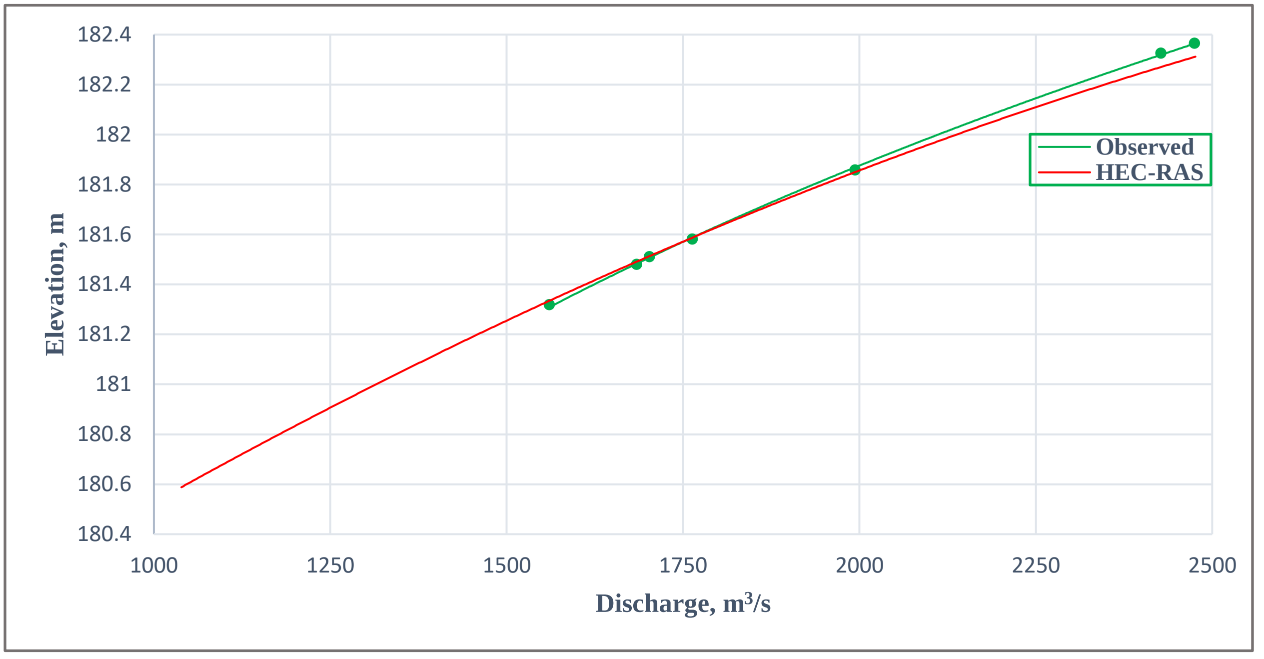

Figure 2.9. Calibration result of HEC-RAS model.

2.9 Vulnerability

Vulnerability is defined as the characteristics and circumstances of a community, system or asset that make it susceptible to the damaging effects of a hazard and varies significantly within a community and over time (UNSIDR, 2009). Vulnerability, with many aspects arising from physical, social, economic, and environmental factors, reflects the 'potential for loss' and depends on the economy, livelihoods, support infrastructure and resilience of the community to cope up with a hazardous event. Examples may include poor design and construction of buildings, inadequate protection of assets, lack of public information and awareness, and disregard for wise environmental management. The influencing indicators of the vulnerability are usually chosen based on the knowledge and experiences of community and experts within the geographical region. Vulnerability assessment aims to estimate the amount of damage to various infrastructures and assets subjected to a certain hazard. The assessment can later be used to choose cost and prioritize mitigation measures according to their short-term and long-term effectiveness. Vulnerability is generally represented as a curve of loss as function of exposure. Such curves are ideally developed using surveys and statistical analysis.

2.9.1 Types of buildings in the floodplain and their vulnerability to flooding

The main factor that controls the vulnerability of a building to flooding is the material of its walls. Most buildings in the floodplain, in the study area, fall into one of the following four categories: a) mud walls (BAN); b) concrete walls (DUR); c) mud walls covered by mortar (SDU), and d) informal constructions – a mixture of sundried clay and straw also known as Banco (CAS) (Figure 2.10).

(BAN) (SDU)

(DUR) (CAS)

Figure 2.10. Examples of the most common types of buildings found in the Niger River floodplain.

Given that information about past losses is not available for the area of interest, a number of assumptions based on expert judgement, known typical construction types in the study area as well as field surveys, were made to generate vulnerability curves (amount of damages to a building as a function of water height) for the area. It is well known that mud and straw constructions are sensitive to water and collapse as soon as the base of the wall is wet. Therefore, it is assumed that 100% of the building is lost when water reaches 0.5 m. Concrete buildings are assumed to collapse when water reaches 2.5 m while mud walls covered by mortar can stand up to 1 m of water before collapsing. This is indeed very subjective but was deemed reasonable enough to proceed with the analysis. Due to the lack of reliable statistics regarding the prevalence of the different building types in the area, six scenarios were considered representing different relative proportions of each of the four types under consideration: (1) 100% CAS; (2) 100% BAN; (3) 100% DUR; (4) 100% SDU; (5) 50% BAN with 10% DUR, 20% SDU, and 20% CAS; (6) 50% BAN with 30% DUR, 20% SDU, and 0% CAS. Scenario (5) is likely to be the scenario that comes closest to the current situation where many houses are built using mud walls. Scenario (6) represents a situation where informal buildings are banned, and where there are more concrete houses.

It is worth to mention that the functions only account for physical elements and not occupancy levels of the buildings. Accordingly, the following assumptions, shown in Table 2.2, are provided for each of the dominant classes of building in the study area.

Table 2.2. Loss estimation assumptions for various construction materials.

	Building type			
	Informal straw walls (CAS)	Mud walls (BAN)	Concrete walls (DUR)	Mud walls covered by mortar (SDU)
Average value of the building, CFA[a] per m^2	35,000	75,000	200,000	150,000
Corresponding water height for 100% of damage, m	0.5	0.5	2.5[b]	1

[a]West African CFA franc

[b]80% is lost when the water height is 2.5 m.

Figure 2.11 (a-d), shows the assigned vulnerability functions to the four various types of buildings which correlate the hazard intensity with mean damage ratio (MDR). The variation of the intensity, given in terms of water depth (m), is illustrated with blue line and standard deviation is depicted with red line. The analysis is carried out using two of the software modules of Central American Probabilistic Risk Assessment (CAPRA) platform (CAPRA, University of the Andes): ERN-Vulnerability, and CAPRA-GIS.

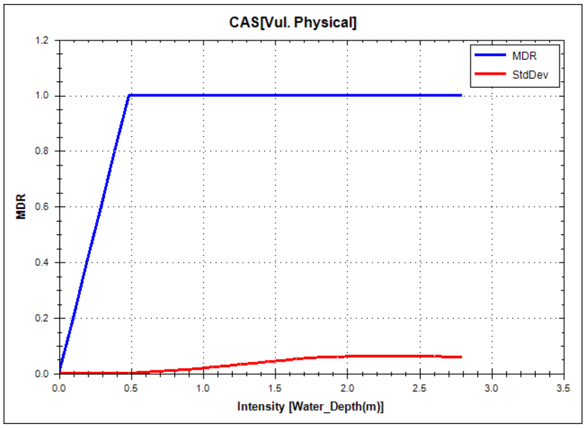

(a)

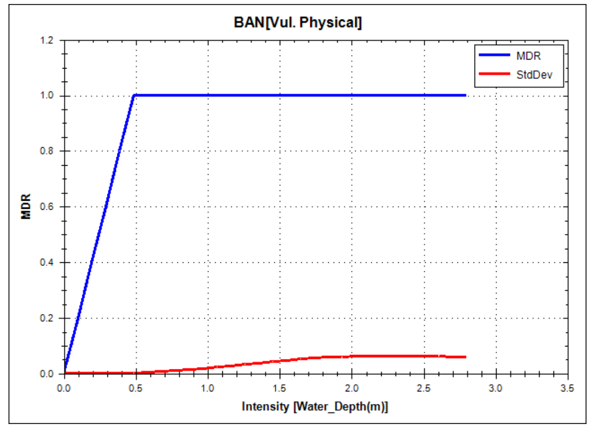

(b)

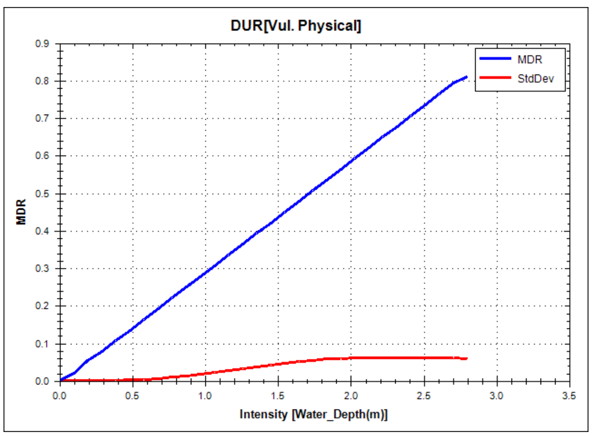

(c)

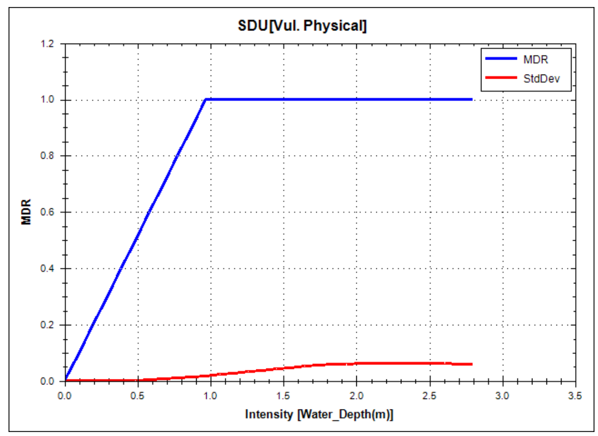

(d)

Figure 2.11. Vulnerability functions for various buildings' material: a) CAS- informal straw walls; b) BAN- mud walls; c) DUR- concrete walls; and d) SDU- mud walls covered by mortar.

2.10 Adaptation options

The realization of yearly flooding of Niger River and its potential impacts on the communities residing along the river has prompted much activity in the realm of 'adaptation', which is typically viewed as actions in response to flooding that seek to limit its impacts. Various definitions for adaptation have been presented so far including both/either adjustment in human and/or natural systems. According to Adger et al. (2009), the way in which humans react to the actual or projected changes in the surrounding environment is frequently termed 'adaptation'. In another definition of adaptation by Smith (1996), it has been defined as all adjustments in behavior or economic structure that reduce the vulnerability of society to changes in the climate system. Adaptation has been also defined as “building resilience” and “increasing capacity” within a system to cope with change and generally refers to reforming, reconstructing, and/or reorganizing to better manage a new situation. The most recent definition of adaptation in UNISDR (2009) refers to the adjustment in natural or human system in response to actual or expected climatic stimuli or their effects, which moderates harm or exploit beneficial opportunities. Numerous adaptation options and coping strategies ranging from the type of houses lived in, to flood preparation and management measures, with the main intend of lessening the effect of the hazard could reduce the risk to some extent. The predominance of a specific coping strategy within an area is generally reflective of the intensity of flooding experienced in the region. Irrespective of expected efficacy, however, the choice of strategies could be influenced by other factors such as finance, or even cultural background.

This section more focuses on suitable mitigation options and strategies in order to decrease the vulnerability to flooding and, hence, to reduce property loss. The targeted groups are stakeholders, governments, consultants, and academic institutions as well as those who are involved in flood projects. Huge budget needs to be spent by the governments in order to mitigate the adverse effect and minimize the damage and losses of floods. The budget depends on an estimation of the cost of and the benefit from the action taken when budget is limited and competitive.

2.11 Results

2.11.1 Flood peak distribution

One important parameter, which is essential for water resources management, is variations in hydrological conditions that would be determined by hydrological measurements. However, quantifying the impact of variations require availability of long-term data. In this study the measured and recorded flow-rate time series at Niamey hydrometric stations were used (Figure 2.12) which shows the discharge measurement (in m^3/s) with available data covering four decades from 1980 to 2014. Thirty-four years of record of the annual peak discharge was considered for use in the flood-frequency analysis. The values of discharge were obtained at the Niamey hydrological station (Longitude 2,099; Latitude 13,510). Data were provided by national meteorological offices of Niger. As seen in the Figure, there is no significant trend identified in annual maximum flow series from 1980 to 2014.

Figure 2.13a shows the applied statistical distribution functions, amongst which Gamma distribution function (Figure 2.13b) with confidence interval (CI) equals to 95% was found to be the best function fitted the observed data. The parameters α and β were 54.81 and 29.68 respectively. Therefore, Gamma distribution function was used to calculate extreme flows associated with each return period. Table 2.3 shows the calculated extreme flow rates, using statistical distribution function, for various floods with different return periods. The flood peaks estimated for various return periods of 2-, 10-, 20-, 50-, 100-, 200-, 500, and 1000-yr were 1608, 2019, 2147, 2297, 2401, 2498, 2620, 2707 m^3/s, respectively.

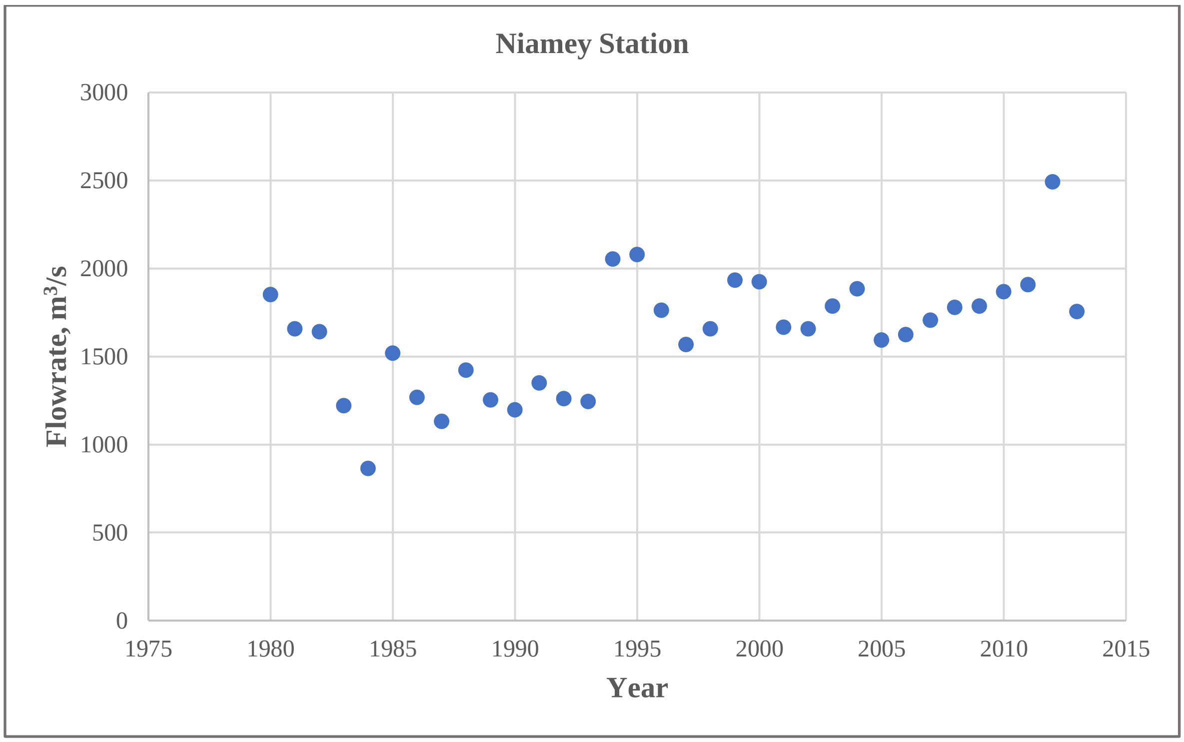

Figure 2.12. Flowrate time series at Niamey Station for 40 years (1980-2014).

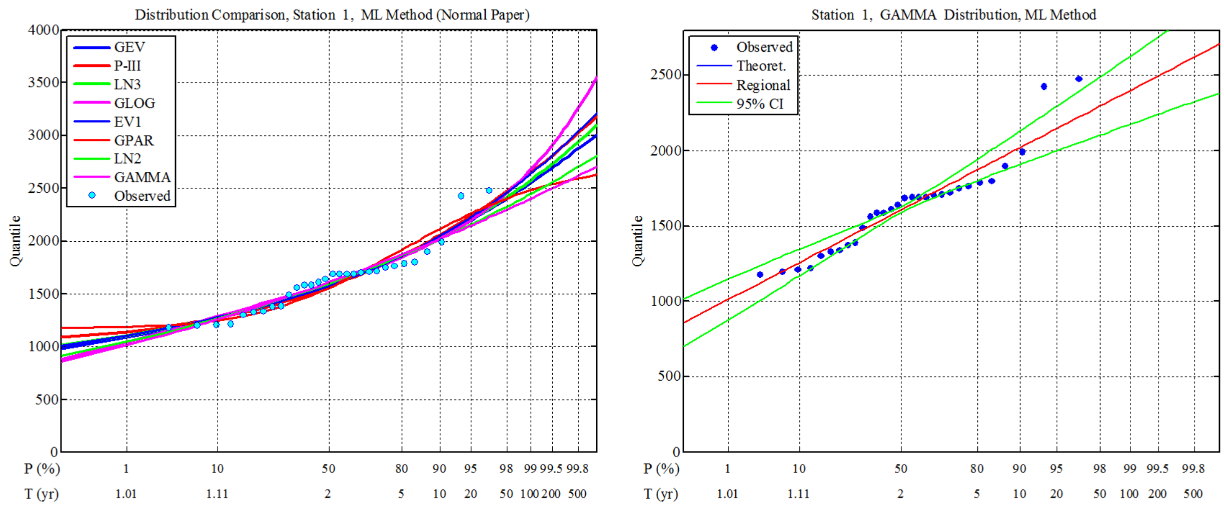

(a) (b)

Figure 2.13. (a) Distribution functions comparison, ML method, Normal paper; (b) GAMMA distribution, ML method, Normal paper.

Table 2.3. Calculated extreme flow rates for various floods with different return periods.

Return Period, (Year)	Exceeding Probability	Flow rate, (m^3/s)
2	50	1608
10	10	2019
20	5	2147
50	2	2297
100	1	2401
200	0.5	2498
500	0.2	2620
1000	0.1	2707

2.11.2 Inundation maps

After developing the hydrodynamic model for the Niger River, floodplain cross-sections from the elevation contour data of the City of Niamey were extracted in order to estimate water-surface profiles. A total of 988 cross-sections were extracted along 160 km of the Niger River within the study area. Accordingly, the companion GIS utility, HEC-GeoRAS, was used to convert the water-surface profiles at all cross-sections from HEC-RAS model into inundation maps and develop plan-view extent of flooding over the length of the modelled stream. Figure 2.14 (a and b) presents flood inundation maps for 100-, and 1000-year flood events in the study area. The floodplain polygons were overlaid on the image of the area in order to compare the extent of various flood frequency events.

(a)

(b)

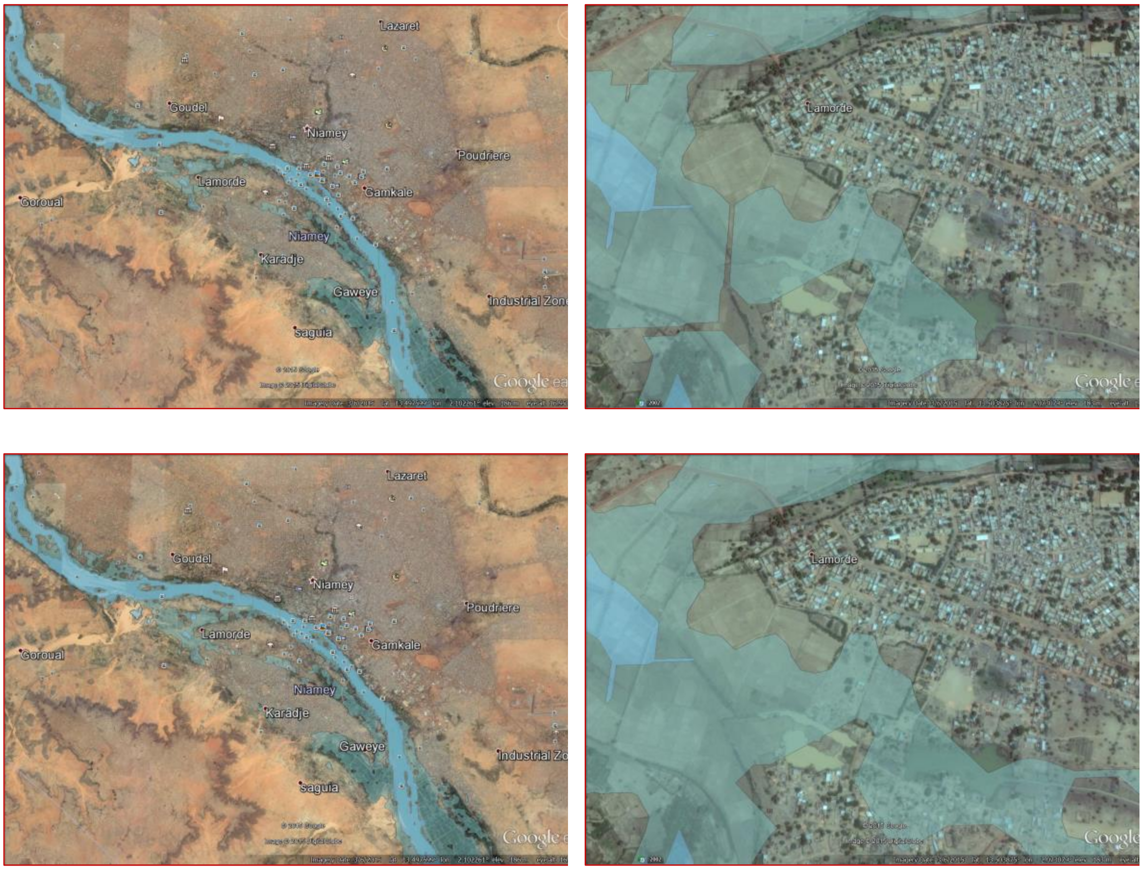

Figure 2.14. Estimated inundated area for various floods with different return periods, (a) 100-yr flood; (b) 1000-yr flood.

2.11.3 Loss exceedance curves

The physical damage to the exposed elements in flood events is calculated by means of hazard and vulnerability of the elements. In this study, Central American Probabilistic Risk Assessment (CAPRA) software (CAPRA, University of the Andes) was used to generate the loss exceedance curves. The software is based on a probabilistic risk assessment methodology and has a set of tools for risk evaluation at different territorial levels. Probabilistic metrics, such as the exceedance probability curve, expected annual loss and probable maximum loss are used by the software to evaluate and estimate losses on exposed elements.

The results illustrate the effect of dike crest height on flood exceedance curves for the six different building material scenarios (Figure 2.15). For each type of building material, the damage exceedance probability becomes zero after a certain threshold: 400 million CFA for mud walls, 300 million CFA for concrete walls, 200 million CFA for informal constructions, and 800 million CFA for mud walls covered by mortar. Irrespective of the type of building material used, increasing the dike crest heights by just 50 cm above present levels might lead to a significant reduction in the exceedance probability of damages. Subsequent increases of the dike heights still lead to further decreases of the exceedance probability. In conclusion, the flood risk mitigation option implemented by the PGRC-DU (Projet de Gestion des Risques de Catastrophes et de Développement Urbain-Disaster Risk Management and Urban Development Project), decreases the probability of physical damages to buildings. It seems likely that this also reduces the probability of casualties, although this aspect was not part of our analysis.

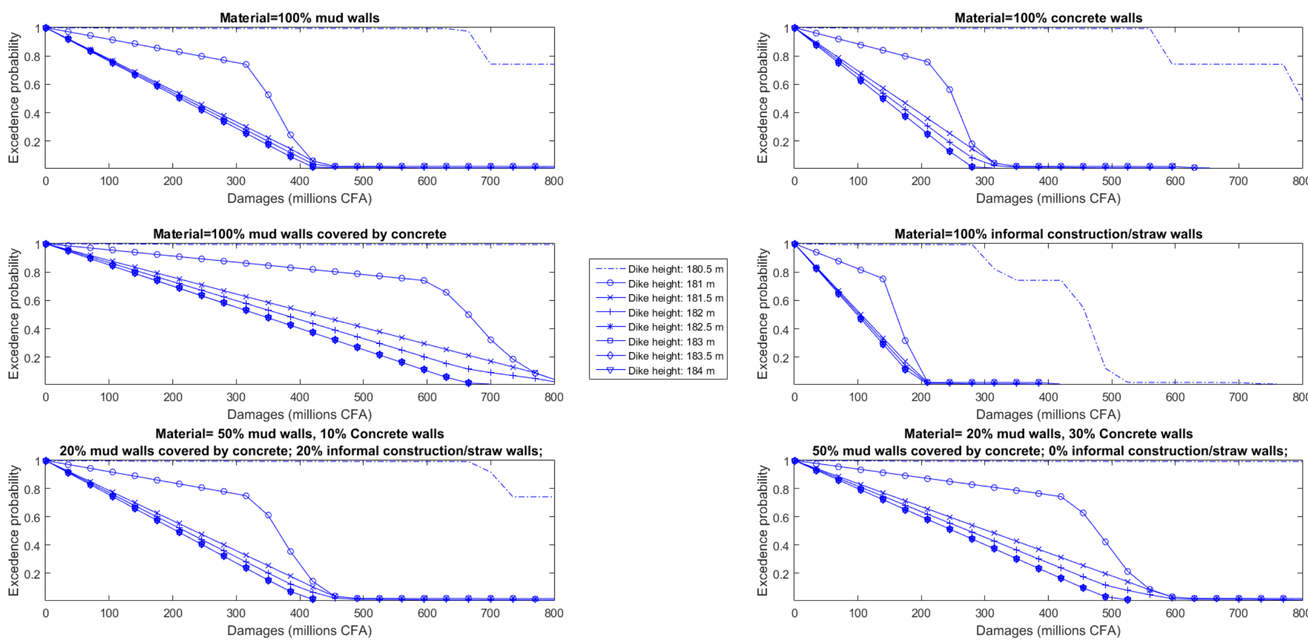

Figure 2.15. Residential flood damage exceedance curves as function of dike crest elevation given the repartition of building types in the floodplain. The current dike height is 181 m.

In order to look more closely at the effect of building materials on the loss exceedance curve for a given dike height, the different scenarios were combined into a single panel and plotted the result for the different dike heights (Figure 2.16). As expected, the loss exceedance curve for the scenario representing the status quo (Scenario 5) is below the loss exceedance for 100% DUR, and above 100% SDU, 100% BAN and 100% CAS. When building materials are improved (Scenario 6), the losses increase without reaching the losses for 100% DUR. Therefore, the adaptation option chosen by local populations in the floodplains would appear to increase the probability of monetary losses, but is likely to decrease the number of casualties.

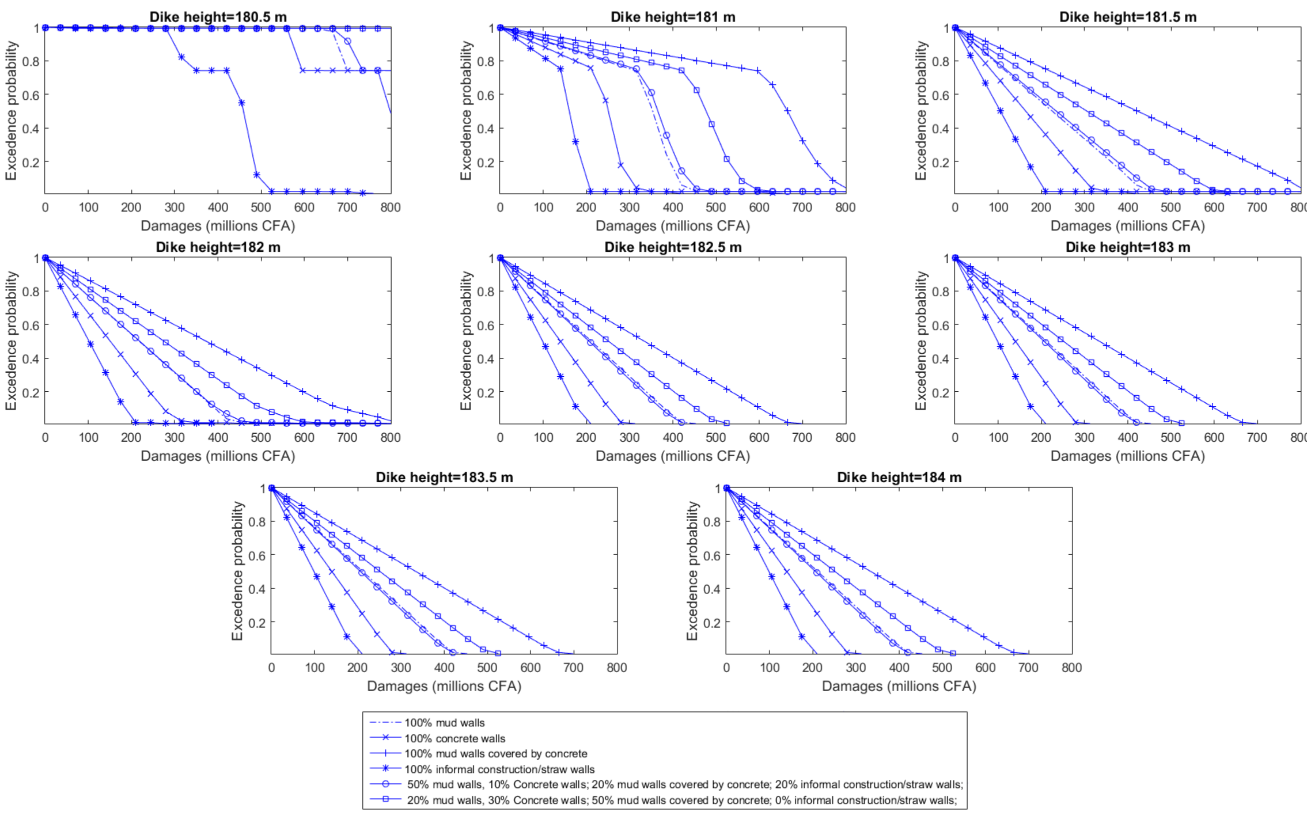

Figure 2.16. Residential flood damage exceedance curves as a function of the mix of building types in the floodplain for different elevations of the flood protection dike crest.

The annual average economic loss for each scenario behaves as expected (Table 2.4), i.e., it decreases with increasing dike height. The lowest economic loss corresponds to 100% informal construction and dike heights greater than or equal to 182.5 m. However, decision-makers should not opt for this scenario since the analysis does not account for the risk of human casualties associated with lower quality material. Another factor that has not been accounted for in this study, is the cost of implementing the adaptation options.

Table 2.4. Estimated average annual losses (in million CFA[a]) as function of dike crest height and building material.

		Building material					
		100 % mud walls	100% concrete walls	100% mud walls covered by mortar	100% informal constructions or straw walls	50% mud walls, 10% Concrete walls; 20% mud walls covered by mortar; 20% informal construction/straw walls	20% mud walls, 30% concrete walls; 50% mud walls covered by mortar; 0% informal construction/straw walls
Dike crest height, m	180.5	932.0	767.1	1729.3	431.4	973.1	1278.1
	181	327.0	233.5	612.2	152.4	337.8	438.7
	181.5	236.0	172.6	440.7	110.5	243.7	316.6
	182	224.5	157.3	389.4	105.3	225.9	285.0
	182.5	213.0	142.0	338.2	100.0	207.3	252.5
	183	213.0	142.0	338.2	100.0	207.3	252.5
	183.5	213.0	142.0	338.2	100.0	207.3	252.5
	184	213.0	142.0	338.2	100.0	207.3	252.5

[a] West African CFA franc

2.11.4 Efficiency of adaptation options

Considering the fact that the area is highly prone to flooding, and often suffers from loss of lives and damages to properties, one proposed adaptation option is changing in the buildings' materials. After the catastrophic floods of 2012, most of the houses made with mud walls were destroyed in the study area. Populations in the most affected areas were offered the option to relocate elsewhere, but a significant number of households chose to rebuild their houses on the same site. Given that most houses built with concrete walls had survived the flood, almost all houses were rebuilt using concrete, resulting in a lower probability of collapse and less human casualties in case of a similar flood. In this study adaptation options in response to the flood risk in Niamey region and the impact of undertaking such options on total loss estimation for residential land-use classes were considered. The total loss was evaluated in response to the likelihood of flooding with various return periods range from 2- to 1000-yr. The options include raising level of the available flood defense (dike), and building or strengthening building structures using various buildings' material. The proposed types of buildings' material which are chosen according to the availability of them in the study area consist of CAS (informal straw walls), BAN (mud walls), DUR (concrete walls), and SDU (mud walls covered by mortar). These adaptation options are more to resist environmental change in order to preserve existing infrastructures; therefore, they might involve significant cost to implement. In the following section, the results of applying the proposed adaptation options to the study area are presented in tabular form.

Accordingly, Tables 2.5 to 2.8 show the total potential loss for residential land-use class for flood with return period of 1000-yr and various type and percentage of buildings' material in the study area.

Table 2.5. (BAN_0%): Total loss value ($\times 10^8$) for different types of buildings, CFA.

DUR (%)	**SDU (%)**										
	0	**10**	**20**	**30**	**40**	**50**	**60**	**70**	**80**	**90**	**100**
0	0.9330	1.2050	1.4770	1.7490	2.0210	2.2930	2.5650	2.8370	3.1090	3.3810	3.6530
10	1.0151	1.2871	1.5591	1.8311	2.1031	2.3751	2.6471	2.9191	3.1911	3.4631	NA
20	1.0972	1.3692	1.6412	1.9132	2.1852	2.4572	2.7292	3.0012	3.2732	NA	NA
30	1.1794	1.4514	1.7234	1.9954	2.2674	2.5394	2.8114	3.0834	NA	NA	NA
40	1.2615	1.5335	1.8055	2.0775	2.3495	2.6215	2.8935	NA	NA	NA	NA
50	1.3436	1.6156	1.8876	2.1596	2.4316	2.7036	NA	NA	NA	NA	NA
60	1.4258	1.6978	1.9698	2.2418	2.5138	NA	NA	NA	NA	NA	NA
70	1.5079	1.7799	2.0519	2.3239	NA	NA	NA	NA	NA	NA	NA
80	1.5900	1.8620	2.1340	NA	NA	NA	NA	NA	NA	NA	NA
90	1.6722	1.9442	NA	NA	NA	NA	NA	NA	NA	NA	NA
100	1.7543	NA	NA	NA	NA	NA	NA	NA	NA	NA	NA

Table 2.6. (BAN_20%): Total loss value ($\times 10^8$) for different types of buildings, CFA.

DUR (%)	**SDU (%)**								
	0	**10**	**20**	**30**	**40**	**50**	**60**	**70**	**80**
0	1.1462	1.4182	1.6902	1.9622	2.2342	2.5062	2.7782	3.0502	3.3222
10	1.2283	1.5003	1.7723	2.0443	2.3163	2.5883	2.8603	3.1323	NA
20	1.3105	1.5825	1.8545	2.1265	2.3985	2.6705	2.9425	NA	NA
30	1.3926	1.6646	1.9366	2.2086	2.4806	2.7526	NA	NA	NA
40	1.4747	1.7467	2.0187	2.2907	2.5627	NA	NA	NA	NA
50	1.5569	1.8289	2.1009	2.3729	NA	NA	NA	NA	NA
60	1.6390	1.9110	2.1830	NA	NA	NA	NA	NA	NA
70	1.7211	1.9931	NA	NA	NA	NA	NA	NA	NA
80	1.8033	NA	NA	NA	NA	NA	NA	NA	NA

Table 2.7. (BAN_40%): Total loss value ($\times 10^8$), CFA.

DUR (%)	SDU (%)						
	0	10	20	30	40	50	60
0	1.3594	1.6314	1.9034	2.1754	2.4474	2.7194	2.9914
10	1.4416	1.7136	1.9856	2.2576	2.5296	2.8016	NA
20	1.5237	1.7957	2.0677	2.3397	2.6117	NA	NA
30	1.6058	1.8778	2.1498	2.4218	NA	NA	NA
40	1.6880	1.9600	2.2320	NA	NA	NA	NA
50	1.7701	2.0421	NA	NA	NA	NA	NA
60	1.8522	NA	NA	NA	NA	NA	NA

Table 2.8. (BAN_60%): Total loss value ($\times 10^8$), CFA.

DUR (%)	SDU (%)				
	0	10	20	30	40
0	1.5727	1.8447	2.1167	2.3887	2.6607
10	1.6548	1.9268	2.1988	2.4708	NA
20	1.7370	2.0090	2.2810	NA	NA
30	1.8191	2.0911	NA	NA	NA
40	1.9012	NA	NA	NA	NA

The results generated in this study allows to quantitatively estimate the gain in resilience that comes from these decisions. It can also demonstrate to the decision-makers the benefits of implementing policies that encourage people to build with different materials. This is the first time a quantitative analysis of flood risk and adaptation options is implemented. For the proposed tool to be more effective, decision-makers should invest in a comprehensive survey of the built environment and exposed assets in the study area. Additional information on building stock and existing building etc. helps in obtaining more accurate information on exposed elements and will be used for decision-making in risk management. Such a survey would allow us to estimate the risk in the current situation and estimate more accurately the benefits of adaptation options.

2.12 Conclusion

There are many different ways of viewing natural hazard adaptation in general, some with main focus on resisting to environment changes, while others are mainly targeting suiting such changes or a combination of both. However, necessity of considering some effective parameters such as budget, time, and available resources, which prioritizes available options for each specific case, makes the decision-makers not to promote one approach over another. Therefore, selection of the best options involves evaluating and assessing various approaches based on specific situation of each case. In this study the residential vulnerability to floods in the city of Niamey was analyzed in a probabilistic framework. Total number of 1000 random flow values, representing maximum annual flow, were generated and converted into loss exceedance curves. The sensitivity of the loss exceedance curves to the altitude of flood protection dikes and to the type of building materials were examined. It was found that increasing the height of the dikes would lead to smaller economic losses, while rebuilding with better materials would increase the average annual economic losses, but might decrease the risk of human casualties. In order to select the best adaptation options, decision-makers have to factor in non-economic values as well as associated implementation costs. These results should be viewed with caution, given the scarcity and low quality of the available data for the study area. The results also demonstrate the individual as well as the combined impact of the two considered variables in flood risk estimation in the Niger River basin, which enable decision-makers as well as the regulators to have a better analysis and estimation in choosing the best preventive measures to alleviate the adverse impacts arising from flood events. The findings contend that although the proposed structural adaptation option as a resisting to environment approach are applied to the area of interest and considered to be technically feasible, other non-structural measures, which have long-term effect of risk mitigation, should be taken into consideration especially for highly hazard-prone areas. Non-structural measures include public awareness programs, policies and laws and their enforcement, changes to land-use, whether through zoning, changes in building codes or in infrastructure design, and location (UNDRR, 2021; Public Safety Canada, 2021).

Chapter 3

Building Extraction from Aerial Imagery and Digital Elevation Model using Artificial Intelligence – Deep Learning

3.1 Introduction

Floods are the most common and widespread of all weather-related natural disasters and more deaths occur each year due to flooding than any other thunderstorm-related hazard (Asian Disaster Reduction Center, 2011; WMO, 2021). In developing countries, where economic damages are more important, low levels of flood protection causes severe flood-induced impacts on the affected communities (Levy and Patz, 2015; De Silva and Kawasaki, 2018). The study area in this research, Niamey (capital city of Niger), has faced more severe and frequent floods, mainly caused by heavy rain, during the past decade. The most catastrophic ones occurred in 2017, 2019, and 2020. The significant flood damage in the region, which is being reported in terms of casualties, affected households, and displaced people (OCHA, 2015, 2017, 2020), indicates the importance and necessity of the assessment of flood risk in the city. To perform a thorough assessment, it is important to identify all three flood risk elements, defined by the World Meteorological Organization (WMO, 2006): hazard; exposure; and vulnerability. Kheradmand et al. (2018) evaluated flood hazards in the city using 1-D hydraulic simulations and limited exposure data delineated from Google Map images. As high-resolution aerial images of flood-prone areas in the city have become available, this study explores more systematic and more accurate approaches for flood exposure estimation in the city of Niamey.

In flood risk assessment, exposure refers to the elements and assets that are subjected to the risk of flood inundation. Buildings are the only type of exposure considered in this research. Buildings' information can be obtained and interpreted through various means and at different scales, spatial, temporal, and spectral resolution. Terrestrial measurements, and airplane surveys as well as spaceborne, airborne, and drone-based imagery using advanced remote sensing technologies provide large amount of data. Ever-developing technology of satellites for Earth monitoring has increased the availability of high-resolution remote sensing imagery. However, high-resolution images can capture more elaborate information of texture and structure of the features. Therefore, managing, processing, analyzing, and applying the vast amount of provided data through high object density satellite images are challenging tasks, especially in dense urban areas, and require dedicated computing resources. Some of these challenges include shadows created by tall objects (trees, buildings, etc.), trees that cover the rooftops, or different reflections due to various roof building materials. Therefore, a great number of attempts have been made by researchers to develop algorithms and techniques to extract buildings automatically (Peraresi and Benediktsson, 2001; Shan and Lee, 2002; Tseng and Wang, 2003; Pandey, 2004; Wu et al., 2004; Khokher and Talwar, 2012; Yee, 2013; Ok, 2014; Salih et al., 2015).

Fradkin et al. (2001) used multiple aerial images in their novel approach (based on accurate surface reconstruction) for building detection in dense urban areas. First, they proposed an algorithm to detect building facades as the main cue for building detection. Subsequently, used a set of confirmation criteria to verify the detected hypotheses in each image. Their method showed 80% detection rate with very high reliability (false detection rate of 1%). Guo and Yasuoka (2002) preprocessed high-resolution IKONOS satellite images using a digital surface model (DSM) and, normalized DSM technique. At the next step, they combined height data and snaked-based approach to extract 2-D building boundaries from the preprocessed images. They achieved promising results of combining spectral signature and height information for extraction of buildings. They suggested that using geometrical information like straight lines, and corners are useful clues and should be investigated in future studies. In another study by Shackelford and Davis (2003) a combined fuzzy pixel-based and object-based approach was used to classify urban land cover from high-resolution multispectral image data. The pixel-based fuzzy classifier used both spectral and spatial information for individual image pixels, followed by an object-based fuzzy logic classification approach. The results led to 76% accuracy in building detection. They suggested that decision rules could be further used to discriminate between different types of buildings, such as residential, commercial, and industrial.

Koc San and Turker (2010) used Hough Transform (a method for finding lines in images) to extract the rectangular and circular shaped buildings from high-resolution pan-sharpened and panchromatic IKONOS images. They tested their proposed technique for the residential and industrial urban blocks in urban area. Kumar and Padmaja (2012) presented a novel method using visual patterns of the objects (Texture approach) to count number of trees in high-resolution images. They first converted RS image to HIS image via the texture approach algorithm to identify the texture difference between Saturation Channel and Intensity Channel. The process followed by removing the noise in the Concatenated HIS image (image smoothing), Thresholding, Histogram Equalization, and Delineating and counting the trees at the last step. However, overlapped tree crowns, and shadows are reported as main errors in counting the number of trees. In another study on automatic building extraction, Wang et al. (2013) proposed a method based on LSD and perceptual grouping to extract buildings. Through three main phases, they first applied bilateral filter to smooth images while preserving edges; and subsequently line segment detection, and perceptual contour line analysis were used to achieve the results. The method was applied on VHR images of challenging examples and showed promising experimental results (overall accuracy of 79.1%).

In an integrated approach proposed by Kumar et al. (2014), main road network was extracted from high-resolution space images (fused IKONOS2, Quick bird, Worldview2 Products with fused resolutions ranging from 0.5 m to 1 m). The first step was segmentation of the urban scene using Multi-resolution Object-Oriented segmentation with the focus on spatial and spectral information of the target features. At the next step, a soft fuzzy classifier was used to automatically identify the road regions. Shape descriptors were also computed to avoid misclassification with spectrally similar objects. The last step was refining the detected roads with morphological operations. They achieved accurate results in extracting main road networks in complex urban scenes. However, objects like trees, vehicles, as well as shadows of high buildings were some of the reported limitations. Benali et al. (2014), used an unsupervised method based on mathematical morphology to extract buildings from high spatial resolution satellite images of urban areas. The applied morphological operations were Hit-or-Miss Transformation (HMT), and noise were eliminated by deformation correction and smoothing. They used an empirically thresholded image as a reference image in their semi-automatic proposed method. They obtained satisfactory results; however, using automatic thresholding technique was suggested to enhance the results. Shrivastava and Rai (2015), extracted buildings from high-resolution satellite data (Cartosat-1 satellite data fused with IRS-1C, LISS IV data) using eCognition software. Despite the overall satisfactory results (overall accuracy of classified image was 0.94 and Kappa accuracy was 0.92), the applied method was not successful in extracting the clear edges of the buildings. Therefore, using thinning algorithms was suggested by the authors for further thinning the edges.

The goal of this chapter is to investigate an Artificial Intelligence (AI) method in building extraction in the area of interest, Niamey, Niger, and compare the results of the method with those of the semi-automated Maximum Likelihood Classification (MLC) method (using ArcGIS software). For this purpose, a Deep Learning (DL) method was applied. Details on the input data, methodology, and the results are explained in the following sections.

3.2 Materials and methods

3.2.1 Study area and available data

Niamey, the largest city of Niger, with a mean elevation below 227 m above sea level, is also the most populated city with a population estimate of 1.336 million inhabitants (Populationstat.com Retrieved in July 2021). Most of the Niamey's population is mainly located along both sides of the Niger River, hence are prone to flooding. Niamey is located between latitudes 13.29° N and longitude 2.09° E in Niger, Africa. Figure 3.1 shows the study area, Niamey.

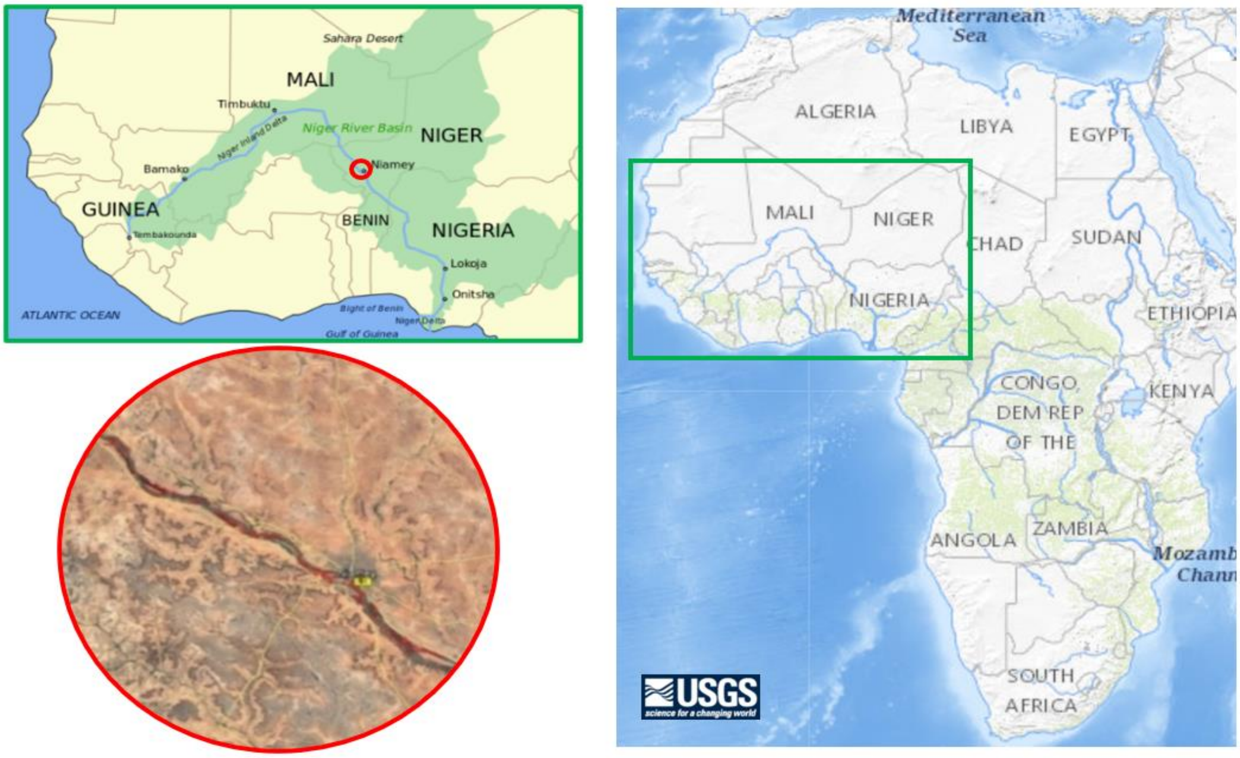

Figure 3.1. Niger River basin (United States Geological Survey - USGS). The red line indicates the section of the River which has been considered in this study.

The data used in this study consist of orthomosaics and a Digital Surface Model (DSM) of an approximately 98.85 km^2 (22.47 km long and 4.40 km wide) band of land along the Niger river in Niamey. The orthomosaics and the DSM were acquired in 2014 using Ultralight Airplane and Photogrammetry. The dataset contains the elevation data of the elements of the natural terrain, vegetation, and the buildings as a set of 3-D points. Figure 3.2 shows the extent of the available DSM data for the study are in this research, city of Niamey, Niger. A sample area is shown in the black square (Figure 3.2a), as well as the high-resolution aerial image (Figure 3.2b), 2-D (Figure 3.2c) and 3-D (Figure 3.2d) view of the DSM for the sample area.

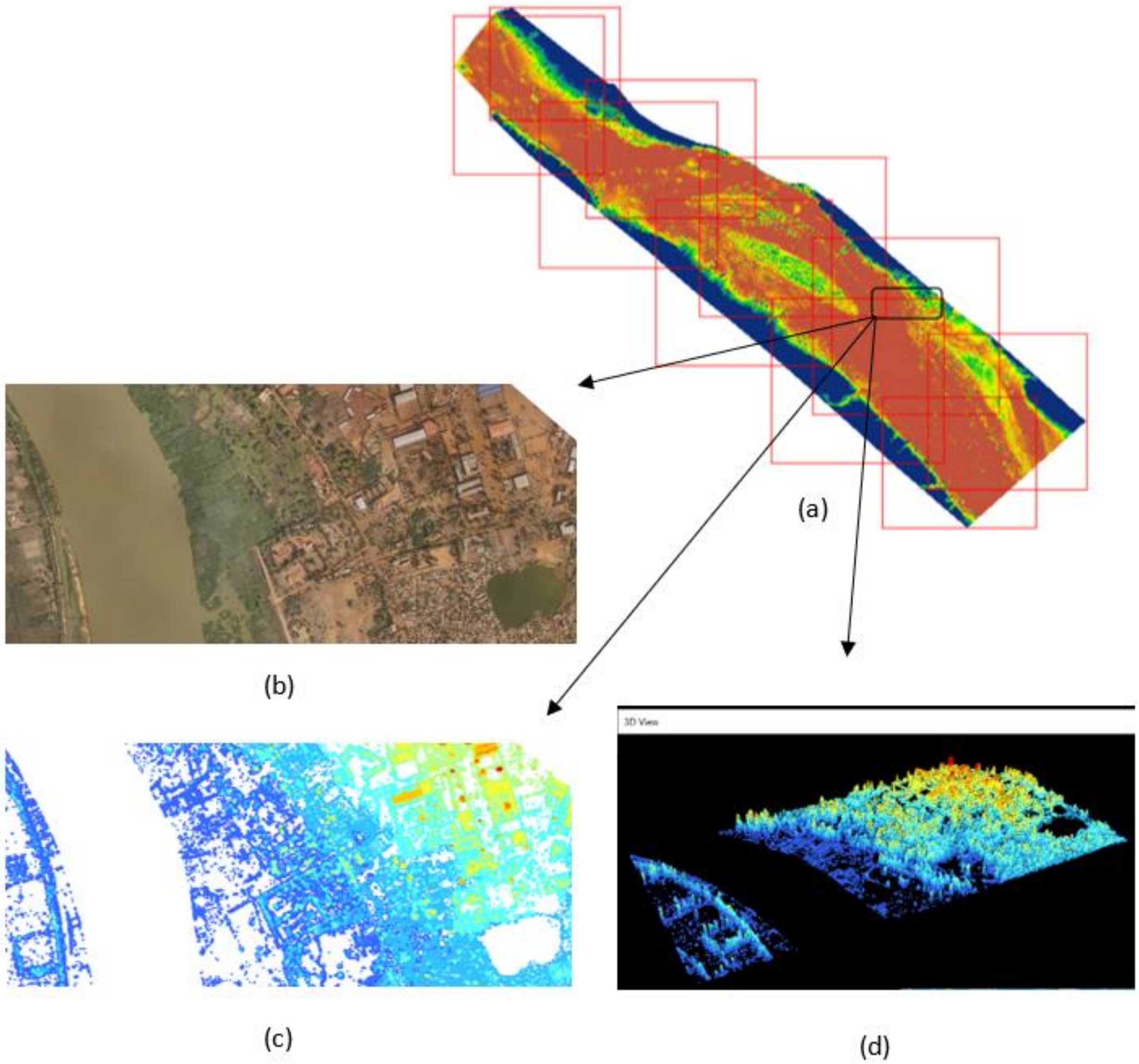

Figure 3.2. a) The extent of the study area, city of Niamey, with a sample area shown in a black square; b) High-Resolution aerial image for the sample area; c) 2-D view of the DSM data for the sample area; and d) 3-D view of the DSM data for the sample area.

3.2.2 Building extraction techniques

Over the past decades, various computer techniques have been developed for interpretation of imagery data such as image processing, pattern recognition, tree base algorithm, artificial intelligence, and Machine Learning (ML) (Wu et al., 2004). By developing computation process like GPUs, machine learning becomes one of the best solutions in solving a variety of problem from feature detection in an image (face, pedestrian, or crop harvesting) to diseases detection.

3.2.3 Semi-automated approach – Maximum likelihood classification

Maximum likelihood classification (MLC) is one of the most popular techniques which estimates parameters using observations. It assumes that a) the distribution is normal for the data; and b) Bayes Theorem of decision making is applied. In image classification, the following function is used to assign the image pixels to a class (Ahmad and Quegan, 2012):

$$P(i \mid \omega) = \frac{P(\omega|i)P(i)}{P(\omega)} \quad (3.1)$$

$$P(\omega) = \sum_{i=1}^{M} P(\omega|i)P(i) \quad (3.2)$$

Where, $P(i \mid \omega)$ is the probability that a pixel with feature vector ω belongs to class i, $P(i)$ is the probability that class i occurs in the study area, $P(\omega|i)$ is the likelihood function, $P(\omega)$ is the probability that ω is observed, and M is the number of classes.

Considering the data given, for all possible parameters, the algorithm computes the probability of observing these data and chooses the parameter for which this probability is highest (maximum likelihood), to identify the specific class that a given image pixel belongs to; all pixels will be classified accordingly.

3.2.4 Automated approach – Machine learning

Image processing using machine learning could be categorized into Image Classification, Object Detection, and Image Segmentation. In image classification, the main goal is to classify the complete image while Object Detection locates an object by drawing a bounding box around the object. In image segmentation, each pixel of image is being classified as a category, therefore location and shape of the object will be recognized. Image segmentation is a popular method in medical studies (where shape of the feature is important) and agricultural research (where land parcels do not have a regular shape). In the following sections, the AI structure is explained, in the scope of this research, with a succeeding section on an overview of the background and various application of deep learning.

Convolutional neural networks

Convolutional neural network (CNN) model is a subset of deep neural network and is mostly used in visual imagery. CNNs are widely used in object segmentation (i.e., classifying an image at a pixel level) (Chellappa and Rosenfeld, 2003) from high-resolutions imagery, e.g., building outline delineation, due to their ability in learning high-level spatial and contextual features (Zhang et al., 2020). Hidden layers in CNN consist of several convolutional layers through which various filters (matrixes) are applied to the input data. The model has two main parts of down-sampling and up-sampling. In down-sampling section, features are being extracted from the image, while in up-sampling the image is being reconstructed from the extracted features. Each of the parts have several hidden layers. The output of each layer is determined by an activation function(s). Activation functions are mathematical functions such as sigmoid, that behave like a gate between two layers. Following the activation function, pooling is used to change the spatial size of the input layer (increasing or decreasing). Subsequently, Normalization is used to normalize and scale the input layers to ensure that each layer can learn independently of previous layers. And loss functions quantify the model prediction from the actual labels.

Deep learning

Deep learning is one of the machine learning methods based on Artificial Neural Networks (ANN); one of its applications is automatic interpretation of satellite imagery through integrating multiple high-resolution remote sensing data sources. The first step in machine learning, is the learning step during which, the chosen algorithm tries to automatically improve its behaviour based on experience; training experience can be expressed as features. In deep learning, basic and general features such as lines, and edges are learned within the first layers while high-level and complicated features are processed and learned in deeper layers. Previous studies showed that by increasing number of layers and becoming deeper, number of parameters increases, and model becomes more capable to fit more complex problems. Neural networks contain weights (W) and biases (b), so-called trainable parameters, which are updated throughout the computational operations based on their effect on the loss function (Kotzé et al., 2020). In a simple neural network such as Multilayer Perceptron (a feedforward artificial neural network), the weights in the layers are updated and adjusted using the backpropagation algorithm; making the small changes to the layers' weights decreases the loss function value of the model. However, increasing the number of layers (deeper models) causes the model's performance to fail by vanishing gradient. In other words, as the gradient flows updating from last layers to initial layers, its value becoming smaller to finally shrinks to zero. Accordingly, layers' weight stops being updated, and the model's performance will not be improved through iterations. Skip (residual) connection is a solution has been used in ResNet. In an ordinary neural network (shallow network), the output of a layer (x) is input of the next layer ($f(x) = x$). Skip connection will skip multiple layers and directly adds information from the previous layers ($h(x) = f(x) + x$). Hence, if $f(x) = 0$, the gradient value will not be shrunk to zero (Figure 3.3).

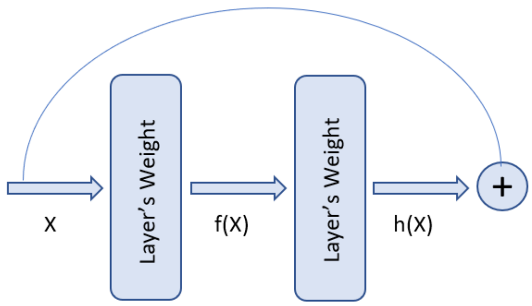

Figure 3.3. Skip connection structure.

In addition to detecting class of features, deep learning models must localize the area of each feature, through classification process for every single pixel. In model classification or object detection, an image is being converted to a vector (number of classes) while in image segmentation, the converted image must be, subsequently, reconstructed to an image. The former is down-sampling (encoding or contraction path), and the latter is up-sampling (decoding or expanding path) which is a more complex procedure than down-sampling. This whole idea is behind U-Net architecture. The U-Net is a CNN model mainly developed for biomedical image segmentation applications. This model has a U shape in which the contraction and the expanding paths are symmetric. The contraction path consists of several convolution layers followed by a rectified linear unit (ReLU). During this path, spatial details are reduced while feature details will be increased. Expanding path consists of several up-convolutional layers during which a segmented image will be reproduced. There are also some skip connections which connect the contraction layers to the expanding layers while ignoring all intermediate layers. The skip connections help reconstructing the segmented image by directly providing the learned spatial information from contraction layers to the up-sampling layers. Training a deep learning model from scratch is a time-consuming task and requires very big dataset which is not accessible in most of the cases. Therefore, in Transfer Learning (TL) a deep model that has been trained (pre-trained model) on large datasets and represents a wide diversity of features and labels, is applied to a new dataset. Figure 3.4 shows an example of the architecture of a U-Net model.

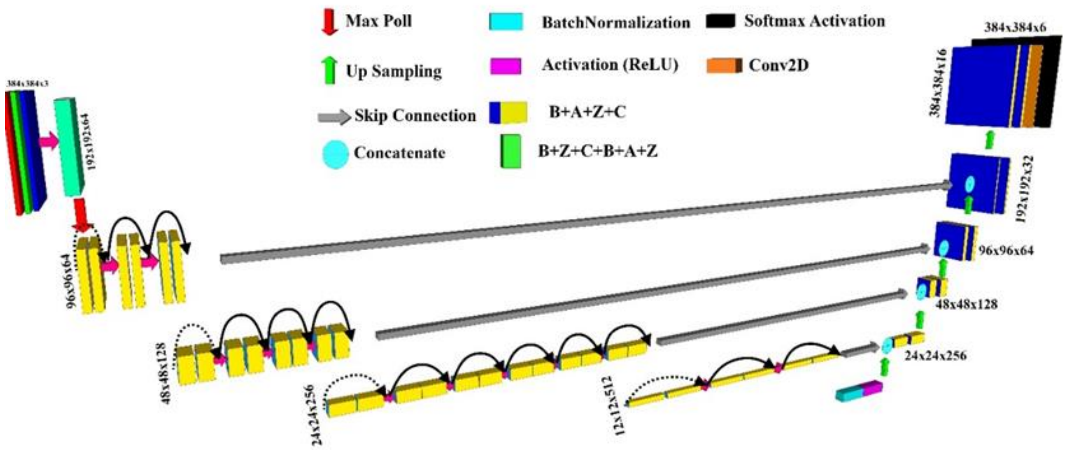

Figure 3.4. An example of a U-Net model.

Loss functions are used to evaluate the ability of a neural network in making predictions by measuring the difference between the actual output and the predicted output. However, the performance of neural networks could be enhanced by using optimizers. Optimizers, in general, define how neural networks learn. They find values of parameters such that a loss function is at its lowest, hence provide the most accurate results possible (Huang et al., 2020; Sewdien et al., 2020). In order to reduce the error, the gradient of a defined loss function with respect to the weights will be used by an optimization function e.g., Gradient Descent (GD) method (Andrearczyk and Whelan, 2017). Adam (Adaptive Moment estimation) and AdaDelta (adaptive learning rate) are amongst the most popular gradient descent optimization algorithms used to train neural networks. They compute adaptive learning rate for each training parameter and for each cycle. AdaDelta resolves the problem of continual decay of learning rate (Adagrad optimizer) by dynamically adapting over time (Zeiler, 2012). Adam is another gradient-based optimizer which updates both the learning rate and momentum for each parameter (Kingma and Ba, 2017).

3.2.5 General methodology

Two methods are used in this section: Maximum Likelihood Classification using ArcGIS MLC tool, and Machine Learning. The flowcharts for the methods are presented in the following figure (Figure 3.5):

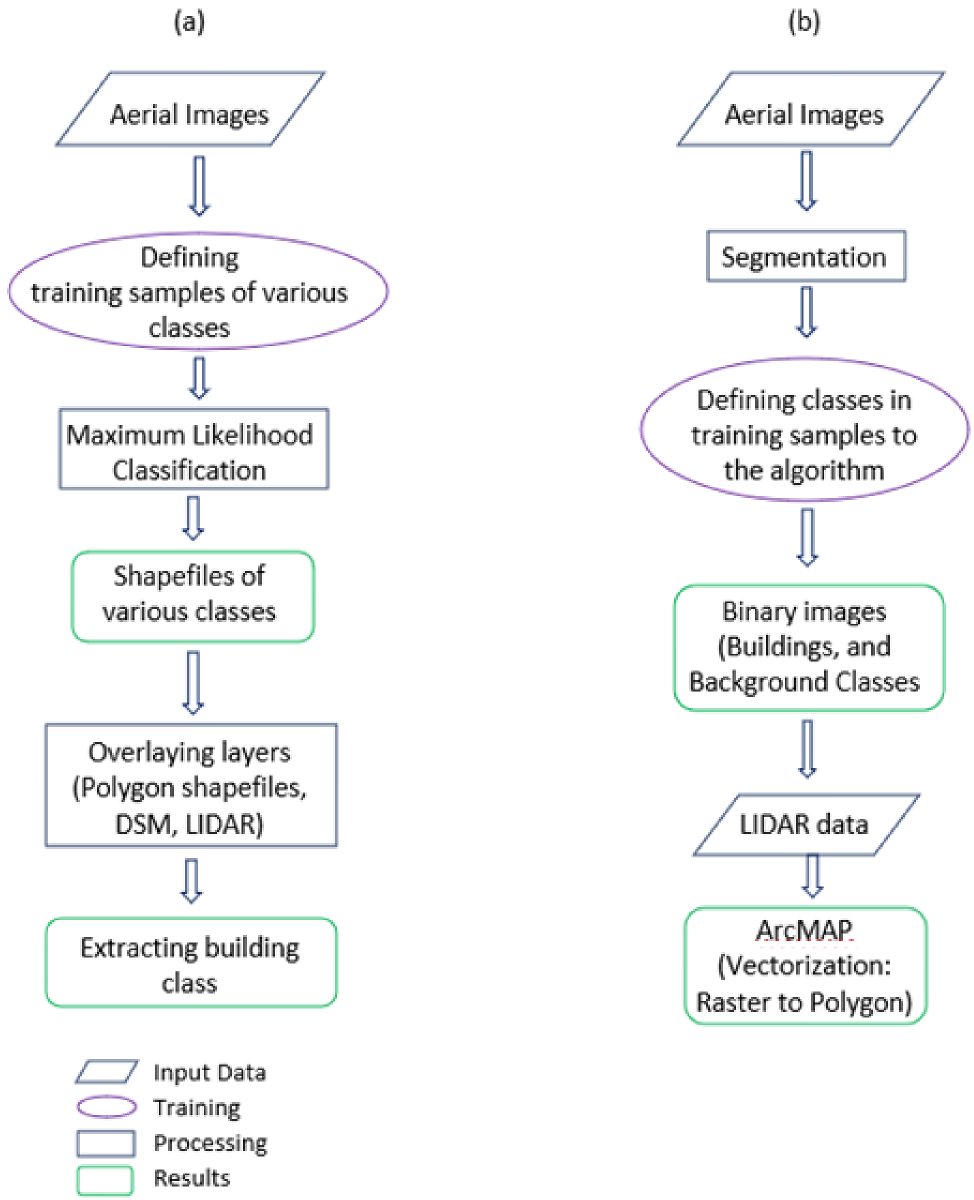

Figure 3.5. Flowchart (workflow) of the applied methodologies: a) ArcGIS MLC tool, b) Machine Learning (ML).

More details on the methods are presented in the following sections.

3.3 Building extraction workflow

3.3.1 Maximum likelihood classification using ArcGIS MLC tool

In this research, the following stepwise approach in ArcGIS Maximum Likelihood Classification tool was followed to apply the maximum likelihood principle. The approach consists of three main steps: Creating training areas; Creating signature file; and Classifying images. During the first step, polygons were drawn for the areas with known land-use purposes. In this study three classes of water, building, and vegetation were used for training samples. Multiple training areas for each class were chosen across the images, to encompass much of the variability for each class, i.e., not all the building sample polygons were selected in one corner of the image, instead several examples of buildings were chosen throughout the image. In the case of this study, it is important to have various samples of building class especially when limitations such as shadows by clouds, or tall trees are seen in aerial images of the area. An example of an area with cloud shadow is shown in the results section (Figure 3.9a). After creating all the training areas for the desired classes, the samples were saved as a signature file to be later used for the classifying step. The MLC method is used to extract information for multiple raster bands in order to compute the probabilities of group membership for each pixel in an aerial image, and subsequently, based on statistical probabilities, assign each cell to the land classes where they belong. The output of the process is a classified image that includes the colors for each class that was previously created and introduced during the previous steps. The output raster files were then converted to polygons using conversion tool on ArcToolbox.

3.4 Deep learning using the Adadelta, and Adam algorithms

Both raw raster images and polygon shape files were divided into small segments to be used as input data to the machine learning grid-based algorithms, where they were further labeled as Building, or Background (training step). At this step, the algorithm is trained based on various terrestrial targets in an image including vegetation, road, pavement, water, etc.; therefore, the most cloud-free images were chosen for the training step. The two algorithms used for this purpose are Adadelta, and Adam algorithms.

After the first step, the trained algorithm was then applied to a new set of image segments of a different area. The output of this step consists of labeled images of Building and Background classes. However, misclassification may occur in the areas where different objects of Background class have same colors of Building class. Therefore, at the next step, DSM data were applied to the output of the algorithms to further select the pixels higher than a certain value.

3.5 Results and discussion

3.5.1 Maximum likelihood classification

Figure 3.6 shows the result of the applied MLC method. At the training phase, two classes of Buildings and non-buildings (including water, vegetation, and bare land), were identified through several sample polygons. A sample of training image is shown in Figure 3.6a. The output of the training step is shown in Figure 3.6b, where the image is classified into two classes of Building (shown in purple), and non-Building (shown in grey). However, classifying the image where various classes share similar colors, results in error and requires post-processing. In this case, some areas of bare lands were classified and identified as buildings due to similarity in their colors. In order to minimize the error, DSM data (Figure 3.6c) have been used and overlaid with the classified raster layer. This step involves trial and error as well as human interpretation. The result of the post-processing step illustrates features with height of over 1 m (Figure 3.6d).

(a)

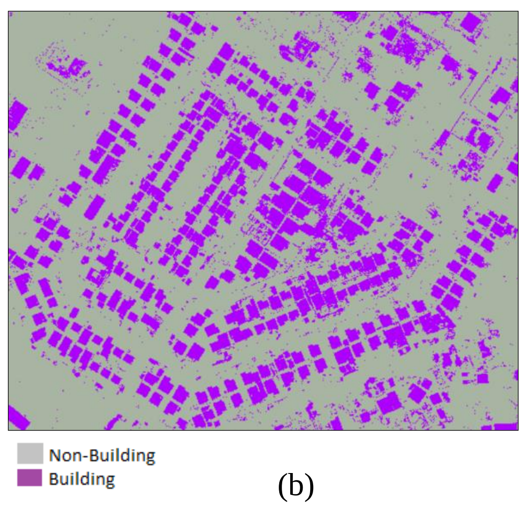

(b)

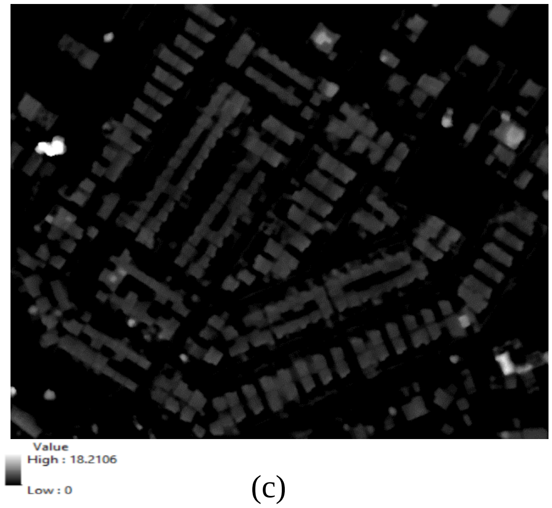

(c)

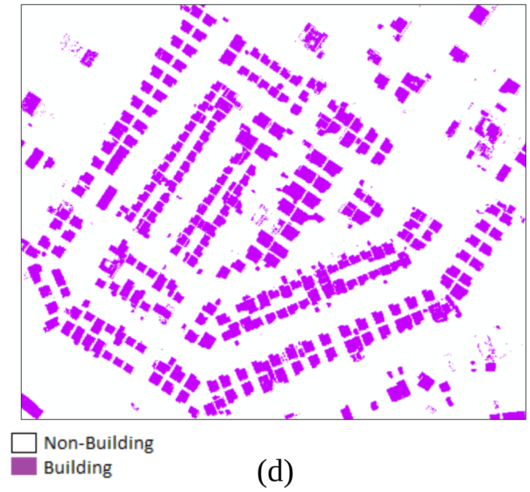

(d)

Figure 3.6. a) HR aerial image; b) Training land-use classes; c) DSM data; and d) Post-processes buildings result.

3.5.2 Machine learning

As the preprocessing step in Deep Learning method, the raw input images needed to be divided into smaller size. Although larger images cover more details, they negatively affect the efficiency by increasing the model input parameters and processing time. Therefore, in the training phase, original images were cropped into 3089 smaller images of size 384 x 384 squared pixels (Figure 3.8a), out of which 2310 images were used for training step, and 779 images were used for validation step. Using both input images (Figure 3.8a), and input shape file of the polygons (Figure 3.8c), the labels are then released as polygon shapes, and further transformed to 2-D labels of the same dimension as the input images to the algorithm, where each pixel is labeled as one of building or background (includes one or more of non-building objects such as vegetation, road, pavement, water, vehicles, etc.). In Figure 3.8, the red and black pixels in observed and algorithms output (Figure 3.8c, Figure 3.8d, and Figure 3.8e) denote buildings and background, respectively. For the first part of this research (preprocessing step), identification of building rooftops was done using human interpretation; which means a vast amount of manual work was done on interpretation and identification of targets (building rooftops) from other objects in aerial images, and their contours delineation. During the training stage, 75% of the input data were used to train the algorithm and 25% were used for the validation step. Performance of Adadelta and Adam algorithms during the training stage (training and validation steps) as well as the testing (on a different data set) step, is shown by Confusion matrixes (Figure 3.7a-f). Confusion matrix is a quantitative performance measurement for machine learning classification and shows how many predicted categories or classes were correctly predicted and how many were not. In this case two classes of Background (BG), and Buildings (BUI) were identified.

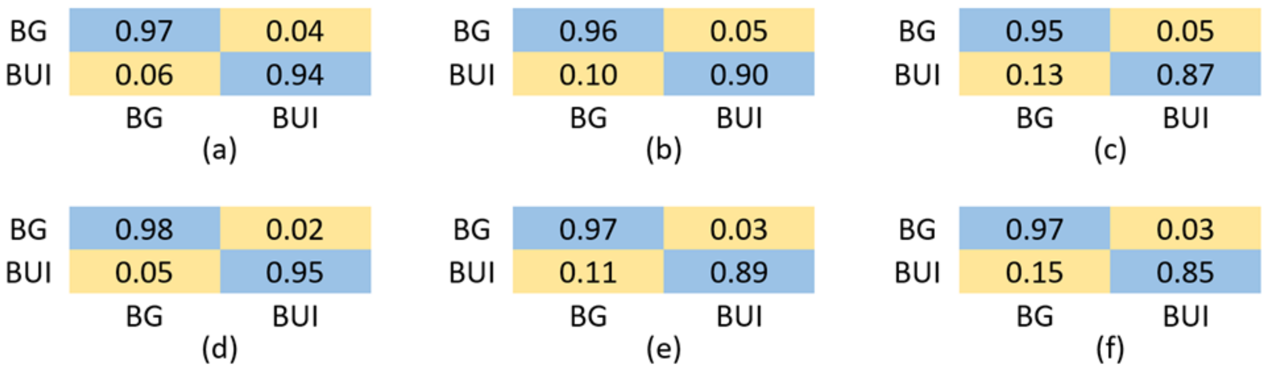

Figure 3.7. Adadelta algorithm performance during: a) Training, b) Validation, c) Prediction; and Adam algorithm performance during: d) Training, e) Validation, f) Prediction steps.

At the final step and in order to assess the final results, two parameters of Loss, and Accuracy are being calculated by the algorithm to compare the predicted data (output) with the observed data. Table 3.1 shows the average values for the Loss and Accuracy for the two algorithms used in this study.

Table 3.1. Loss function and Accuracy of Adadelta and Adam algorithms.

	Function	
Algorithm	Loss	Accuracy
Adadelta	0.080678	0.693074
Adam	0.053333	0.676982

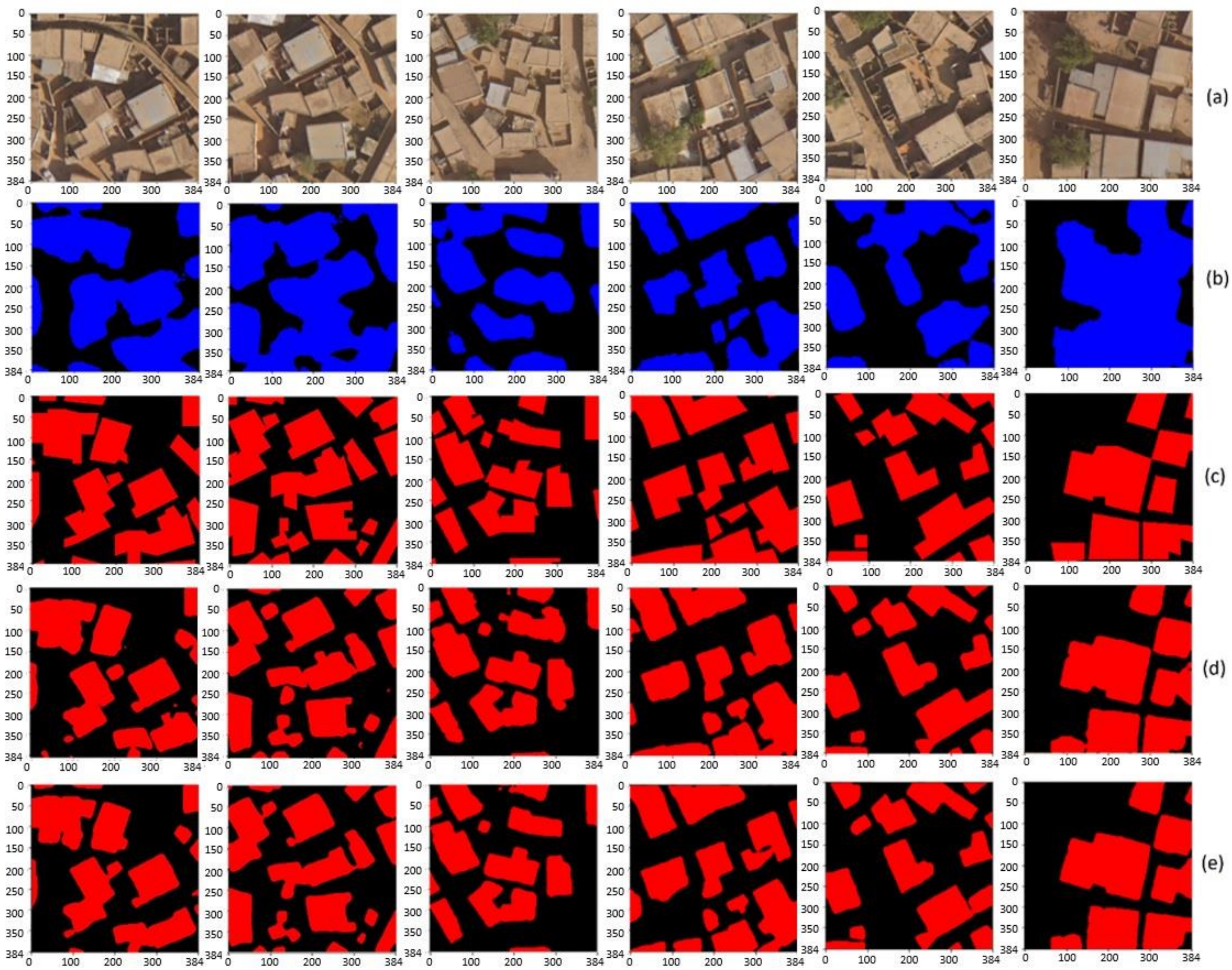

Figure 3.8. a) Aerial image segments, b) LIDAR point elevation data layer, c) Observed polygons, d) Adadelta algorithm output, e) Adam algorithm output.

The final output of the deep learning method consists of Building class objects. A sample of the input data, and the results of both algorithms are presented in Figure 3.8d and 3.8e. Similar to the final step in MLC method, the output raster files of DL method were converted to polygons in ArcMAP using the conversion tool. In Figure 3.10, building polygons are shown for the total study area. The average density in terms of square kilometer of residential area per square kilometer of the study area is 0.041 (Table 3.2).

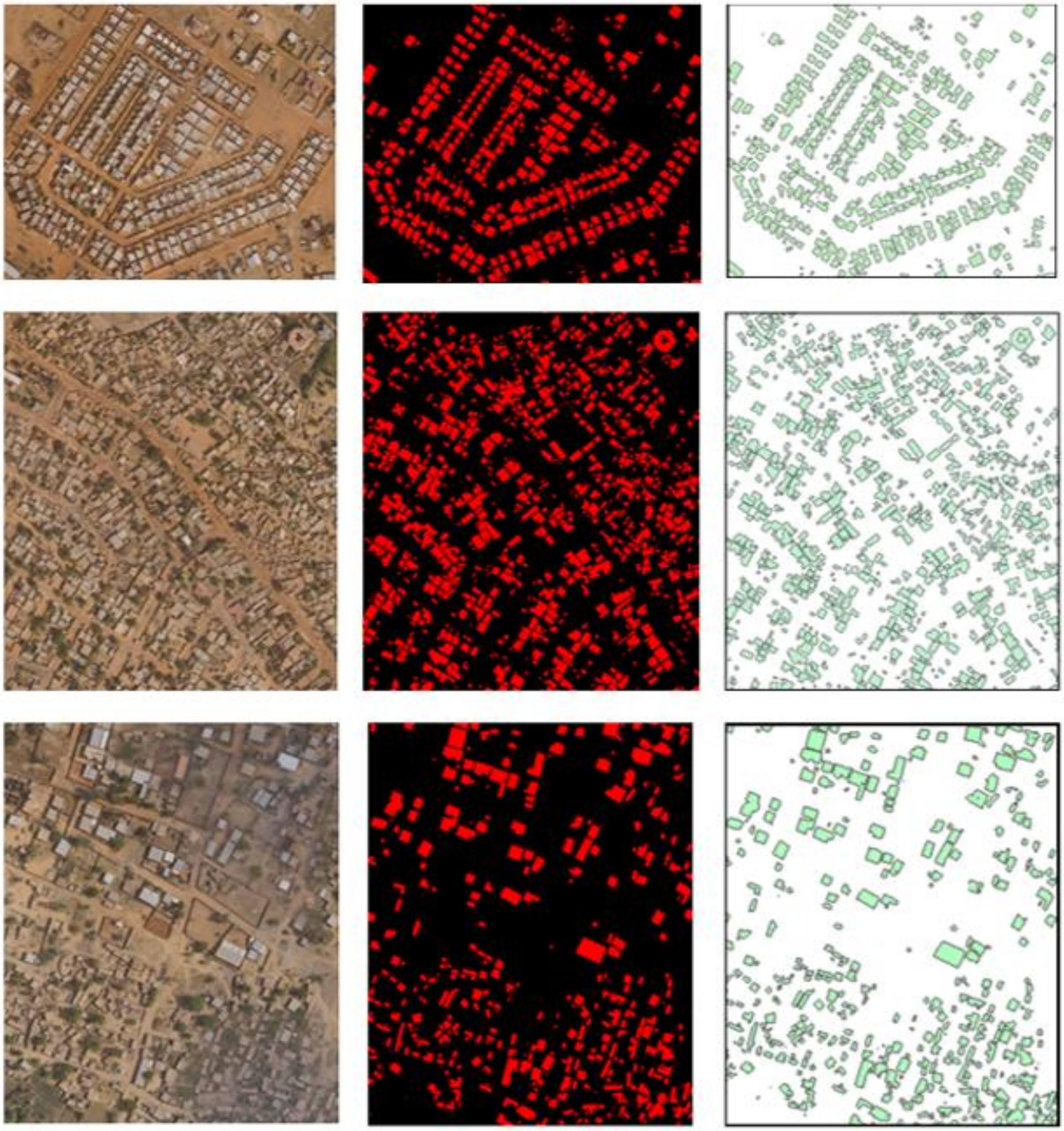

(a) (b) (c)

Figure 3.9. Experiment Results: a) Images in original testing set of Niamey area, b) The binary predictions by Adam algorithm, and c) Buildings' polygons.

Table 3.2. Density of residential area per square km of study area.

	Area	Unit
Total Study area	98.85	km^2
Residential area (polygons)	4.09	km^2
Density	0.041	km^2 Residential area/km^2 Study area

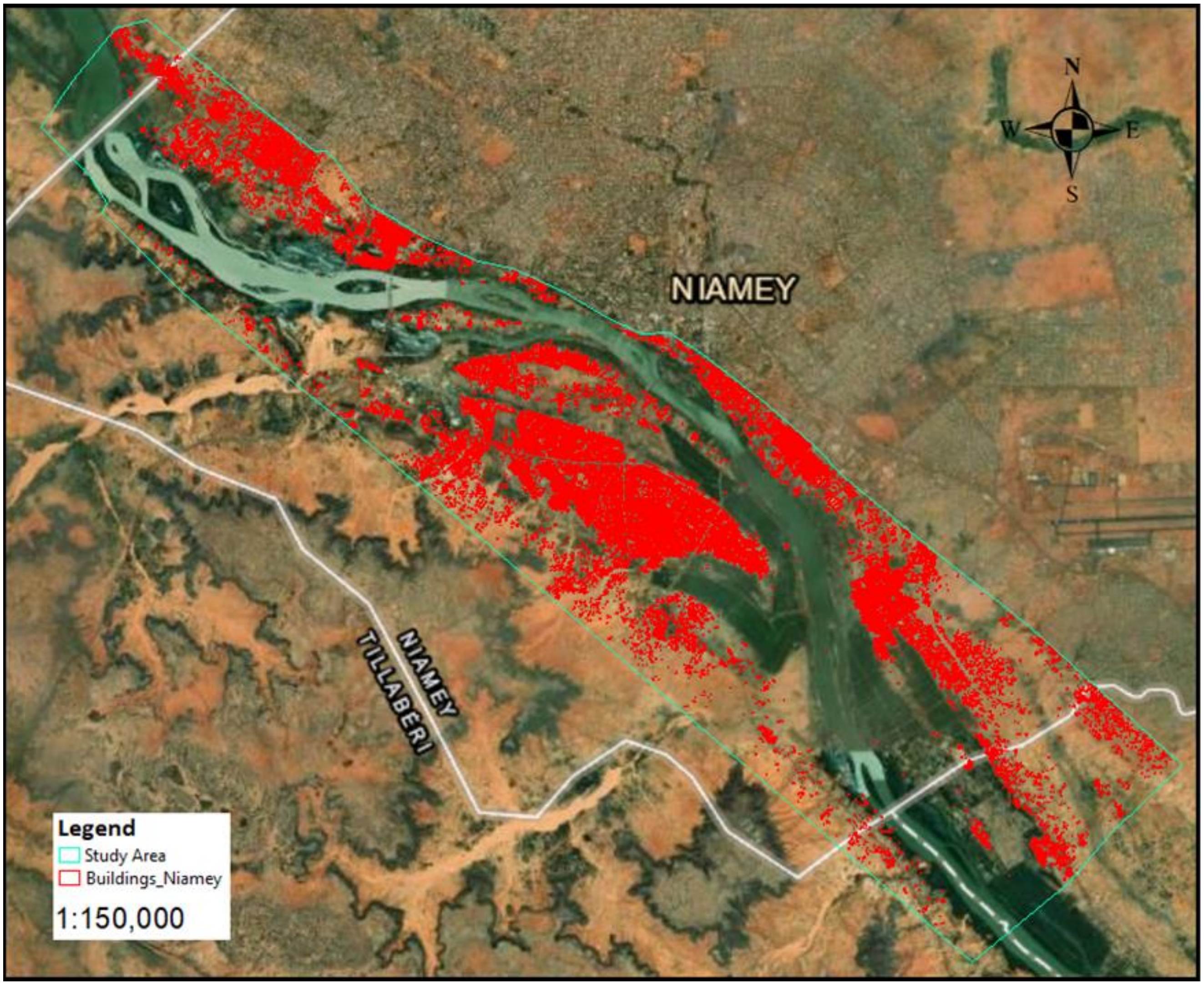

Figure 3.10. Extracted buildings in the study area.

3.6 Conclusion

The aim of this chapter was to investigate a feasible yet fast and precise method of extracting buildings from high-resolution aerial images. To achieve this goal, the possibility of applying an automated building detection technique was explored. The applied deep learning method showed promising results with high accuracy rate for the area of interest in this study. The model was able to identify the two introduced classes of Building and Background (non-building).

In multi-rooftop buildings, where identifying the actual size of the building with manual and Maximum Likelihood Classification methods would be very difficult, the Deep Learning method reported highly accurate results. However, tall trees have been observed as a major limitation and a problem in full-size roof detection of the buildings from very high-resolution aerial images. Therefore, in order to obtain more accurate building boundaries, the overall classification accuracy of the model needs to be improved.

The results of this study would significantly help in loss estimation to the buildings due to the yearly floods in the region of the interest, Niamey, Niger. However, since the buildings are of various type of material, having an accurate building database has a great importance in assessing the expected level of damage in the inundated area, especially to the critical buildings (hospitals, schools, research labs, etc.) in the area.

Chapter 4

Development of flood vulnerability curves using limited survey data[2]

4.1 Introduction

Floods are the most devastating natural disasters, causing more than USD 40 billion in damage worldwide annually (OECD, 2016). Despite emerging new technologies and advancements in research methods, flood damages are predicted to continue to grow (Kundzewicz et al., 2013). While economic damages are more critical in the developed world, socio-economic impacts are higher because of the lack of drainage systems and poor building standards. Niamey, Niger, is located along both sides of the Niger River and is exposed to yearly floods during the rainy season – May through October. During the most recent floods, caused by heavy rains, which began in June 2020, 65 people have died, and at least 432,613 people (52,404 households) have been affected (OCHA Niger, 2020). Therefore, city managers must understand the monetary and social impacts of floods in the city. It is essential to identify risk components to have a better assessment and management. The World Meteorological Organization (WMO, 2006) defines the risks as three elements: hazard, exposure, and vulnerability. Hence, a thorough risk assessment requires that each component in a given area be evaluated. Floods hazards in the city have been evaluated by Kheradmand et al. (2018) using 1-D hydraulic simulations and limited exposure data delineated from Google Map images. Flood exposure estimation were later performed using a more precise method (artificial intelligence) by which buildings were extracted from high-resolution aerial images of the study area (details of the approach, and the results are presented in Chapter 3). This

[2] Kheradmand, S., Seidou, O., Konte, D., and Barmou Batourec, M.B., 2021. Flood vulnerability derivation using Artificial intelligence and limited ground truth: a case study of the city of Niamey, Niger, West Africa. *Draft to submit to Journal of African Earth Sciences*.

section of the study explores the feasibility and capability of 2-D flood modeling (using HEC-RAS 2-D) in a data-scarce region. In flood forecasting studies, both one-dimensional (1-D) and two-dimensional (2-D) models have been widely used and showed satisfactory results (Horritt and Bates, 2002, Alfieri et al., 2014, Bates and de Roo, 2000, Di Baldassare et al., 2010, Domeneghetti et al., 2013, and 2015, Falter et al., 2013, Quiroga et al., 2016, Yang et al., 2006, Alzahrani, 2017, Rubiu 2018, Liu et al., 2019, Shustikova et al., 2019). Two-dimensional (2-D) numerical simulation has gained popularity in understanding flood events, and several research have been performed using 2-D simulations. HEC-RAS with 2-D capabilities, is one of the most popular models. In the following section, some of the studies which used HEC-RAS 2-D are presented.

Quiroga et al. (2016) applied HEC-RAS 2-D (version 5) to simulate the February 2014 flood event in the vast plains of Llanos de Moxos in Bolivian Amazonia. The geographic data used in their study was based on the Digital Elevation Model (DEM) from the Shuttle Radar Topography Mission (SRTM) with a grid cell size of 90 m. The flow data in the study includes 16 years of daily discharge from the Mamore River provided by the Flood Observatory. They simulated the floods for the period that was the most affected by the flood event (February 02, 2014 to March 02, 2014). The results of the applied numerical model in their study were compared with satellite image – Moderate Resolution Imaging Spectroradiometer (MODIS) of the flood event and shows good performance. In a recent study by Liu et al. (2019), 1-D and 2-D modules of HEC-RAS and LISFLOOD-FP were applied to four study reaches with different geometry, and the model performances were compared. Their land-use characterization set up the models by assigning distributed Manning's *n* values in a floodplain. Lateral structures linked the 1-D channel and 2-D floodplain using a uniform grid resolution of 30 m. Each model's performance was then compared by model simulated flood inundation extent with the reference flood map; 2-D models showed better results in their study. Shustikova et al. (2019) tested HEC-RAS 2-D and LISFLOOD-FP 2-D models on an inundation event, occurred on January 19, 2014, in northern Italy and compared the results of the two models. They used various grid sizes of 25, 50, and 100 m, generated from a LiDAR DEM of 1-m resolution. No 1-D component was included in the simulations since their study aimed to evaluate codes' ability to simulate inundation propagating over complex and highly anthropogenically altered topography. They concluded that the optimum solution for HEC-RAS would be the configuration of 1-m sub-grid terrain and 100-m mesh size, whereas the LISFLOOD-FP model performed better with a 50-m resolution. Also, HEC-RAS performed better at representing spatial distribution details (i.e., inundation boundary). They suggested using codes with simplified physics as a necessary tool for probabilistic/preliminary flood-risk assessment to avoid the computational cost. In another study, Rubiu (2018) used HEC-RAS to apply three models on the Minija river: a 1-D model for both river and floodplain; a combined 1-D-2-D model where River and floodplain were modeled in 1-D and 2-D, respectively; and a 2-D model for both River and floodplain. The results showed that more detailed information on flood propagation and velocities could be achieved using 1-D and 1-D-2-D models while all three models successfully reproducing a historical flood event and a reliable estimation of the inundation extent was provided by the models. However, computational time significantly varies from 1-D to a combined 1-D-2-D and 2-D models. Therefore, it is suggested to use a 1-D model where the primary research goal is determining maximum inundation extent. Alzahrani (2017) performed a study using HEC-RAS 1-D and 2-D models on the 7.38-miles reach of the Great Miami River and Bear Creek, Ohio, United States. They used two mesh computational resolutions of 80 × 80 feet (in GMR) and 20 × 20 feet (in Bear Creek). 2-D model's results proved to be better and more realistic than those of 1-D when compared with measured inundation extent from LiDAR topographic datasets.

The objective of this chapter is to develop flood loss exceedance curves and flood vulnerability curves using relatively low-quality data available in the city. Building polygons derived from high resolution aerial imagery using artificial intelligence (explained in detail in Chapter 3), are used in this study. Building material are assigned to the polygons using a limited (and spatially imprecise) ground survey data set. A HEC-RAS 2-D model of the study area is set-up and used to generate a set of 1000 probabilistic flood maps, which in turn are converted into loss exceedance curves for the city. following sections describe the study area, the general methodology, available data sets and finally the algorithms used to process the data and generate crucial vulnerability information. The implications for flood risk management as well as recommendations for vulnerability reduction are discussed.

4.2 Material and methods

4.2.1 Study area

Niger is located in the Sahelo-Saharan region of Africa and is characterized by an arid climate. Although recurring droughts constitute the main natural hazard, the country also faces frequent and sometimes catastrophic floods during the rainy seasons – May through October, with most rain in July and August. Therefore, climate variability has long been a challenge for the development of the region. Unpredictable dry and wet seasons and extreme weather events regularly devastate communities in Niger, one of the poorest countries. Rainfall in Western Sahel region, including Niger, increases, proceeding from the north of the country to the southern parts of it (Lebel and Ali, 2009). The yearly floods are mainly caused by the Niger River, which flows through the country's capital city, Niamey (Figure 4.1); many people are affected by the floods, and some lose their lives. Niamey is the capital city of Niger, also the largest and most populated city in Niger. With a total area of about 239.30 km^2, the city is located in the southwest corner between latitudes 13.29° N and longitude 2.09° E in Niger. Annual precipitation is around 570 mm – mean annual value between 1905 to 2003 at Niamey Airport (Descroix et al. 2012). Niamey's population (in 2021) is estimated at around 1.336 million (Populationstat.com Retrieved in July 2021). The majority of people are located along both sides of the Niger River. Their main activities are agriculture and fish farming; hence, they are more vulnerable to extreme weather and rising water levels.

Available topographic and imagery of the city generally comes from global data sets (e.g., Google Earth, Shuttle Radar Topography Mission) and does not have the adequate resolution for precise floodplain mapping and vulnerability estimation. The city does not have a GIS database of exposed assets. This study was only possible because in 2014, the Word Bank (WB) commissioned orthoimagery acquisition and the development of a high-resolution Digital Elevation Model (DEM) on a small portion of the urban footprint, shown in (Figure 4.1). In 2017, the WB commissioned a ground survey where the geographical location of exposed assets (buildings, municipal infrastructure, agricultural lands) in flood-prone areas were determined. Both data sets will be described in detail in the next sections.

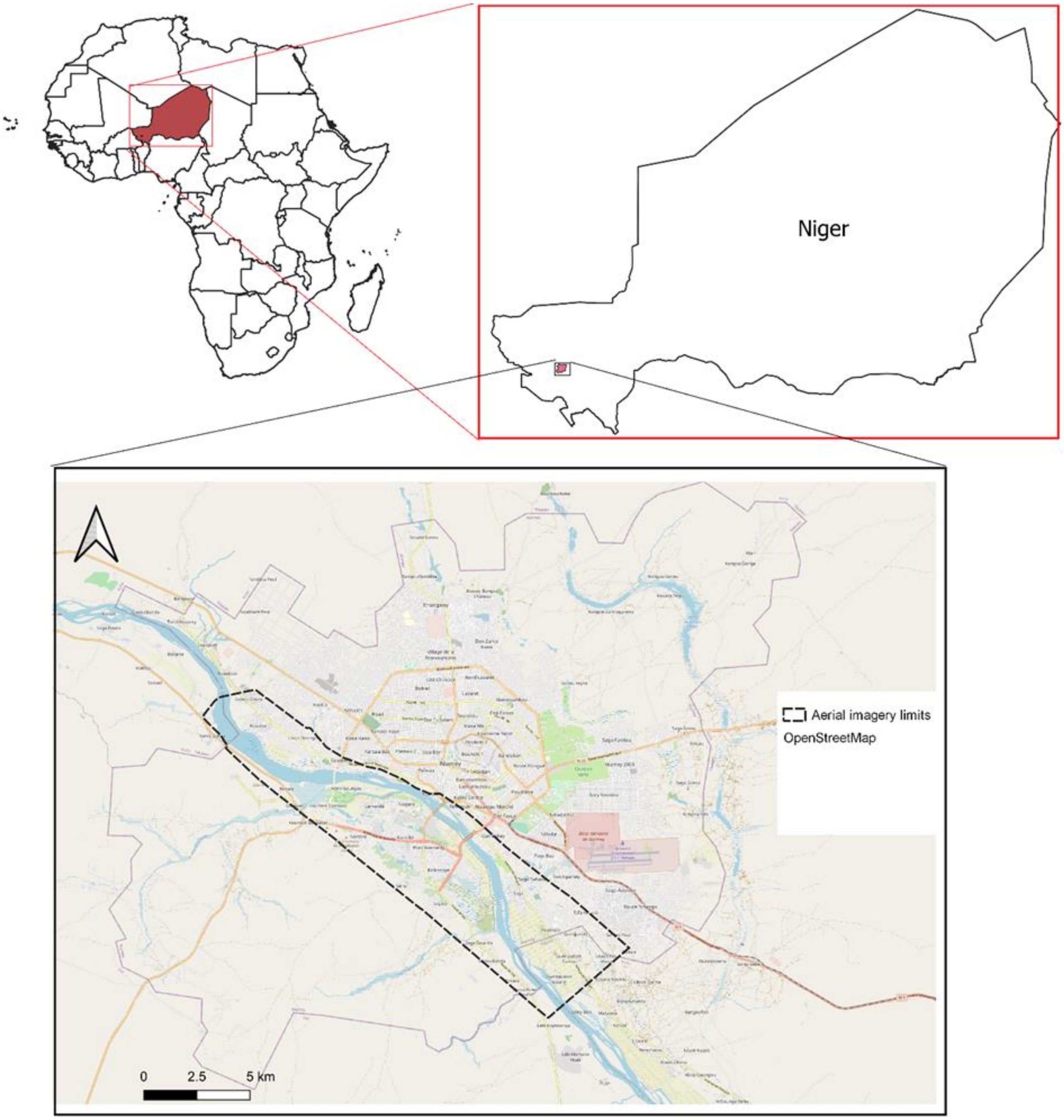

Figure 4.1. Study area and limits of available aerial imagery and high resolution DTM.

4.2.2 General methodology

The proposed methodology comprises three main parts of exposure quantification, hazard estimation, and flood loss calculation, which are described in detail herein, and is conceptually represented in Figure 4.2.

Exposure quantification

The initial step in exposure quantification is to detect and extract buildings from high-resolution aerial imagery of the area of interest, Niamey; for this purpose, artificial intelligence (AI) method was used (explained in detail in Chapter 3). The output of this step was the building polygons which were further processed using ArcMAP (the main component of ArcGIS software) to create GIS layer of building shapefile. The total area of the polygons was used as the total residential buildings when calculating flood losses. Moreover, another parameter in flood loss estimation to residential building, is the construction material type. Therefore, a probabilistic approach (inverse distance weighting) has been applied on the available ground survey data of the study area to calculate the probability that each building detected belongs to a particular type of material in the region. More details on ground survey data, and the applied probabilistic approach are presented in Sections 4.2.4 and 4.2.7, respectively.

Hazard estimation

At the next step, probabilistic set of flood maps, were generated by forcing a HEC-RAS model with a stochastically generated ensemble of flood peaks representing the river regime at Niamey. Accordingly, statistical distribution functions were applied on flow data from one hydrometric station at Niamey region, and peak discharge values for the Niger River watershed, within the study area were calculated. The calculated extreme flowrates were then given to the hydraulic model, HEC-RAS, in order to determine the associated water level. Results were, subsequently, converted to the floodplain map associated with each return period.

Flood loss calculation

At the last step and in order to estimate the possible economic losses induced by various flooding scenarios happen in the defined area, total loss was calculated. The loss was estimated based on vulnerability functions, damage criteria for residential land-use class, and various type of buildings' material (CAS - informal material; BAN - mud wall; SDU - mud walls with concrete cover; DUR – concrete; or a combination of different material estimated based on IDW method). More details on loss functions developed in this study is presented in Section 4.2.8. Estimated average annual losses (in thousand West African CFA franc) as a function of building construction material, were illustrated by loss exceedance curves (more details in Section 4.3.2).

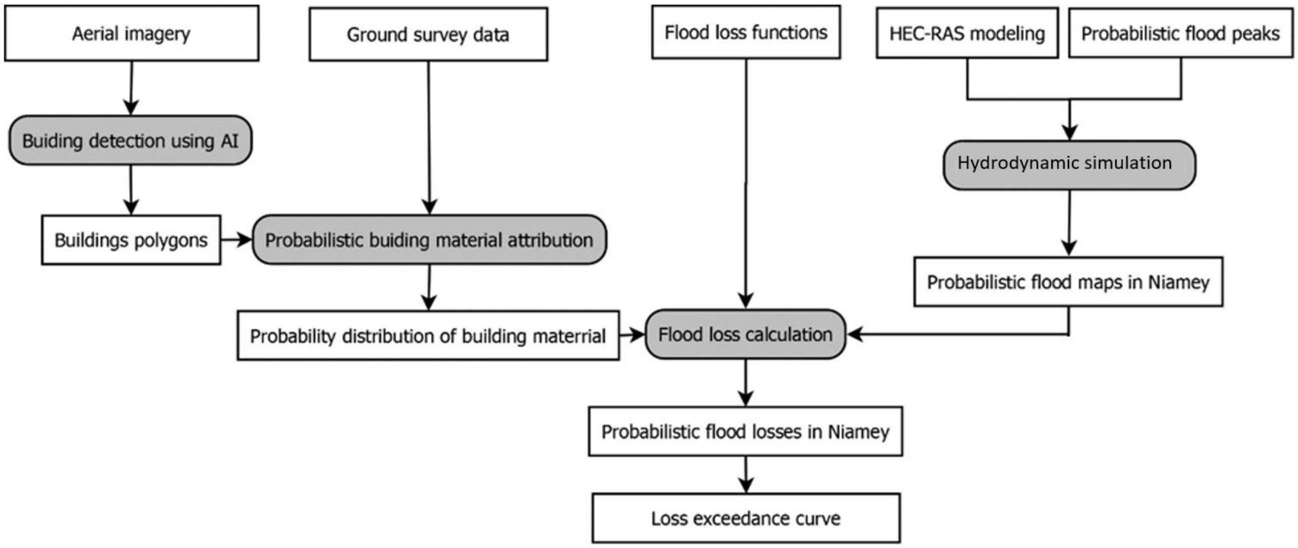

Figure 4.2. General methodology.

4.2.3 Aerial imagery

The data used in this study consist of orthomosaics and a Digital Surface Model (DSM) of an approximately 98.85 km^2 (22.47 km long and 4.40 km wide) band of land along the Niger river in Niamey. The orthomosaics and the DSM were acquired in 2014 using Ultralight Airplane and Photogrammetry. The dataset contains the elevation data of the elements of the natural terrain, vegetation, and the buildings as a set of 3-D points. Characteristics of the images and the covered area are presented in detail in Chapter 3, Section 3.2.

4.2.4 Ground survey data

The survey took place between August 28 and September 28, 2017. Two teams each composed of 10 investigators and a supervisor traveled through the flood-prone areas and gathered a certain amount of socio-economic information using the GeoODK mobile application (GeoMarvel, 2017). The geographic information collected is of point type (latitude, longitude). The information collected depends on the type of infrastructure. In the case of buildings, the information collected includes the use of the building (commercial, residential), the number of occupants and the material used to construct the walls. A total of 27,296 points were collected of which 12,944 are buildings with information on the type of building material (Figure 4.3). Unfortunately, due to the imprecision of the GPS of the mobile phones used, it is not possible to assign a polygon among the buildings to each point in the survey. This is why a probabilistic approach has been developed in this article to calculate the probability that each building detected belongs to a particular type of material. The approach adopted is presented subsequently in section 4.2.7.

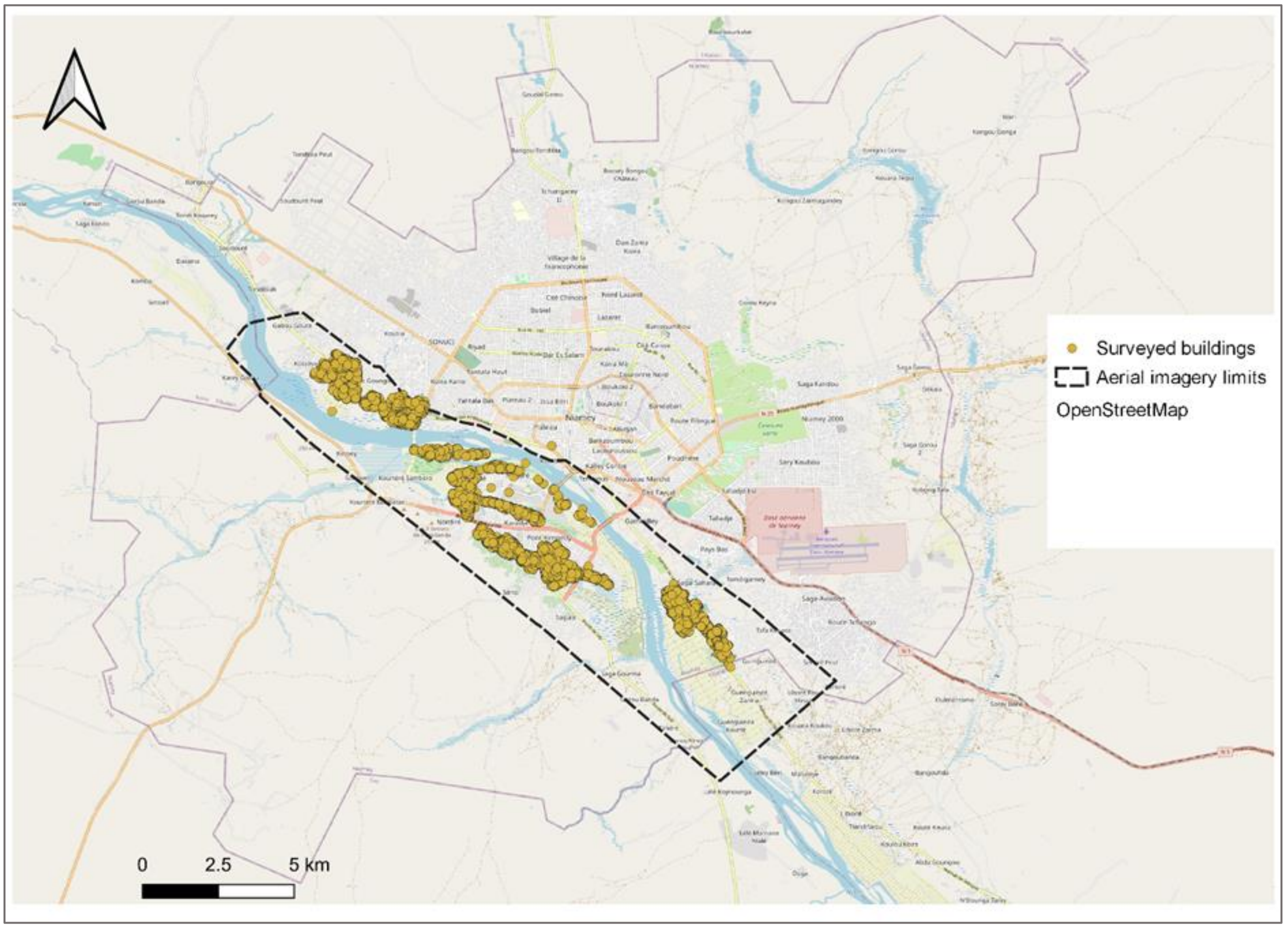

Figure 4.3. Surveyed buildings.

4.2.5 Exposure quantification

In order to quantify the exposure (here residential buildings), artificial intelligence (AI) method was used; for this purpose, a deep learning (DL) method was applied to extract building from the aerial raster images in the area of interest, Niamey, Niger. The main steps include preprocessing the data (identifying the buildings in the aerial images of the sample area, and saving polygon shapefile for training step, and dividing the images into smaller segments), applying the deep learning algorithms to the raw data, exporting binary images from the algorithms, and converting raster binary images to polygon shapefiles using vectorization tools in ArcMAP. Further details are explained in Chapter 3 - Methodology section. Also, the results of building detection using deep learning method are presented in Chapter 3 – Results Section.

4.2.6 Hydrodynamic modelling

In the current study, the hydraulic model HEC-RAS 2-D was selected, which is a widely used computer program for modelling the hydraulics of water flow in natural or artificial river channels and floodplains. The HEC-2 model was originally developed by the United States Army Corps of Engineers (ACOE) Hydrologic Engineering Center (HEC) in 1970s, and later in 1995 was upgraded to HEC-RAS with an easy-to-use graphical user interface. The program is designed to calculate water surface profiles for steady, gradually varied flow in natural or constructed channels, and can handle a number of hydraulic computations in a single run. It can be applied to floodplain management to delineate flood hazard zones.

The computational procedure for 2-D modeling is based on solution of the shallow water equations, which are derived from the conservation of mass (Eq. 4.1), and momentum equations in the x and y-direction (Eq. 4.2 and Eq. 4.3):

$$\frac{\partial H}{\partial t} + \frac{\partial (hu)}{\partial x} + \frac{\partial (hv)}{\partial y} + q = \theta \qquad (4.1)$$

where, t is time, q is the source/sink term, and u and v are velocity components in x- and y-directions, respectively. H is the water surface elevation and is defined as the sum of the surface elevation $z\ (x, y)$ and water depth $h\ (x, y, t)$.

$$\frac{\partial HU}{\partial t} + \frac{\partial HU^2}{\partial x} + \frac{\partial HUV}{\partial y} = \frac{\partial HT_{xx}}{\partial x} + \frac{\partial HT_{xy}}{\partial y} - gH\frac{\partial z}{\partial x} - \frac{\tau_{bx} + \tau_{wx}}{\rho} + D_{xx} + D_{xy} - \Omega HV \qquad (4.2)$$

$$\frac{\partial HV}{\partial t} + \frac{\partial HV^2}{\partial y} + \frac{\partial HVU}{\partial x} = \frac{\partial HT_{yy}}{\partial y} + \frac{\partial HT_{xy}}{\partial x} - gH\frac{\partial z}{\partial y} - \frac{\tau_{by} + \tau_{wy}}{\rho} + D_{yy} + D_{yx} - \Omega HU \qquad (4.3)$$

where x and y are Cartesian coordinates, t is time, H is depth of water, U is depth average velocity of water in the x-direction, V is depth average velocity of water in y-direction, θ is net mass input (rainfall + exfiltration – infiltration), z is WSE (bed elevation + h), g is gravitational acceleration,

$T_{xx,xy}$ is depth average turbulent shear stresses, $D_{xx,xy}$ is dispersion terms, $\tau_{bx,by}$ is bed shear stress, $\tau_{wx,wy}$ is wind shear stress, and Ω is Coriolis parameter.

The application of the St. Venant equations in flood routing involves solving them simultaneously down the length of a stream channel. Discrete solution over a grid and iteration are the two major processes in the computational process in solving the St. Venant equations. HEC-RAS uses an implicit finite-difference scheme in the stage of discretization to determine the new values of water level and discharge at a discrete point based on all discrete points and with at least two time steps solved simultaneously. This implicit scheme is found more stable than other explicit schemes. Solving the implicit equations requires an iteration approach, which means that at a given time step, successive solutions of water level and discharge are obtained until the difference of the latest values and the values from the previous iteration is small enough. Thus, it is regarded to have converged on the correct value.

Solving the 2-D Saint Venant flow equations requires more computational power and thereby results in longer run times. In addition, the 2-D Saint Venant flow equations can become numerically unstable in regions of the 2-D mesh where the water surface profile or flow direction is changing rapidly. To avoid an unstable model, a finer mesh and a corresponding smaller time step will need to be used. Some of the situations where the Full Momentum computational method should be used includes: Dynamic flood waves (i.e., dam failure, rapid rise and fall); Sudden expansion or contraction of flow with high velocity changes; Detailed flow solutions around hydraulic structures and obstacles (i.e., bridge openings, piers and abutments).

The main objective of the program is to compute water surface elevation at cross-section locations of interest along River or stream, for given flow values. Data requirements include flow regime, starting elevation, flow rate, roughness, cross-sectional geometry, and reach length. The domain of the HEC-RAS model is exactly the extent of the high resolution DTM (Figure 4.4a). The model also contains four flood protection dikes (Figure 4.4a), and one submerged weir used to maintain water levels high enough for the municipal water management plant. The land use (Figure 4.4b) was obtained from the European Space Agency (ESA) Prototype Land Cover 20 m Map of Africa (ESA, 2017). The topographical data (Figure 4.4c) comes from World Bank (2014). The bathymetric data is the same as the one used in Kheradmand et al. (2018).

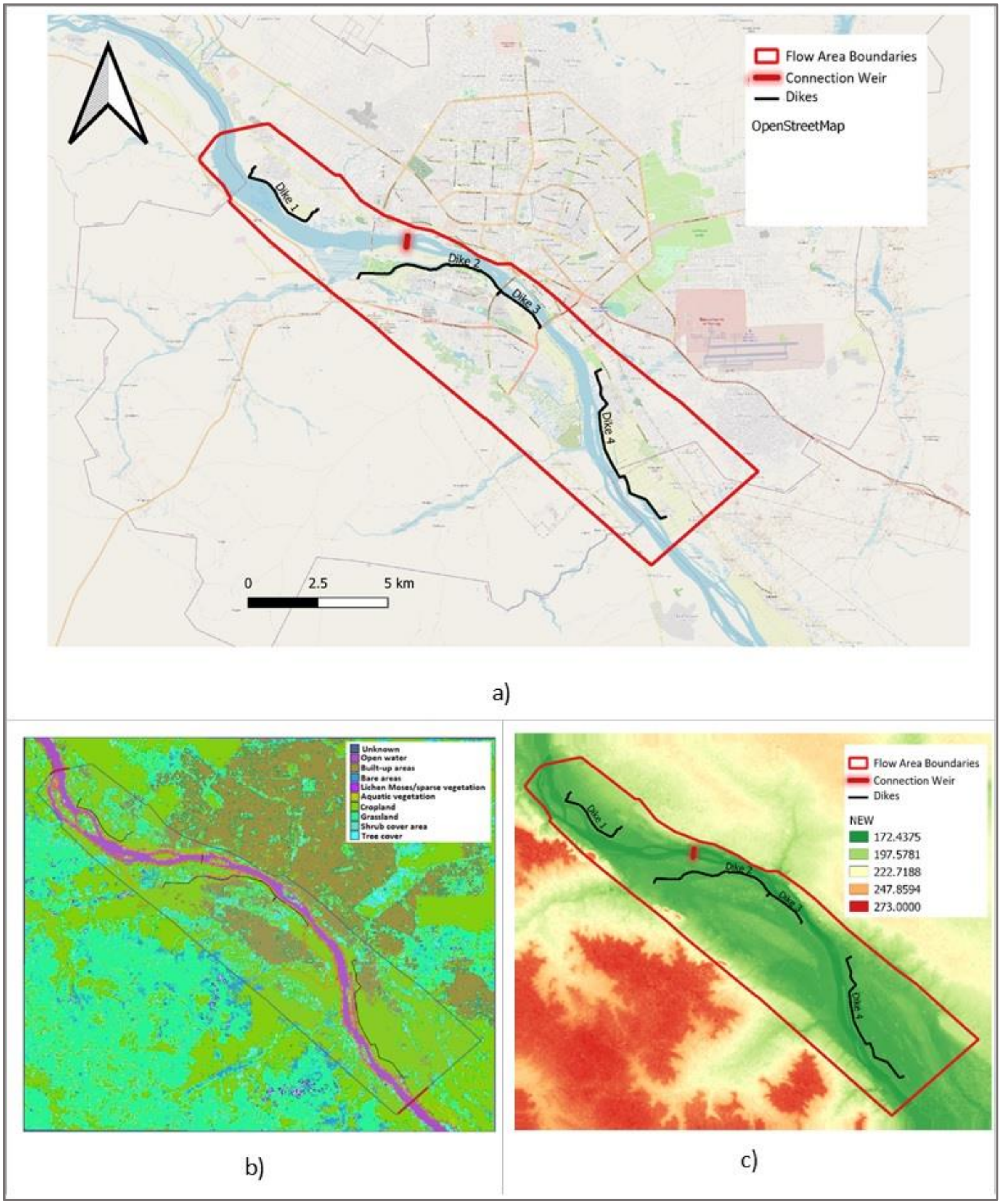

Figure 4.4. a) HEC_RAS model domain and hydraulic structures; b) land use map; c) topographical map.

A number of break lines representing riverbanks, inlands, major streets in the flood plain as well as hydraulic structures were added to the model (Figure 4.5a). A regularly spaced 30 m grid was generated on the model domain (Figure 4.5b, c, and d).

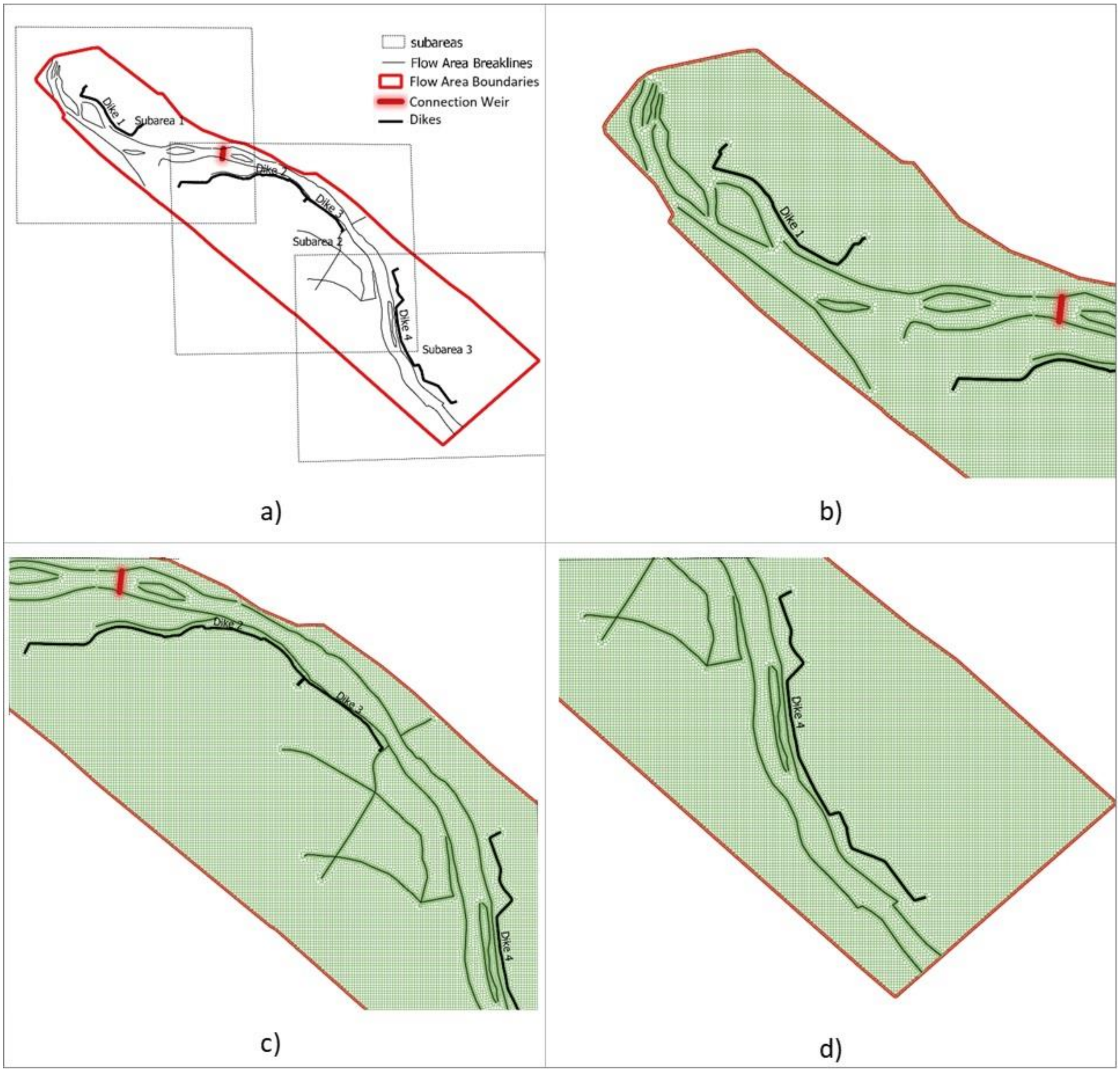

Figure 4.5. HEC-RAS model break lines and grid.

The HEC-RAS model was set-up with the following parameters. The crest of the submerged weir was set at 179 m. The four dikes in Niamey regularly undergo deterioration due to floods and vandalism, as well as emergency repairs. Their crest has an elevation that vary along the dikes, and constantly changes. Figure 4.6a-d show profile of the dikes in the study area. For the sake of this exercise, the crest is set as max (182 m, natural terrain elevation). The manning coefficient in the floodplain is a function of the land use. The association between the manning coefficient and the land use is shown in Table 4.1.

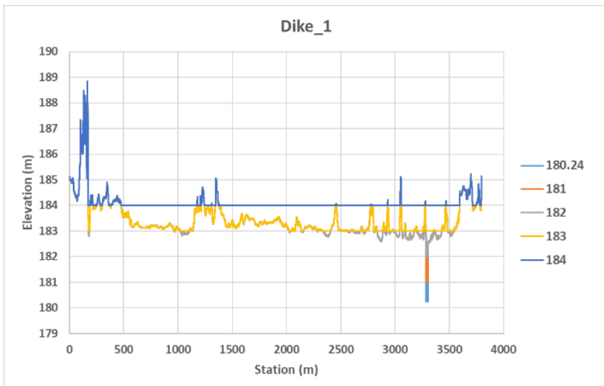

(a)

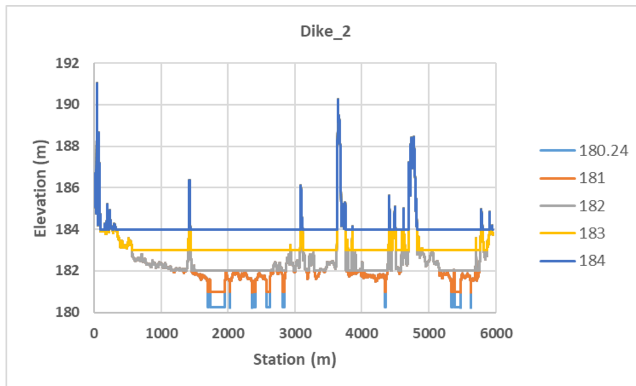

(b)

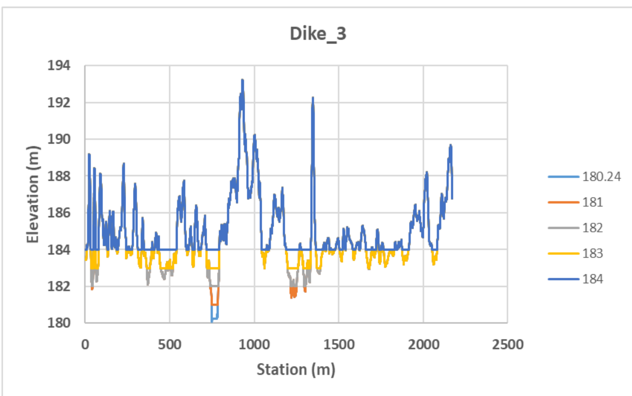

(c)

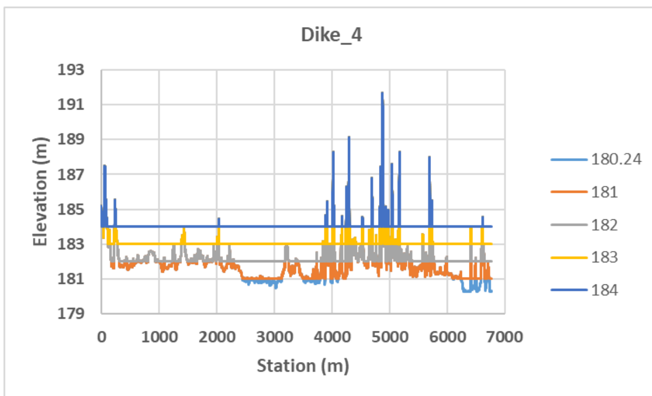

(d)

Figure 4.6. Dikes' profile in the study area: a) Dike 1; b) Dike 2; c) Dike 3; and d) Dike 4.

Table 4.1. Manning coefficient associated with land uses.

Class	Description	Manning n
0	NoData	-
1	Tree Cover	0.4
2	Srub cover area	0.4
3	Grassland	0.368
4	Cropland	0.3
5	Aquatic vegetation	0.04
6	Lichen Moses/sparse vegetation	0.182
7	Bare area	0.04
8	Built-up areas	0.06
9	Open water	0.03
10	Unknown	0.03

The inflow is a triangular hydrograph going from 0 m^3/s to 3000 m^3/s in 12 days. The upstream boundary condition is the incoming flow and a bed slope of 0.089%, measured from the bathymetric data. The outflow condition is a normal depth condition with a slope of -0.039%, measured from the terrain model. Digital terrain model with 50 m resolution was used in the 2-D model set-up. Once the simulation is completed, a series of 1000 flood maps, corresponding to the 1000 peaks flows developed in Kheradmand et al. (2018) are extracted. Kheradmand et al. (2018) sampled the 1000 peak flow from a Gamma distribution fitted to the 1980-2014 annual maximum flows at Niamey. The resulting 1000 maps will hence represent the flood regime in Niamey.

4.2.7 Building material attribution – probabilistic approach

To identify the material of the buildings in the study area, Inverse Distance Weighting (IDW) interpolation technique was used. This technique is widely used due to its robustness and simplicity and is a quite popular and a simple way to apply Tobler's law (Babak and Deutsch, 2009). It works by using an unbiased weight matrix based on the distances from an unknown value to known values. Weights may be defined in several different ways. Using the neighboring points allow us to interpolate a value based on distance. IDW method has been applied in the current study to estimate the material for a given building based on the surrounding known buildings' material. For this purpose, the existing point values from the survey, which represent the buildings' material, were taken and weighted according to their distance from digitized buildings in the study area. Various exponents (0, 1, 2, 5 and 10) for the inverse distance method were used to see the difference; and it is minimal.

As shown in Equations below, type of material for each building is determined as follows:

$$D_i = \sum_{j=1}^{n} \frac{1}{d_j^n} \tag{4.4}$$

$$P_i = \frac{D_i}{D_{BAN} + D_{DUR} + D_{SDU} + D_{CAS}} \tag{4.5}$$

where, i is the type of building material: BAN (mud walls); DUR (concrete walls); SDU (mud walls covered by mortar); and CAS (informal constructive – a mixture of sundried clay and straw), D_i is sum of inverse squared distance of a building with material of type i to all other buildings with the same type of material, d_j is the distance between any two building of the same material, and P_i is the probability of a building having type i material, and n is the exponent value (0, 1, 2, 5 and 10).

4.2.8 Flood loss functions

The flood loss functions used in this study were developed by Kheradmand et al. (2018) for four types of material: CAS (informal material), BAN (mud wall), SDU (mud walls with concrete cover) and DUR (concrete). In this study, a building cannot be classified in a single class – it rather has four probabilities (summing to 1) of being CAS, SDU, DUR or BAN. Accordingly, loss in terms of amount of damage as a function of water height, is calculated using the following equation (Eq. 4.6):

$$Loss = A \times \sum_{mat \in \{CAS,BAN,SDU,DUR\}} p(mat) \times value\_m_{mat}^2 \times f_{mat}(h) \tag{4.6}$$

Where, A is area of the building, $p(mat)$ is the probability for the building to be of a given material ($mat \in \{CAS, BAN, SDU, DUR\}$), $value\_m_{mat}^2$ is monetary value per square meter of the area based on the type of the building material, and $f\_mat(h)$ is the loss fraction which is a function of water height (h) at the building and is defined according to the type of the building material. It is worth to mention that in this study only direct tangible losses were considered when estimating the flood loss in the area of interest, Niamey. Also, human casualties were not taken into account.

4.3 Results

4.3.1 HEC-RAS modelling

The HEC-RAS model was run for 12 days using a variable time step (between 5 s and 5 min). In order to check how the model performs in the study area, the predicted extent of the inundation in floodplain and observed flood map (from the 2020 flood season) are compared in Figure 4.7, where green polygon indicates the simulated flood map in the current study, using HEC-RAS 2-D model, overlaid onto orange polygon which shows the observed extent for the 2020 flood.

Results show that the developed model in this study provided an accurate estimation of the inundation extent, and successfully reproduced the flash flood flows and water surface levels resulted from the 2020 flood season. Although the developed model tends to identify less flooding than the observed extent on floodplain, it is suitable, to an acceptable degree, for predicting and assessing flood risks in the study area. The observed error could be attributed to the limitations such as scarcity and low quality of the available data, limits of historical data on past flood losses as well as long-term hydrological data for the study area.

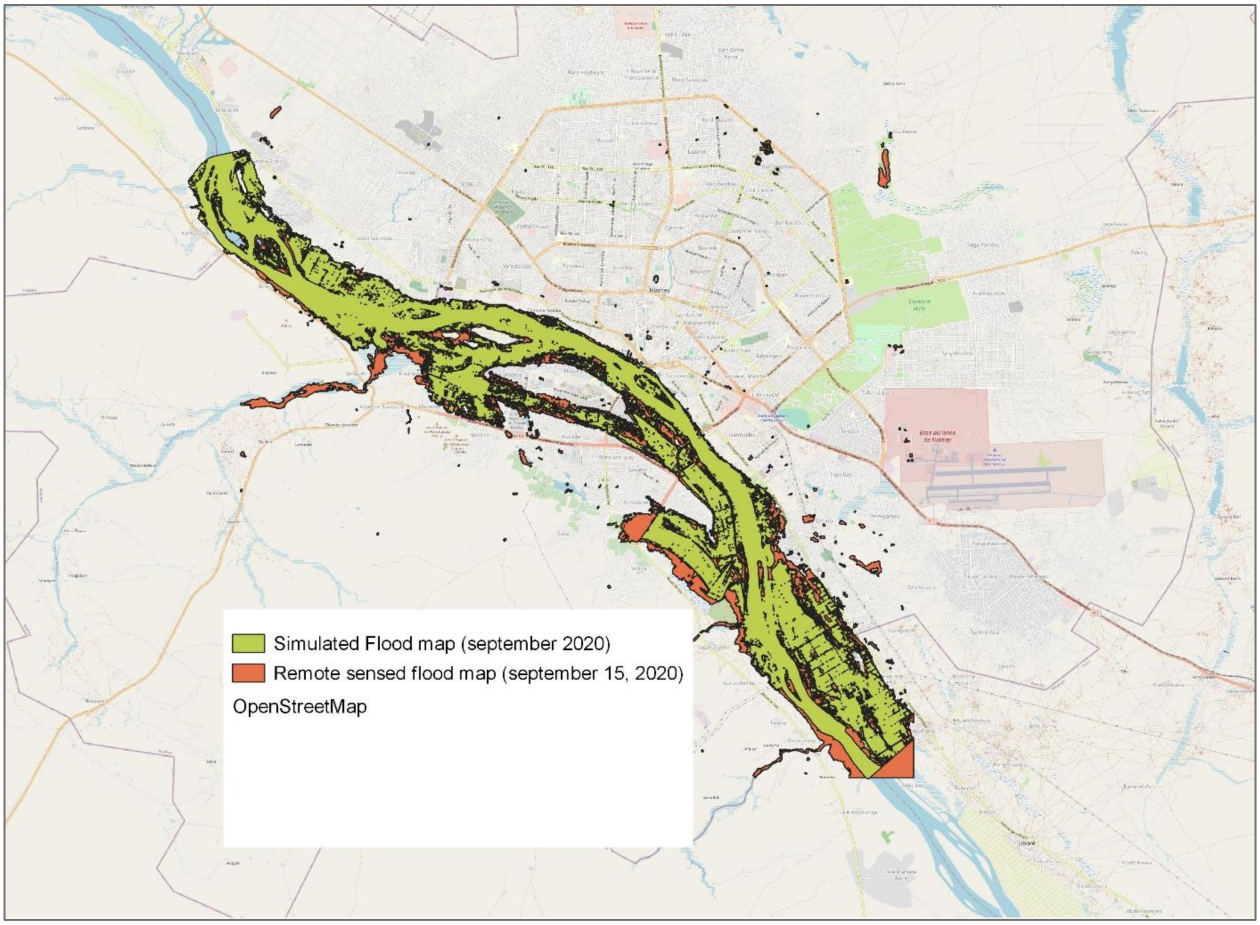

Figure 4.7. Simulated versus observed flood maps in September 2020.

4.3.2 Loss exceedance curves

Figure 4.8 and Table 4.2 show estimated average annual losses (in thousand West African CFA franc) as a function of building construction material. The scenarios for building construction material consider 100% of the buildings in the area to be of: Mud walls (BAN); Concrete walls (DUR); Mud walls covered by mortar (SDU), Informal constructions – a mixture of sundried clay and straw also known as Banco (CAS), or a combination of different material estimated based on Inverse Distance Weighting method (the method has been explained in detail in section 4.2.7). The current dike height is 182 m for four available dikes. Location of the dikes is shown in Figure 4.4.

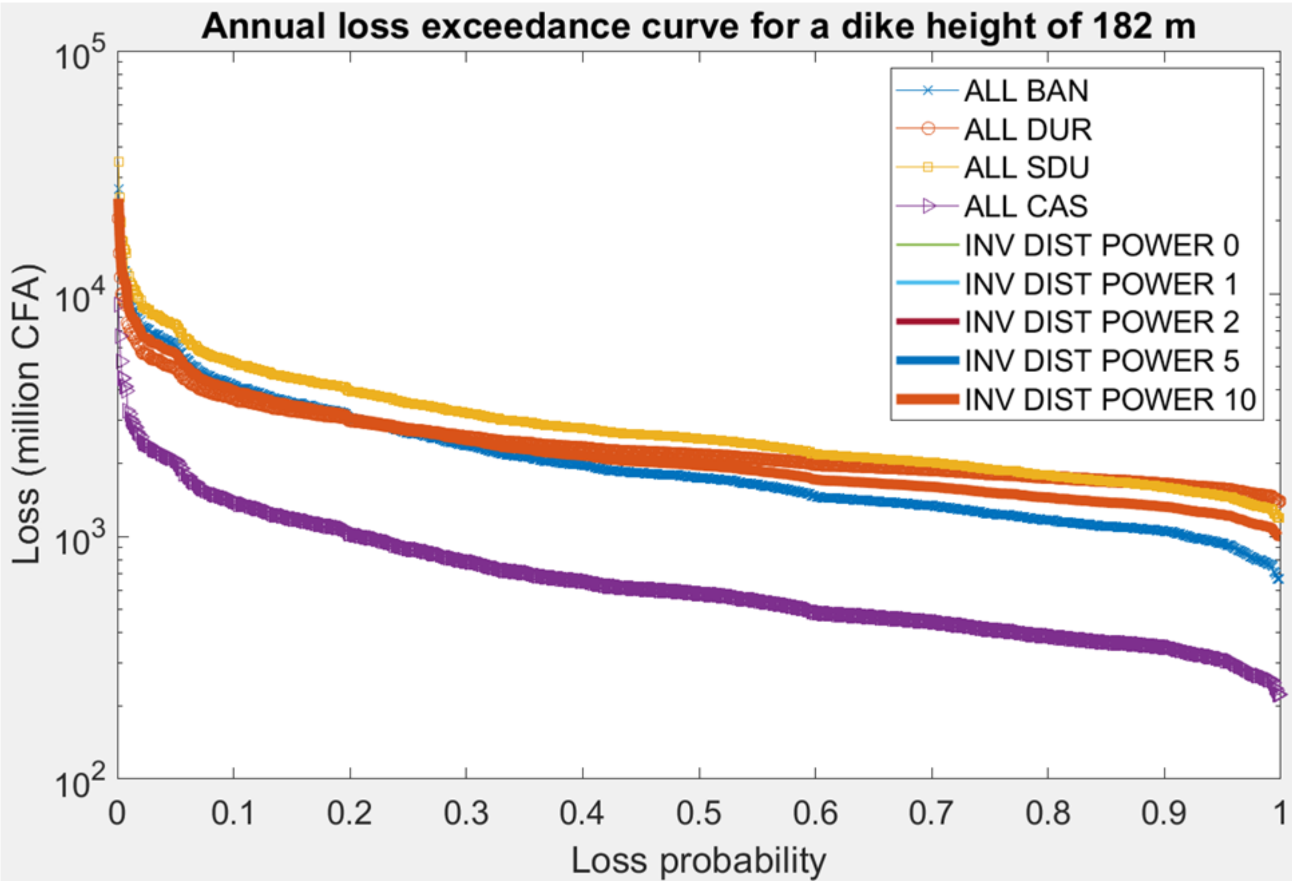

Figure 4.8. Annual loss exceedance curve as a function of building construction material for the reference situation (dike height =182 m).

Table 4.2. Average annual loss (in thousand CFA[a]) for different dike crest height and building construction material.

Minimum dike crest height, m	**Scenarios**								
	All SDU[b]	**All DUR[b]**	**All CAS[b]**	**All BAN[b]**	**IDW[c] (0)**	**IDW (1)**	**IDW (2)**	**IDW (5)**	**IDW (10)**
182	314,319	251,979	77,598	232,793	244,176	244,180	244,184	244,197	244,220

[a] West African CFA franc.

[b] Mud walls covered by mortar (SDU); Concrete walls (DUR); Informal constructions (CAS); Mud walls (BAN).

[b] Inverse Distance Weighting method using various exponents (0, 1, 2, 5 and 10).

As seen in Figure 4.8, using various values for exponent when applying IDW method, does not make any significant changes. In this Figure, the lines corresponding to exponent values of 0, 1, 2, 5, and 10 are overlapped due to similar values. Difference in losses for other scenarios (all BAN, all Dur, all CAS, and all SDU) also reflects the difference in the applied depth-damage curves for each material; hence, improving buildings' material to concrete will show an increase in losses due to the higher value of the concrete compared to other materials. It is worth to mention that, in addition to the feasibility assessment of various mitigation measures, the effect of such measures on human casualties should also be considered.

4.4 Discussion

Climate change is already altering weather patterns which makes floods and droughts more common and more severe. But it also makes them much harder to predict. Around the world, floods devastate millions of lives, undermine the economy and add more challenges to water management. Natural disasters such as floods, can disrupt the country's trade, and destroy infrastructure as well as transport networks, hence, significantly impact Gross Domestic Product (GDP) in the impacted regions. GDP which represents the overall market value of all the goods and services a country produces, is one of the most common indicators used to gauge a country's economic health.

Resilience to such hazards demands joined-up thinking from policymakers, and land, water, and urban managers to take care of water services and resources continuously, especially in transboundary water management. Better preparation for flooding will lead to more impactful future investments and help governments achieve the sustainable development goals. Therefore, it is important for water managers to determine the level of risk, assess planning options, and better prepare for flood hazards especially when population increase leads in faster growth in the number of people living in flood-prone areas.

The objective of this study was to develop flood loss exceedance curves and flood vulnerability curves for city of Niamey. However, given the scarcity and low quality of the available data, limits of historical data on past flood losses as well as long-term hydrological data for the study area, the authors took probabilistic approach to develop a methodology to generate loss exceedance curves despite low quality data. Results show that losses are distributed throughout the city, and only a fraction of residential areas are protected by the dikes. Therefore, the available dikes seem to be mainly considered to protect agricultural lands from flooding. Since, in the current study, only residential land-use class was considered, the results do not reflect the total loss, including flood damage to agricultural crops in the study area.

The 1000 flow used in Kheradmand et al (2018) are anterior to 2014. Since then, large and sometimes catastrophic floods have occurred in 2017, 2019 and 2020. The statistical analysis (and hence the 1000 maps) may not be representative of the current flood regime and should be updated. Because of the climate change and sedimentation in the Niger river, flood regime is actually nonstationary. A nonstationary flood analysis coupled with the methodology developed in this study may help provide a more accurate picture of the changing flood risk in the study area.

The findings of the current study must be seen in light of some other limitations such as: lack of consideration of variations in hydrological conditions e.g., climate change projections, which requires availability of long-term data; rainfall-induced losses were not taken into account; in order to generate vulnerability (depth-damage) and accordingly, loss exceedance curves, a number of assumptions were made based on expert judgement; moreover, the digital elevation model used to characterize dikes' height in the study area, do not represent the most recent terrain changes, especially after the 2020 floods.

The abovementioned limitations may have impacted the interpretation of the findings and should be taken into account in future works.

4.5 Conclusion and recommendations

A methodology was developed in this study to generate loss exceedance curves using imperfect data. Given that the geographical information in the ground survey data is too imprecise to associate a collected point to a building polygon, inverse distance weighting with various exponents were used to evaluate the probability of each building in the floodplain to belong into one of these four categories: Mud walls (BAN); Concrete walls (DUR); Mud walls covered by mortar (SDU), Informal constructions-a mixture of sundried clay and straw and is also known as Banco (CAS). A HEC-RAS model was used to generate 1000 maps representing the flood regime in the study area. The probabilistic information on building material and loss curves were used to derive loss exceedance curves for the city of Niamey. Results show that the exponent in the IDW algorithm has a very little impact on the loss exceedance curves. Therefore, using exponent value of 2, the common value in literature (Babak and Deutsch, 2009), is being suggested when applying

IDW technique in future studies. Results also show that residential losses are spread throughout the city and that the current configuration of the dikes seems to be designed to protect agricultural lands rather than residential buildings. If nothing is done, the changing hydrological regime may lead to even more catastrophic losses.

Chapter 5

Assessment of two flood mitigation options for the city of Niamey[3]

5.1 Introduction

The Republic of Niger, West Africa, is located between the Sahelian zone and the Sahara desert. It is at the same time one of the driest countries and the most vulnerable to floods. It often experiences intense rainy seasons lasting for two to four months depending on the region. Niamey, the capital city, located on the banks of the Niger River, is in the Middle Niger River basin. It is exposed to both pluvial and fluvial flooding. The Niger River hydrograph has two flood peaks: the local flood (also known as red flood), occurs between August and September. The Guinean flood (also known as black flood) occurs during the rainy season, June to September (Descroix et al., 2013). The city has incurred several extreme flooding events, caused by heavy rainfall, coupled with rising water levels in the major river basins, during the last decade. The reason for the observed increase in the frequency of the flooding events is not known with precision. However, several researchers attribute it to the changes in the hydrological regime and hydroclimatic behavior of the Niger River since the end of the great droughts of the 1970s (Massazza et al., 2021; Descroix et al., 2012). Moreover, in the absence of proper land-use planning, the impacts of flooding are expected to rise due to population growth which causes a higher number of people living in the flood-prone areas, i.e., riverbanks. In 2020, the western region of Niger, including Niamey, has been hit by days of heavy rain starting in June. Accordingly, the Niger River in Niamey reached its all-time highest levels and overflowed. The flood event claimed 65 lives,

[3] Kheradmand, S., and Seidou, O., 2021. Assessment of two flood mitigation options for the city of Niamey. *Draft to submit to Journal of African Earth Sciences*.

affected more than 50,000 houses, left 53,000 people homeless, and caused the displacement of more than 225,000 people. It also caused many rice fields being submerged (OCHA Niger, 2020).

A study performed by Austrian flood expert Prof. Günter Blöschl from TU Wien (Vienna) in collaboration with 34 research groups shows that the past three decades were among the most flood-rich periods in Europe during the past 500 years (Vienna University of Technology, 2020). It also states that, compared to the past, floods tend to be more prominent in many places, the timing has shifted, and the relationship between flood occurrence and air temperatures has reversed. The future trend of extreme floods, and flood-related impacts in West Africa, has been studied by several researchers (Aich et al., 2016; Amogu et al., 2010; Descroix et al., 2009, 2012, and 2018; Fiorillo et al., 2018; Massazza et al., 2019, and 2021; Nka et al., 2015; Tarhule, 2005; Wilcox et al., 2018). Therefore, with the current hydrological changing trend, if nothing is done in the region, more catastrophic events will happen in the future. Moreover, increasing the frequencies of extreme events will reduce the rehabilitation time for the region. Most of these areas are particularly vulnerable because of the high poverty levels, aggravating flood risk, and adverse impacts. Various measures can be taken to prevent flooding of rivers. The strategy taken in Niamey to reduce its vulnerability and mitigate the risk to the lives and properties was constructing dikes along the Niger River. Currently, there are four dikes in the Niamey area, two dikes on each of the right and left banks of the Niger River which are designed to protect the area from flooding. However, the extreme floods in 2012, 2019, and 2020 overwhelmed the dikes in the area, indicating the necessity of the strategies to be re-evaluated.

At the end of August 2020 and the beginning of September 2020, heavy rains have caused flooding across Niamey, followed by rising water levels of the Niger River and breaching the dikes in the right riverbank of Niger River in Niamey. Thousands of houses in the districts of Nogare and Lamordé were reported to be inundated. The districts of Banga Bana, Karadjé, Kirkissoye, and Saguia were also affected. Several roads in the affected areas have also been rendered impassable due to floodwaters, hampering disaster response efforts and hindering overland movements. Local communities residing along Niger's main rivers are more exposed to flood hazards. The lack of means and funds to effectively reduce the impacts of flooding has significantly increased the vulnerability of local communities. The flooding event in August 2020 led to the overtopping and partial collapse of the dikes after several days of water rising beyond record levels (Figure 5.1a, b).

In this chapter, the benefits of two previously proposed adaptation options (increasing dikes' height, and improving buildings' material) are examined.

5.2 Study area

The study area in this chapter is the green polygon in Figure 5.2b and covers the affected area in the flood event of September 2020 (Nogare and Lamordé). The study area is only being protected by two dikes: Dike 2 and Dike 3 (Figure 5.2a).

(a) (b)

Figure 5.1. a) The August flood broke the record level of the Niger River; b) Dikes were overflowed after several days of heavy rain (CLIMATESERVICES.IT).

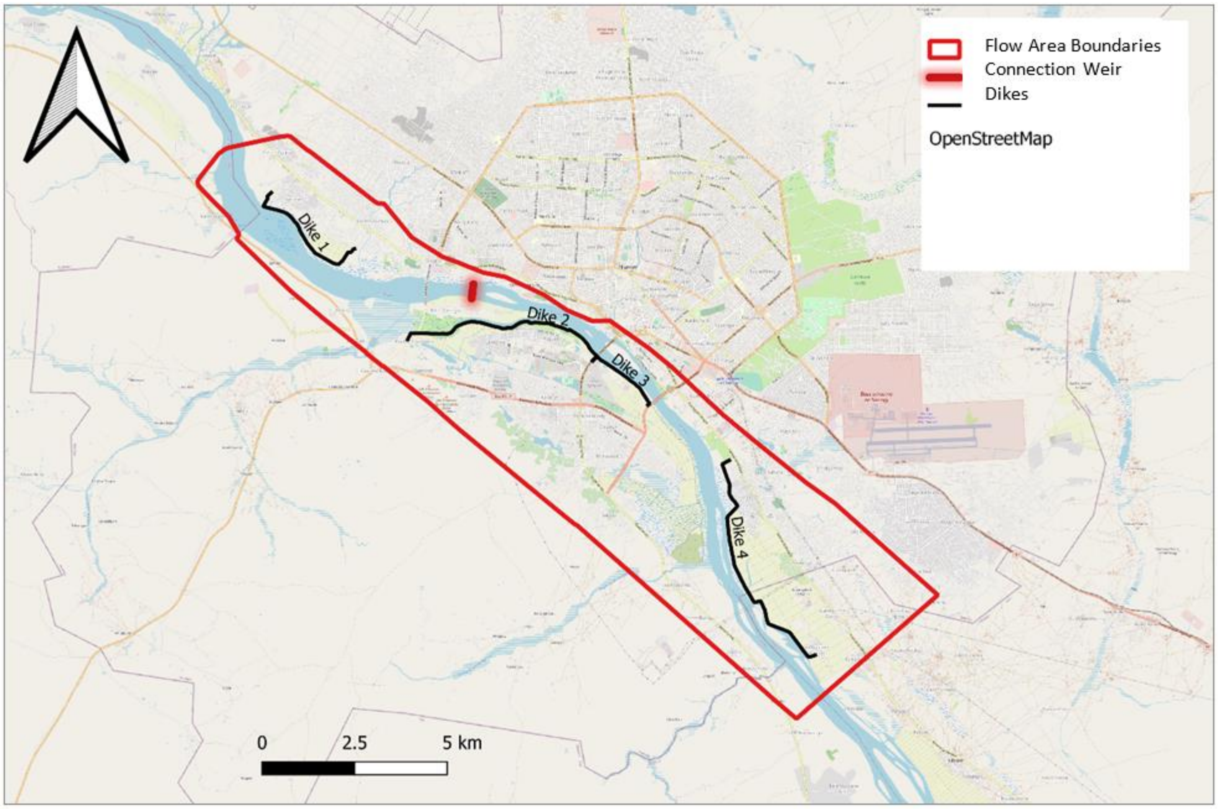

(a)

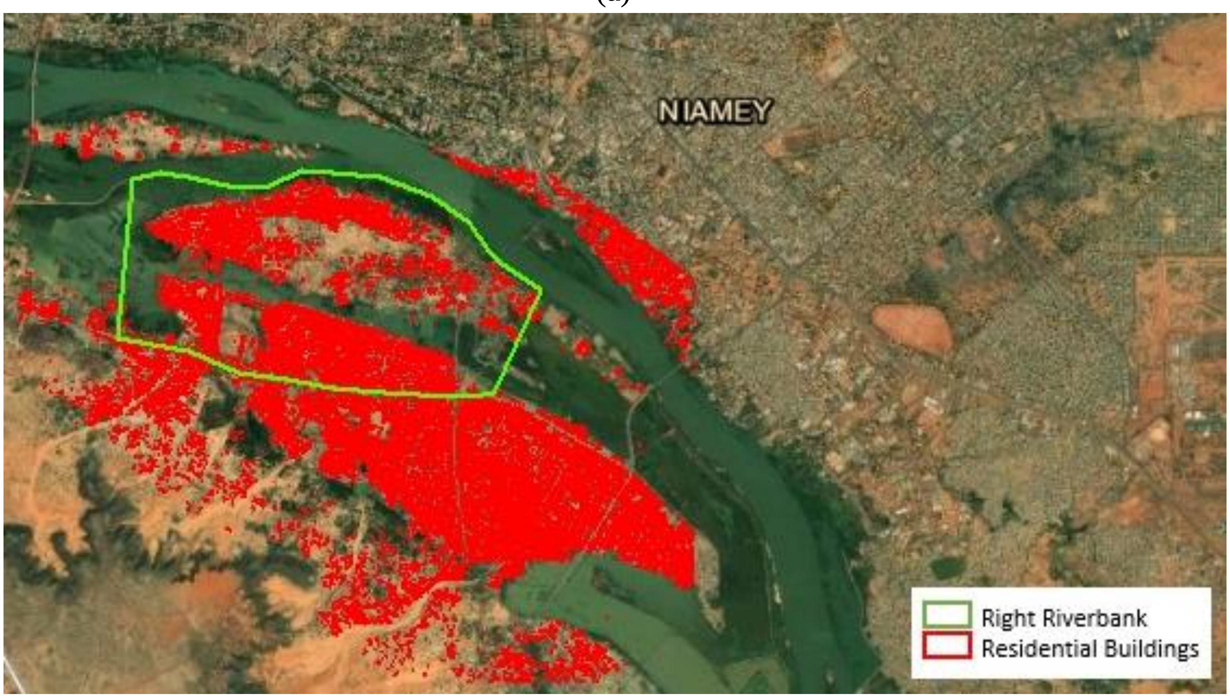

(b)

Figure 5.2. a) Dikes' locations in the study area; b) Right riverbank of the Niger River, Niamey, Niger, West Africa.

5.3 Adaptation options

Climate change is causing significantly more frequent and more extreme flooding, especially in densely populated areas of the world. Moreover, the flooding magnitude has changed over the last few decades due to the increase in precipitation. Therefore, existing flood control measures may not perform as expected in the future. Various adaptation and risk management options could be taken by the communities at risk to improve their resilience and prepare for extreme flood events. The possibilities involve efforts to modify and strengthen the environment subjected to flooding. The general goal of implementing any adaptation options is to mitigate hazard risk and its adverse impacts in the affected areas. Since flood risk assessment includes flood hazard, exposure, and vulnerability, increasing or building resilience in the hazard-prone communities and accordingly decreasing the risk could be effectively done by improving all or any risk components. Finding the right approach to ensure sufficient preparedness requires more strategizing and planning and taking several factors into account, especially for poor communities. A huge budget needs to be spent by the governments to mitigate the adverse effect and minimize the damage and losses of floods. Given that resources are limited, the budget depends on the estimation of the cost of, and the expected benefit from the action taken. While short-term strategies are being implemented to help address current flood concerns, they should also align with long-term strategic directions.

According to the definition by the United Nations Office for Disaster Risk Reduction (UNDRR, 2021), risk management measures could be structural and/or non-structural. Structural measures are any physical construction used to reduce or avoid potential impacts of hazards, or any engineering techniques or technology applied to achieve hazard resistance and resilience in structures or systems. Examples of such measures include flood management systems (dikes, dams, flood levies, ocean wave barriers, spillways, etc.), earthquake-resistant construction and evacuation shelters. On the other hand, non-structural measures are measures do not involve any physical construction. Instead, they use knowledge, practice, or agreement to reduce disaster risks and impacts, and manage vulnerability. Examples include policies and laws, flood warning systems, public awareness-raising, training and education such as building codes, land-use planning laws and their enforcement, research and assessment, information resources, and public awareness programmes. While structural measures are designed to reduce flood hazards, non-structural measures focus more on reducing exposure and vulnerability elements of risk management.

In most cities in developing countries such as Niamey, poor governance and spontaneous development due to rapid growth and urbanization increase the vulnerability, hence worsening the flood consequences. Moreover, increasing urbanization, especially in riverbanks, increases the runoff instead and decreases the storage capacity of the land. In such flood-prone areas where loss level is directly proportional to the area’s level of vulnerability and exposure, growing vulnerability to floods could be related to various economic, social, cultural, political, and environmental drivers. In the case of Niamey, several other causal factors of vulnerability played a role in in diminishing resilience and capacity to cope with and adapt to the extreme events, such as: the lack of proper runoff collection systems, the use of low-strength constructional material in the residential areas which are mainly located in the vicinity of the Niger River, the mismanagement in the exploitation of the land mainly in more vulnerable regions on sides of the rivers, and the lack of enough disaster recovery and rehabilitation time due to yearly flooding in the area . The most commonly encountered buildings’ materials in Niamey are informal straw walls, mud walls, concrete walls, and mud walls covered by mortar. There are also some temporary houses, which are inappropriate in terms of resiliency towards floods.

The prevalence of this house type is possibly its low cost, since most of the inhabitants are seasonal settlers who are reluctant to invest in the construction of more durable houses. In such places where implementing strategies to keep people away from the hazard-prone areas seem unrealistic, our proposed adaptation options in this study aim to assist decision-makers in choosing the best practices to mitigate flood risks. After the catastrophic floods of 2012, most of the houses made with mud walls were destroyed in the study area. Populations in the most affected areas were offered the option to relocate elsewhere, but a significant number of households chose to rebuild their houses on the same site. The majority of people are located along both sides of the Niger River, and their main activities are agriculture and fish farming. Therefore, in this study, the impact of undertaking such options in the area of interest, on total loss estimation for residential land-use classes was also considered. The proposed adaptation options in this study are more to resist environmental change to preserve existing infrastructures.

The proposed adaptation options aim to mitigate the risk by decreasing all three risk components in the current study. The two proposed adaptation options include a) Increasing dike height and b) Improving or rebuilding the residential buildings. Option a) will decrease both hazard (water height in this case), and exposure (the number of areas being inundated) in case of extreme flooding events. Figure 5.3 shows the various height values considered for two available dikes in the right riverbank of the Niger River. The heights range from 180.24 to 184 m at 1 m intervals. Option b) aims to decrease the vulnerability of the exposed buildings in the affected areas. The dikes' crest has an elevation that varies along the dikes because of the natural terrain. The minimum height has been measured to be 180.24 m. Each of the proposed alternatives in option a) consists of increasing the minimum elevation of the dike to a certain height *h*. Therefore, the dike height variable considered in this section ranged from 180.24 m to 184 m, at a 1 m interval (Figure 5.3). Of course, when the dike crest is set to *h*, portions of the dike are higher due to the elevation of the natural terrain. The second variable (building material) is considered to be any of: CAS: Informal constructions – a mixture of sundried clay and straw and is also known as Banco; BAN: Mud walls; DUR: Concrete walls; and SDU: Mud walls covered by mortar. The effect of implementation the abovementioned adaptation options in the right riverbank of Niger River were evaluated and the results are presented in subsequent sections.

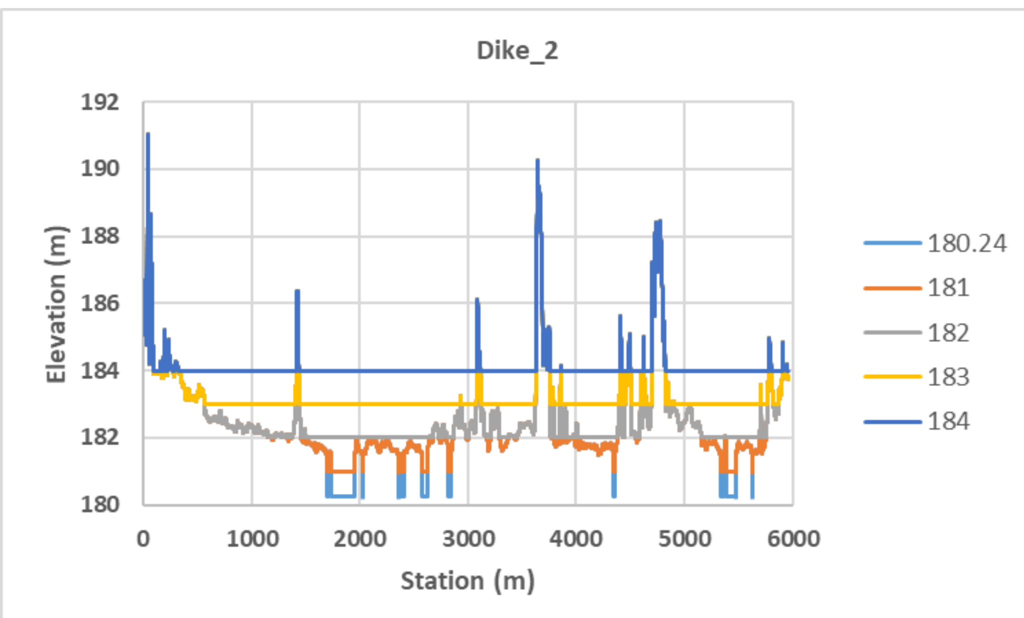

(a)

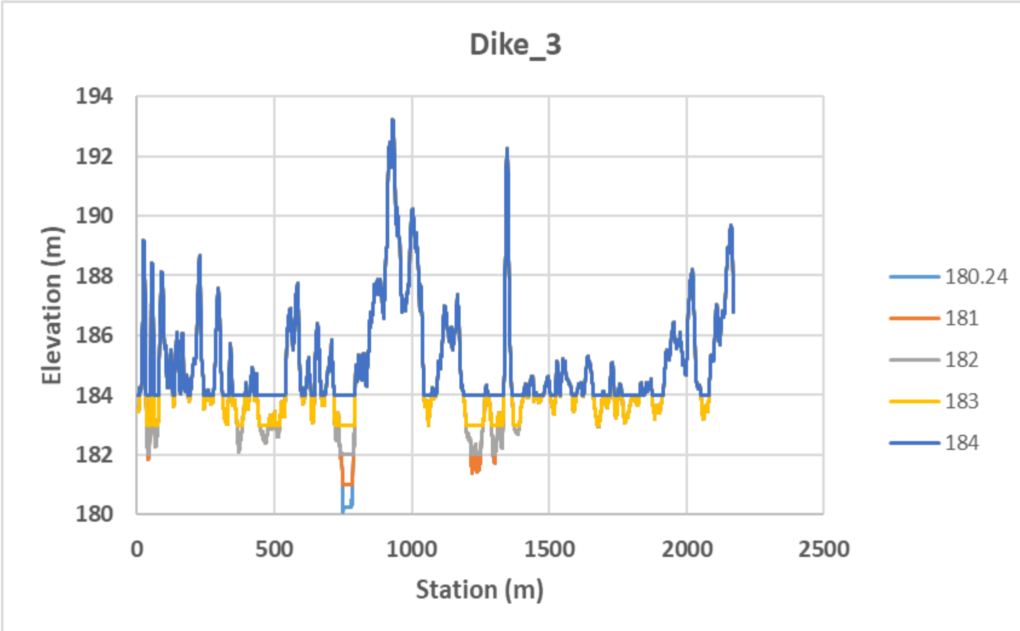

(b)

Figure 5.3. Dikes' profile in the right riverbank of the Niger River: a) Dike 2; b) Dike 3.

5.4 Flood loss and adaptation option benefits estimation methodology

The general methodology used in this section of the study is similar to what has been considered in Chapter 4. It includes flood hazard, exposure, and vulnerability components of flood risk estimation for the right riverbank of the Niger River within the area of interest, Niamey. For the flood hazard part of the methodology, the probabilistic set of flood maps (representing water level) generated by the HEC-RAS 2-D model were used (details are explained in Chapter 4).

For the exposure component of the study, an artificial intelligence method was applied to extract the buildings from high-resolution aerial images of the area. The methodology on building extraction using AI has been explained in detail in Chapter 2; the results (buildings' polygons) were used in this study section. To estimate the type of material for each polygon, a probabilistic approach (Inverse Distance Weighting) has been applied to estimate the probability that each building detected belongs to a particular type of material in the region (the method has been explained in Chapter 4).

At the last step, the total loss for the residential land-use class were calculated using the depth-damage functions and the proposed adaptation options. Similarly to the total loss calculation performed in chapter 4, total loss estimation is restricted to direct tangible loss of available land-use classes (residential buildings) in right riverbank area. Results are presented as average annual loss exceedance curves for building construction material and dikes' height.

5.5 Results

Table 5.1 presents the effect of building material on the average annual loss for a given dike height (ranging from 180.24 to 184). As shown in Table 5.1, increasing the dike height significantly reduces the flood-induced loss to the residential buildings on the river's right bank. Increasing the dike height to 183 m (less than 3 m above the current level) leads to 0.0% loss to the buildings, i.e., 100% protection against flooding for all types of buildings construction material. Increasing the dike height to 183 m will also reduce the probability of casualties in the region and decrease physical damages to the residential buildings.

As seen in Table 5.1, and considering the status quo scenario, improving the buildings material to concrete (All DUR scenario) without increasing the dike height, results to a decrease in loss to the buildings from 2213 to 1698 thousands CFA. The status quo scenario corresponds to a minimum dike crest height of 180.24 m, and the distribution of buildings material obtained in chapter 4 by applying inverse distance weighting method – exponent of 2. However, it should be mentioned that the cost of implementing the adaptation options has not been considered here.

Table 5.1. Average annual loss (in thousand CFA[a]) for different dike crest height and building construction material scenarios.

Dike crest height, m	Scenarios				
	All BAN[b]	All DUR[b]	All SDU[b]	All CAS[b]	IDW (2)[c]
180.24	11113	7976	13671	3704	9874
181	11036	7856	13509	3679	9773
182	2566	1698	3072	855	2213
183	0	0	0	0	0
184	0	0	0	0	0

[a] West African CFA franc.

[b] Mud walls covered by mortar (SDU); Concrete walls (DUR); Informal constructions (CAS); Mud walls (BAN).

[b] Inverse Distance Weighting method – exponent of 2.

Exceedance probability curves were generated for average annual loss using the hazard and vulnerability of the exposed buildings. The results are illustrated in Figure 5.4a-c. As seen in the figure, irrespective of the type of building material used, increasing the dike crest heights to 183 m led to a significant reduction in the exceedance probability of damages, and average annual loss becomes zero. It is therefore reasonable to expect a substantial decrease in casualties by increasing the dike heights. The scenarios for building construction material consider 100% of the buildings in the area to be of: Mud walls (BAN); Concrete walls (DUR); Mud walls covered by mortar (SDU), Informal constructions – a mixture of sundried clay and straw and is also known as Banco (CAS), or a combination of different material estimated based on Inverse Distance Weighting method.

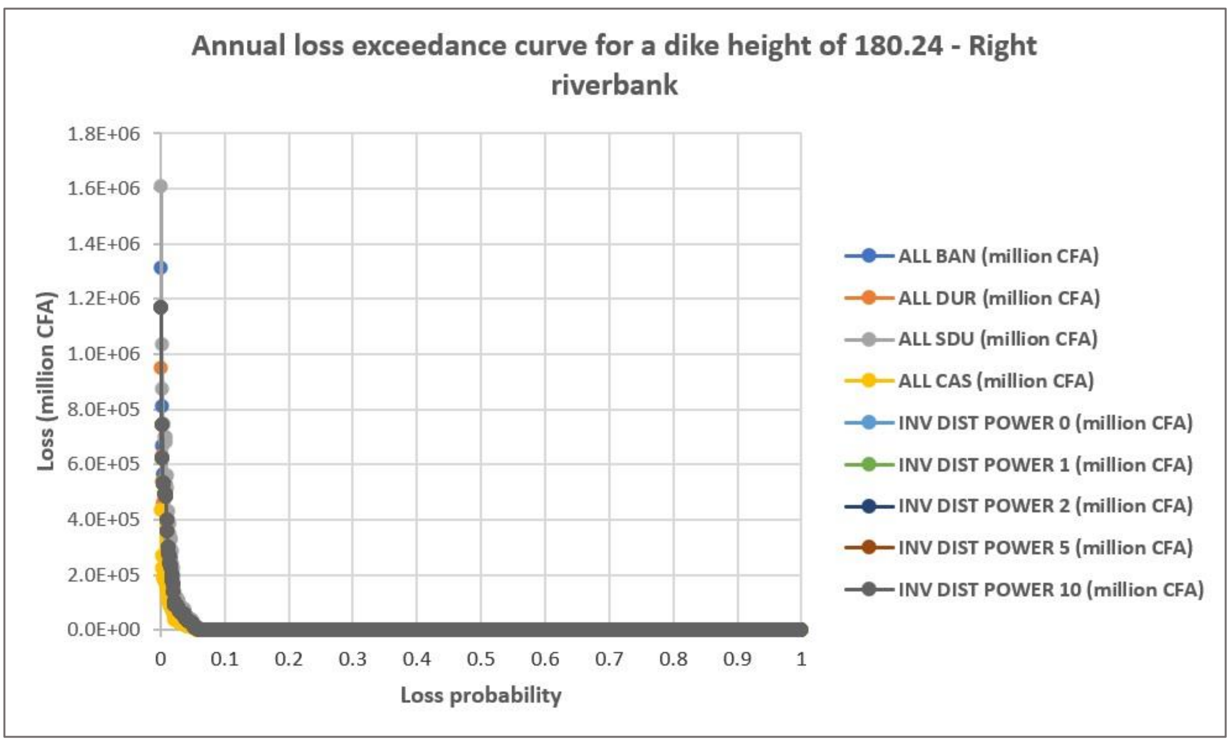

(a)

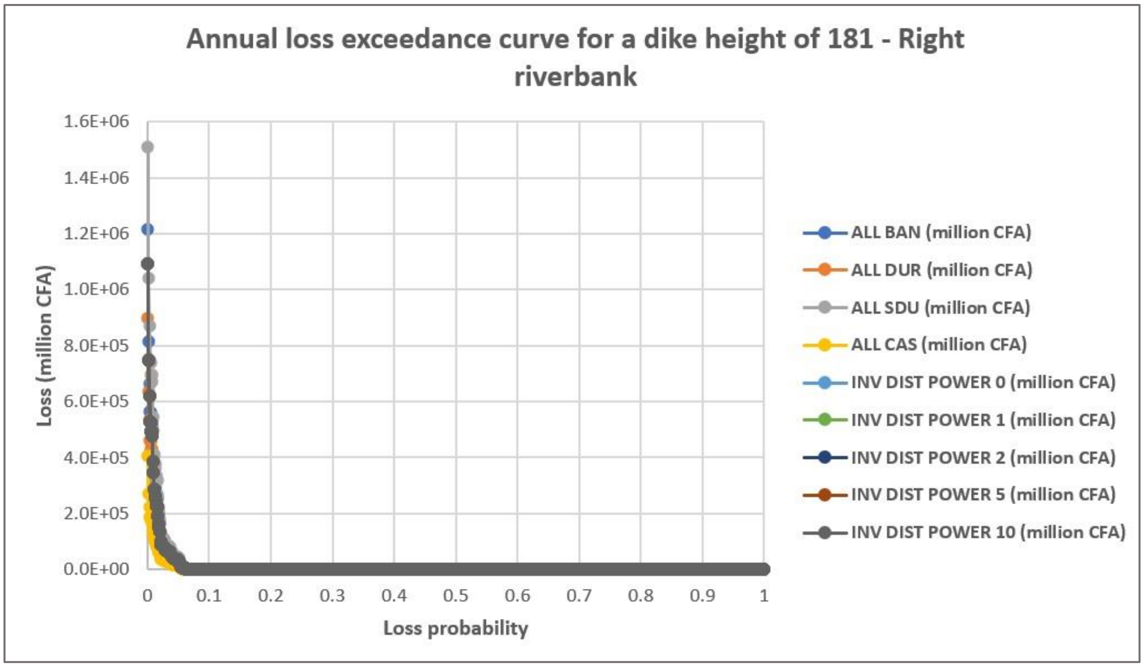

(b)

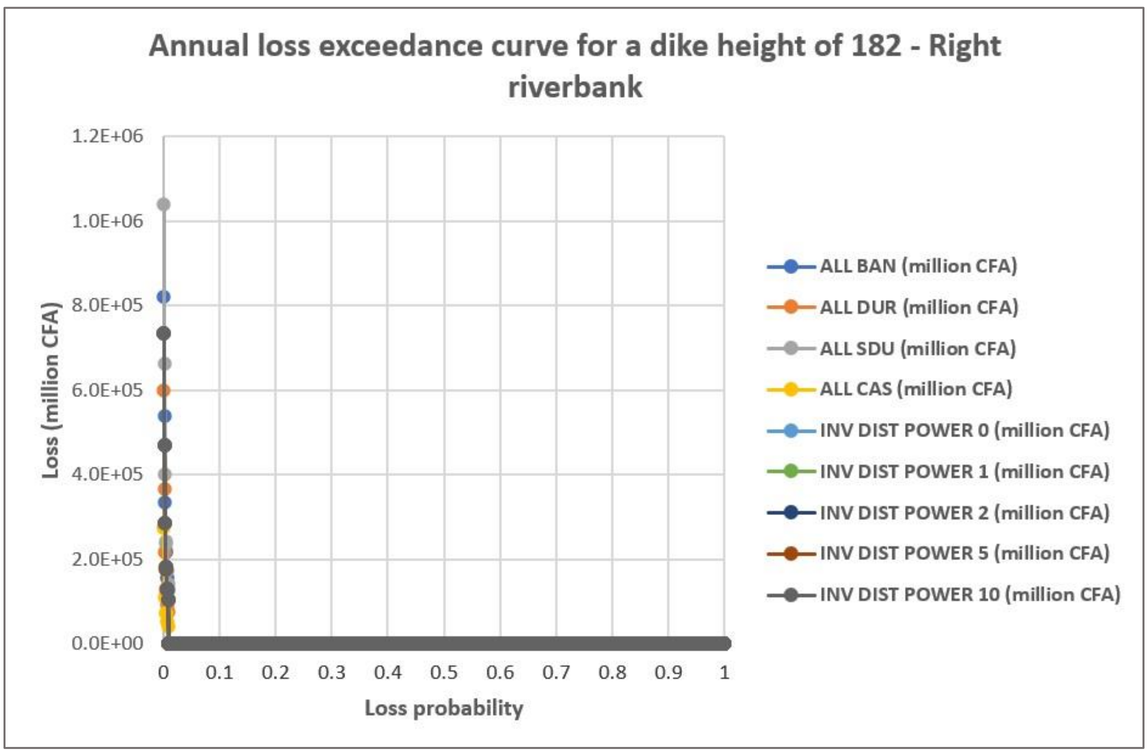

(c)

Figure 5.4. Annual loss exceedance curve as a function of dike crest height and building construction material: a) 180.24 m; b) 181 m; and c) 182 m.

Results show that both adaptation options proposed for the area of interest behave as expected and decrease the probability of monetary losses to the residential building class, and are likely to reduce the number of casualties (which was not considered in this study).

The analysis presented in this chapter could have been expanded to a complete cost-benefit analysis of the adaptation options that would have helped the decision-maker choose the best solution given the available budget. The formula the decision-maker could use to estimate the length of time the investment would be paid off could be (Eq. 5.1):

$$D = \frac{C_d + C_{br}}{AAL_b - AAL_a} \tag{5.1}$$

Where D is the investment return length in years, C_d *is the* cost of dike retrofitting, C_{br} is the cost of building conversion, AAL_b is the average annual loss in the study area before dike retrofitting and building conversion, and AAL_a is the average annual loss in the study area after dike retrofitting and building conversion. The above formula can be applied to any dike height and subset of building. Mathematical programming could be used to identify the optimal dike height and best set of buildings to retrofit. Additional adaptation options could be included, such as flood zoning (buying out the buildings in the floodplain), and damages to other sectors (e.g., agriculture could be considered).

There is, however, one significant limitation to this study. One of the limitations is that the inflow scenarios were calculated using flood peaks up to 2012, and hence do not reflect the current flood peaks. When it occurred, the 2012 flood peak in Niamey was considered a 1/100 year flood and had a magnitude that was never seen since streamflow measurements started in the city in 2012. Since 2012, that '100-years flow' was exceeded three times: in 2017, 2019, and 2020. These unexpected events suggest that the hydrological regime of the river has shifted and that the 100-year flood has probably increased. Therefore, the flooded areas and losses calculated in this paper are not representative of the current flood risk, even more so future flood risk. Further investigation on how the flood risk evolves and how it affects the optimal adaptation strategies is needed. Two potential areas for improvement include the attribution of building material to the remote-sensed building polygons, and the development of loss exceedance curves that are representative of local conditions.

5.6 Conclusion

This chapter examined the sensitivity of the loss exceedance curves to the height of flood protection dikes in the right riverbank of the Niger River and the type of building materials. Results show that in the absence of any other mitigation measurements in the study area, increasing the height of the dike up to 3 m above the current dike crest height could significantly protect the area against flooding and decrease the physical damages to the residential buildings in the region. Results also confirmed that improving the constructional material for the buildings to concrete will cause 23% less flood-induced damages to the buildings in the region than the current situation. Concrete is being suggested due to the maximum durability against damages due to water height increase. Depth-damage curves used in this study have been explained in Chapter 2. The benefits of implementing the proposed adaptation options in the area include a reduction risk of flooding as well as the number of the area inundated by water, avoiding the possible loss of lives and adverse economic impacts to the affected communities and the people of Niamey overall.

It was also found that, irrespective of the type of building material used, increasing the dike crest heights to 183 m led to a significant reduction in the exceedance probability of damages, and average annual loss becomes zero. It is reasonable to expect a significant decrease in casualties, too, by increasing the dike heights. Therefore, implementing any or both adaptation options proposed for the area of interest will cause a decrease in the probability of monetary losses to the residential building class and are likely to decrease the number of casualties.

Chapter 6

Summary and conclusion

Climate change is already altering weather patterns which makes floods and droughts more common and more severe. But it also makes them much harder to predict. Floods could affect our environment and cause damages including loss of human life; damage to property and crop; interruption to transportation and utility services; and other damages arising from economic activity disruption. Therefore, the need for flood risk evaluation and assessment is more recognized in flood-prone and vulnerable regions since the loss level is directly proportional to the area's level of vulnerability and exposure. There are many different ways of viewing natural hazard adaptation in general. Some focus on resisting environmental changes, while others mainly target suiting such changes or combining both. However, the necessity of considering some effective parameters such as budget, time, and available resources, which prioritizes available options for each specific case, makes the decision-makers not to promote one approach over another. Therefore, selection of the best options involves evaluating and assessing various approaches based on specific situation of each case.

This study investigated the possibility of developing and implementing a probabilistic flood risk estimation framework where all flow ranges are accounted for. The probability of flood occurrence and the probabilistic distribution of hydraulic parameters, and the probability of damages are spatially calculated for the decision-makers to take optimal adaptation decisions (flood protection dike design, recommendations for new buildings, etc.). The challenges of inferring the probability distribution of the different physical flood parameters in a context of sparse data, linking their parameters to flood damages, and finally translating the estimation risk into decision were also explored. The proposed methodology is a strategy encompassing hazard, exposure, and vulnerability components of flood risk. A first case study on Niamey, Niger, was performed using readily available data and a 1-D and 2-D HEC-RAS model.

Adaptation options to flood risk in Niamey (Niger, West Africa) area were examined by looking at two main variables: a) Buildings' material (CAS: Informal constructions – a mixture of sundried clay and straw also known as Banco, BAN: Mud walls, DUR: Concrete walls, and SDU: Mud walls covered by mortar), and b) Dike height within a scenario-based framework, where numerical modelling was undertaken to quantify the inundated area. The focus was on adaptation to the associated direct tangible losses to residential land-use classes due to flooding. The 1-D and 2-D hydraulic model, HEC-RAS, was tested on a 160 km reach of the Niger River. water levels within the inundated areas have been identified using the numerical modeling. The range and domain of residential areas have been evaluated associated with each scenario. Floods with various return periods (2-, 10-, 20-, 50-, 100-, 200-, 500-, and 1000-yr) were designed and considered in estimating total loss. The benefits and costs of different adaptation options were then compared for residential land-use class to implement flood risk maps in Niamey. Dike heights ranged from 180.24 m to 184 m, and buildings' material were considered 0% to 100% of each type, respectively.

In order to generate vulnerability curves (amount of damages to a building as a function of water height), a number of assumptions based on expert judgment, known typical construction types in the study area, and field surveys were made. It was assumed that 100% of the mud and straw building is lost when water reaches 0.5 m. Concrete buildings were assumed to collapse when water reached 2.5 m, while mud walls covered by mortar were assumed to stand up to 1 m of water before collapsing. Due to the lack of reliable statistics regarding the prevalence of the different building types in the area, six scenarios were considered representing different relative proportions of each of the four types under consideration: (1) 100% CAS; (2) 100% BAN; (3) 100% DUR; (4) 100% SDU; (5) 50% BAN with 10% DUR, 20% SDU, and 20% CAS; (6) 50% BAN with 30% DUR, 20% SDU, and 0% CAS.

Since the study area does not have detailed information on the exposed infrastructure elements to estimate economic losses associated with flooding, exposure quantification was performed using two different methods. For the first method, the output of the HEC-RAS model, describing flood-prone areas (hazard maps), was imported to Google Earth software. Potential floodplain polygons, which identify the buildings in the flood-prone areas, were then digitized in Google Earth. For this purpose, visual interpretation was applied to the Google Earth images to identify the number of properties (buildings) at risk of flooding. Subsequently, the digitized buildings' polygons were exported to ArcMAP to calculate the total area of the potentially affected region. As high-resolution aerial photos of flood-prone areas in the town have become available, this study applied more systematic and accurate approaches (as another method of exposure quantification) for flood exposure estimation in Niamey. Therefore, an artificial intelligence method was evaluated to extract buildings from high-resolution aerial images in the area of interest, Niamey, Niger. For this purpose, a deep learning (DL) method was applied. The data used in this study consist of orthomosaics and a Digital Surface Model (DSM) of an approximately 98.85 km^2 (22.47 km long and 4.40 km wide) band of land along the Niger river in Niamey. Subsequently, a probabilistic approach (inverse distance weighting – IDW) has been applied to calculate the probability that each building detected belongs to a particular type of material in the region. The probabilities for a particular building are based on the inverse distance to the available ground survey data of the study area. Results show that using various values for exponent when applying IDW method does not make any significant changes.

Following general conclusions could be drawn based on the results of this study:

- A methodology was successfully developed for estimating flood vulnerability curves for the city using aerial imagery, artificial intelligence, and limited ground truth on building material and evaluating the proposed adaptation options' impact on flood risk in Niamey, Niger.
- It was found that increasing the height of the dikes would lead to smaller economic losses while rebuilding with better materials would increase the average annual economic losses but might decrease the risk of human casualties. To select the best adaptation options, decision-makers have to factor in non-economic values as well as associated implementation costs.
- Without detailed information on the exposed infrastructure elements, a feasible yet fast and precise method of extracting buildings from high-resolution aerial images was investigated using an artificial intelligence method – deep learning. The applied deep learning method showed promising results with a high accuracy rate for the area of interest in this study. It was able to successfully identify the two introduced classes of Building and Background (non-building).

- In multi-rooftop buildings where identifying the actual size of the building with manual and Maximum Likelihood Classification methods would be very difficult, the Deep Learning method reported highly accurate results. However, tall trees have been observed as a major limitation and a problem in full-size roof detection of the buildings from very high-resolution aerial images. Therefore, to obtain more accurate building boundaries, the overall classification accuracy of the model needs to be improved.
- Despite imperfect and scarce data in the study area, quantitative tools were developed to help decision-makers and regulators choose the best preventive measures to mitigate flood risk.
- Results demonstrate the individual and the combined impact of two variables in flood risk estimation in Niamey. Results showed that proposed measures can, individually, decrease the potential for direct tangible flood damage (from 23% to 100%), by reducing the probability of residential building to be inundated; a combination of the proposed options could also be considered depending on the available budget.
- It was concluded that the extent of individual residential losses is highly affected by building material.
- Results show that the developed model in this study accurately estimated the inundation extent and successfully reproduced the flash flood flows and water surface levels resulting from the 2020 flood season. Although the developed model tends to identify less flooding than the observed extent on the floodplain, it is suitable, to an acceptable degree, for predicting and assessing flood risks in the study area. The observed error could be attributed to the limitations such as scarcity and low quality of the available data, limits of historical data on past flood losses, and long-term hydrological data for the study area.
- Results also show that residential losses are widespread along the Niger river throughout the city. The current configuration of the protection dikes seems to be designed to protect agricultural lands rather than residential buildings; they only protect a small fraction of the exposed residential buildings. If nothing is done, the changing hydrological regime may lead to even more catastrophic losses.
- Results show that the exponent in the IDW algorithm has very little impact on the loss exceedance curves. Therefore, using the exponent value of 2 (the common value in literature) is being suggested when applying IDW technique in future studies.

The findings contend that although the proposed structural adaptation option as a resisting to environment approach is applied to the area of interest and considered technically feasible, other non-structural measures, which have long-term effect of risk mitigation, should be taken into consideration, especially for highly hazard-prone areas. Examples of non-structural measures include but not limited to public awareness programs, policies, and laws and their enforcement, changes to land-use whether through zoning and changes in building codes, or in infrastructure design and location. Moreover, the results of this study would significantly help in loss estimation to the buildings, according to construction type, due to the yearly floods in the region of the interest, Niamey, Niger. However, since the buildings are of various types of material, having an accurate building database is important in assessing the expected level of damage in the inundated area, especially to the critical buildings (hospitals, schools, research labs, etc.).

The results generated in this study allow us to quantitatively estimate the gain in resilience that comes from these decisions. It can also demonstrate to the decision-makers the benefits of implementing policies that encourage people to build with different materials. This is the first time a quantitative analysis of flood risk and adaptation options is implemented. For the proposed tool to be more effective, decision-makers should invest in a comprehensive survey of the built environment and exposed assets in the study area. Additional information on building stock and existing buildings, etc., helps the collection of more accurate information on exposed elements and will be used for decision-making in risk management. Such a survey would allow us to estimate the risk in the current situation and estimate more accurately the benefits of adaptation options.

The findings of the current study must be seen in the light of some other limitations such as the lack of consideration of variations in hydrological conditions, e.g., climate change projections, which requires the availability of long-term data; rainfall-induced losses were not taken into account. The study area in this research, Niamey, is located in Sahel region – the vast semi-arid region of Africa separating the Sahara Desert to the north and tropical savannas to the south (UN, 2021). The Sahelian rainfall pattern is directly being affected by the West African Monsoon (WAM), a highly variable climate system (Cornforth, 2013). Therefore, using a combined hydrological and hydraulic model is being suggested for the futures studies in order to incorporate the effects of variations in hydrological conditions and achieve more realistic results.

Application of fragility curves is also recommended for future studies, in order to better understand the failure mechanism of the dikes in case of extreme flooding. Fragility curves are typically used to relate the percentage damage for elements such as buildings, to flood characteristics such as inundation depth, velocity or duration (Reese and Ramsay, 2010).

Also, to generate vulnerability (depth-damage) and accordingly, loss exceedance curves, several assumptions were made based on expert judgment. Moreover, the digital elevation model used to characterize dikes' height in the study area does not represent the most recent terrain changes, especially after the 2020 floods. The abovementioned limitations may have impacted the interpretation of the findings and should be considered in future works.

References

Abah, R.C., 2013. An application of Geographic Information System in mapping flood risk zones in a north central city in Nigeria. African Journal of Environmental Science and Technology. 7 (6), 365–371. <https://doi.org/10.5897/AJEST12.182>.

ACTED, OXFAM, UNICEF, 2012. Enquête auprès des ménages sinistrés par les inondations à Niamey, République du Niger. Présenté par ACTED et OXFAM Niamey, République du Niger En partenariat avec UNICEF.

Adeaga, O., 2009. Planning and warning tools for flood disaster management in Lagos Mega city. In: Proceedings of the 5th Urban Research Symposium. June 28–30, World Bank, Marseille, France.

Adelekan, I.O., 2009. Vulnerability of poor urban coastal communities to climate change in Lagos, Nigeria. In: Proceedings of the 5th Urban Research Symposium. June 28–30, World Bank, Marseille, France.

Adger, W.N., Lorenoni, I., and O'Brien, K.L. (Eds.), 2009. Adapting to Climate Change. Cambridge, p. 514.

Ahmad, A., Quegan, S., 2012. Analysis of maximum likelihood classification on multispectral data. Appl. Math. Sci. 6 (129), 6425–6436.

Aich, V., Koné, B., Hattermann, F.F., and Paton, E.N., 2016. Time Series Analysis of Floods across the Niger River Basin. Water. 8, 165.

Alfieri, L., Salamon, P., Bianchi, A., Neal, J., Bates, P., and Feyen, L., 2014. Advances in pan-European flood hazard mapping. Hydrological Processes. 28 (13), 4067–4077. <http://dx.doi.org/10.1002/hyp.9947>.

Alher, F., 2017. Enquete de cartographie pour la preventions de risques des catastrophes dans les communes v et i de niamey : zarmagandeye, banguisto, goudel et lossou goungou. Technical report, Projet de Gestion des Risques de Catastrophe et de Développement Urbain (PGRCDU), Niamey.

Alfonso, L., Mukolwe, M.M., and Di Baldassarre, G., 2016. Probabilistic Flood Maps to support decision-making: Mapping the Value of Information, Water Resources Research, 52, 1026–1043. <https://doi:10.1002/2015WR017378>.

Alzahrani, A., 2017. Application of Two-Dimensional Hydraulic Modeling in Riverine Systems Using HEC-RAS. (Electronic Thesis or Dissertation). Retrieved from <https://etd.ohiolink.edu/>.

Amogu, O., Descroix, L., Yéro, K.S., Le Breton, É., Mamadou, I., Ali, A., Vischel, T., Bader, J.-C., Moussa, I.B., Gautier, E., et al., 2010. Increasing River Flows in the Sahel? Water. 2, 170–199.

Andrearczyk, V., and Whelan, P.F., 2017. Chapter 4 - Deep Learning in Texture Analysis and Its Application to Tissue Image Classification, Editor(s): Adrien Depeursinge, Omar S. Al-Kadi, J.Ross Mitchell, In The Elsevier and MICCAI Society Book Series, Biomedical Texture Analysis, Academic Press, 95-129.

Apel, H., Thieken, A. H., Merz, B., and Blöschl, G., 2004. Flood risk assessment and associated uncertainty, Nat. Hazards Earth Syst. Sci., 4, 295–308, <https://doi.org/10.5194/nhess-4-295-2004>.

Apel, H., Thieken, A.H., Merz, B., and Bloschl, G., 2006. A Probabilistic Modelling System for Assessing Flood Risks, Nat. Hazards (2006) 38: 79–100. <https://doi.org/10.1007/s11069-005-8603-7>.

Apel, H., Merz, B., Thieken, A.H., 2008. Quantification of uncertainties in flood risk assessments. Int. J. River Basin Manage. 6 (2), 149–162. <https://doi.org/10.1080/15715124.2008.9635344>.

Asian Disaster Reduction Center (ADRC), 2011. Natural Disaster Data Book 2009 (an analytical review). Asian Disaster Reduction Center (ADRC), Kobe, Japan. pp. 23.

Babak, O. and Deutsch, C.V., 2009. Statistical approach to inverse distance interpolation, Stoch Environ Res Risk Assess. 23, 543–553. <https://doi.org/10.1007/s00477-008-0226-6>.

Bates, P.D. and de Roo, A.P.J., 2000. A simple raster-based model for flood inundation simulation. Journal of Hydrology, 236 (1–2), 54–77. <http://dx.doi.org/10.1016/S0022-1694(00)00278-X>.

Ben Khalfallah, C., Saidi, S., 2018. Spatiotemporal floodplain mapping and prediction using HEC-RAS - GIS tools: Case of the Mejerda river, Tunisia. Journal of African Earth Sciences. 142, 44–51, <https://doi.org/10.1016/j.jafrearsci.2018.03.004>.

Benali, A., Dermeche, H., Belhadj, S., Adnane, A., Elhachemi, A.H., 2014. Building extraction of very high spatial resolution satellite images. 978-1-4799-3824-7/14/$31.00, 2014 IEEE.

Central American Probabilistic Risk Assessment (CAPRA), University of the Andes, Colombia. <https://ecapra.org/>.

Chellappa, R., and Rosenfeld, A., 2003. Image Processing. Editor(s): Robert A. Meyers, Encyclopedia of Physical Science and Technology (Third Edition), Academic Press, 595-630.

Chang, C.H., Chung, M.K., Yang, S.Y., Hsu, C.T., and Wu, S.J., 2018. A Case Study for the Application of an Operational Two-Dimensional Real-Time Flooding Forecasting System and Smart Water Level Gauges on Roads in Tainan City, Taiwan. Water 10(5), 574. <https://doi:10.3390/w10050574>.

Cardona, O.D., M.K. van Aalst, J. Birkmann, M. Fordham, G. McGregor, R. Perez, R.S. Pulwarty, E.L.F. Schipper, and B.T. Sinh, 2012: Determinants of risk: exposure and vulnerability. In: Managing the Risks of Extreme Events and Disasters to Advance Climate Change Adaptation [Field, C.B., V. Barros, T.F. Stocker, D. Qin, D.J. Dokken, K.L. Ebi, M.D. Mastrandrea, K.J. Mach, G.-K. Plattner, S.K. Allen, M. Tignor, and P.M. Midgley (eds.)]. A Special Report of Working Groups I and II of the Intergovernmental Panel on Climate Change (IPCC). Cambridge University Press, Cambridge, UK, and New York, NY, USA. pp. 65-108.

Chormanski, J., Okruszko, T., Ignar, S., Batelaan, O., Rebel, K.T., Wassen, M.J., 2011. Flood mapping with remote sensing and hydrochemistry: a new method to distinguish the origin of flood water during floods. Ecol. Eng. 37 (9), 1334–1349. <https://doi.org/10.1016/j.ecoleng.2011.03.016>.

CLIMATESERVICES.IT a, Web. <https://climateservices.it/a-niamey-les-digues-de-protection-tiennent-la-hauteur-record-du-fleuve-de-650-centimetres/>.

CLIMATESERVICES.IT b, Web. <https://climateservices.it/la-crue-du-fleuve-niger-se-poursuit-et-des-nouveaux-quartiers-de-niamey-sont-sous-leau/>.

Cornforth, R.J., 2013. West African Monsoon 2012. Weather 68: 256-263.

De Silva, M.M.G.T., Kawasaki, A., 2018. Socioeconomic Vulnerability to Disaster Risk: A Case Study of Flood and Drought Impact in a Rural Sri Lankan Community, Ecological Economics 152, 131–140 .

Daffi, R.E., Otun, J.A., Ismail, A., 2014. Flood hazard assessment of river DEP floodplains in North-Central Nigeria. International Journal of Water Resources and Environmental Engineering 6 (2), 67–72. <https://doi.org/10.5897/IJWREE2013.0457>.

Dale, M., Wicks, J., Mylne, K., Pappenberger, F., Laeger, S., Taylor, S., 2014. Probabilistic flood forecasting and decision-making: an innovative risk-based approach. J. Nat. Hazards 70, 159–172. <https://doi.org/10.1007/s11069-012-0483-z>.

de Moel, H., Aerts, J., Koomen, E., 2011. Development of flood exposure in the Netherlands during the 20th and 21st century. J. Glob. Environ. Change 21 (2), 620–627. <https://doi.org/10.1016/j.gloenvcha.2010.12.005>.

Descroix, L., Mahé, G., Lebel, T., Favreau, G., Galle, S., Gautier, E., Olivry, J.-C., Albergel, J., Amogu, O., Cappelaere, B., et al., 2009. Spatio-temporal variability of hydrological regimes around the boundaries between Sahelian and Sudanian areas of West Africa: A synthesis. J. Hydrol., 375, 90–102.

Descroix, L., Genthon, P., Amogu, O., Rajot, J.L., Sighomnou, D., and Vauclin, M., 2012. Change in Sahelian Rivers hydrograph: The case of recent red floods of the Niger River in the Niamey region, Global and Planetary Change, Volumes 98–99, Pages 18-30. <https://doi.org/10.1016/j.gloplacha.2012.07.009>.

Descroix, L., 2018. Processus Et Enjeux D'eau En Afrique De l'Ouest Soudano-Sahélienne; Editions des Archives Contemporaines: Paris, France.

Di Baldassarre, G., Schumann, G., Bates, P.D., 2009a. A technique for the calibration of hydraulic models using uncertain satellite observations of flood extent. J. Hydrol. 367 (3-4), 276–282. <https://doi.org/10.1016/j.jhydrol.2009.01.020>.

Di Baldassarre, G., Castellarin, A., Montanari, A., Brath, A., 2009b. Probability-weighted hazard maps for comparing different flood risk management strategies: a case study. J. Nat. Hazards 50, 479–496. <https://doi.org/10.1007/s11069-009-9355-6>.

Di Baldassare, G., Schumann, G, Bates, P.D., Freer, J.E., and Beven, K.J., 2010. Flood-plain mapping. A critical discussion of deterministic and probabilistic approaches. Hydrological Sciences Journal, 55 (3), 364–376. <http://dx.doi.org/10.1080/02626661003683389>.

Domeneghetti, A., Vorogushyn, S., Castellarin, A., Merz, B., and Brath, A., 2013. Probabilistic flood hazard mapping. Effects of uncertain boundary conditions. Hydrology and Earth System Sciences, 17 (8), 3127–3140. <http://dx.doi.org/10.5194/hess-17-3127-2013>.

Domeneghetti, A., Carisi, F., Castellarin, A., and Brath, A., 2015. Evolution of flood risk over large areas. Quantitative assessment for the Po river. Journal of Hydrology, 527, 809–823. <http://dx.doi.org/10.1016/j.jhydrol.2015.05.043>.

Doorn, A., 2014. Rationality in flood risk management: the limitations of probabilistic risk assessment in the design and selection of flood protection strategies. J. Flood Risk Management, 7, 230-238.

Dutta, D., Herath, S., Musiake, K., 2003. A mathematical model for flood loss estimation. Journal of Hydrology, 277, 24–49. <https://doi.org/10.1016/S0022-1694(03)00084-2>.

Dyck, J.V., and Willems, P., 2013. Probabilistic flood risk assessment over large geographical regions. Water Resour. Res., 49, 3330–3344. <https://doi.org/10.1002/wrcr.20149>.

Environmental Agency, 2003. Strategy for Flood Risk Management (2003/4-2007/8). Version 1.2. EA. Environment Agency, London, pp. 31.

ESA., 2017. Land Cover CCI Product User Guide Version 2. Tech. Rep. Available online: <http://www.esa-landcover-cci.org/?q=node/199 (accessed on 8 August 2021)>.

Falter, D., Vorogushyn, S., Lhomme, J., Apel, H., Gouldby, B., and Merz, B., 2013. Hydraulic model evaluation for large-scale flood risk assessments. Hydrological Processes, 27 (9), 1331–1340. <http://dx.doi.org/10.1002/hyp.9553>.

FAO (Food and Agriculture Organization of the United Nations), 1997. Irrigation potential in Africa: A basin approach. Web. <http://www.fao.org/docrep/w4347e/w4347e0i.htm>.

Fiorillo, E., Crisci, A., Issa, H., Maracchi, G., Morabito, M., Tarchiani, V., 2018. Recent Changes of Floods and Related Impacts in Niger Based on the ANADIA Niger Flood Database. Climate, 6, 59.

FloodList, Africa, Web. <http://floodlist.com/africa/niger-floods-niamey-tillaberi-june-2017>.

Fradkin, M., Maitre, H., and Roux, M., 2001. Building detection from multiple aerial images in dense urban areas. Computer vision and image understanding, Vol 82.

Freer, J., Beven, K.J., Neal, J., Schumann, G., Hall, J., Bates, P., 2013. Flood risk and uncertainty. In: Rougier, J., Sparks, S., Hill, L. (Eds.), Risk and Uncertainty Assessment for Natural Hazards. Cambridge University Press, UK, pp. 190–233. <https://doi.org/10.1017/CBO9781139047562>.

Fuchs, S., Röthlisberger, V., Thaler, T., Zischg, A., Keiler, M., 2017. Natural hazard management from a coevolutionary perspective: exposure and policy response in the European Alps. Ann. Am. Assoc. Geogr. 107 (2), 382–392. <https://doi.org/10.1080/24694452.2016.1235494>.

Ganguli, P., Reddy, M.J., 2013. Probabilistic assessment of flood risks using trivariate copulas. J. Theor. Appl. Climatol. 111, 341–360. <https://doi.org/10.1007/s00704-012-0664-4>.

Garrote, J., Peña, E., Díez-Herrero, A., 2021. Probabilistic Flood Hazard Maps from Monte Carlo Derived Peak Flow Values—An Application to Flood Risk Management in Zamora City (Spain). Appl. Sci. 2021, 11, 6629. <https://doi.org/10.3390/app11146629>.

Gleick, P.H. 2000. The World's Water, 2000-2001: The Biennial Report on Freshwater, Island Press, p. 33. ISBN 1-55963-792-7; online at Google Books.

Guimarães Nobre, G. (2019). Floods, droughts and climate variability: From early warning to early action. Thesis. Vrije Universiteit Amsterdam.

Guo, T., and Yasuoka, Y., 2002. Snake-based approach for building extraction from high-resolution satellite images and height data in urban areas, Proceedings of 23rdAsian Conference on Remote Sensing.

Hagen, E., Lu, X.X., 2011. Let us create flood hazard maps for developing countries. Nat. Hazards 58 (3), 841–843. <https://doi.org/10.1007/s11069-011-9750-7>.

Hallegatte, S., Green, C., Nicholls, R.J., Corfee-Morlot, J., 2013. Future flood losses in major coastal cities. J. Nat. Clim. Change 3 (9), 802–806. <https://doi.org/10.1038/nclimate1979>.

Haq, M., Akhtar, M., Muhammad, S., Paras, S., Rahmatullah, J., 2012. Techniques of remote sensing and GIS for flood monitoring and damage assessment: a case study of Sindh Province, Pakistan. Egypt. J. Remote Sens. Space Sci. 15 (2), 135–141. <https://doi.org/10.1016/j.ejrs.2012.07.002>.

Horritt, M.S. and Bates, P.D., 2002. Evaluation of 1-D and 2-D numerical models for predicting river flood inundation. Journal of Hydrology, 268 (1–4), 87–99. <http://dx.doi.org/10.1016/S0022-1694(02)00121-X>.

Huang, H., Wu, J., Lim, T.C., Yang, M., and Ding, W., 2020. Pure electric vehicle nonstationary interior sound quality prediction based on deep CNNs with an adaptable learning rate tree, Mechanical Systems and Signal Processing, 148, 1-22. <https://doi.org/10.1016/j.ymssp.2020.107170>.

Huizinga, J., Moel, H. de, and Szewczyk, W., 2017. Global flood depth-damage functions. Methodology and the database with guidelines. EUR 28552 EN. <doi: 10.2760/16510>.

IPCC, 2012. In: Barros, C.B., Stocker, V., Qin, T.F., Dokken, D., Ebi, D.J., Mastrandrea, K.L., Mach, M.D., Plattner, K.J., Allen, G.-K., Tignor, S.K., Midgley, M., IPCC, P.M. (Eds.), Managing the Risks of Extreme Events and Disasters to Advance Climate Change Adaptation A Special Report of Working Groups I and II of the Intergovernmental Panel on Climate Change. With Assistance of Field. Cambridge University Press, Cambridge, UK; New York, NY, USA.

Jalayer, F., De Risi, R., De Paola, F., Giugni, M., Manfredi, G., Gasparini, P., Topa, M.E., Yonas, N., Yeshitela, K., Nebebe, A., Cavan, G., Lindley, S., Printz, A., and Renner, F., 2014. Probabilistic GIS-based method for deliniation of urban flooding risk hotspots. Nat. Hazards 73, 975–1001. <https://doi.org/10.1007/s11069-014-1119-2>.

Japan International Cooperation Agency (JICA), March 2003. Manual of Flood Control Planning, Project for the Enhancement of Capabilities in Flood Control and Sabo Engineering of the Department of Public Works and Highways (DPWH).

Kerres, M., 2010. Adaptation to Climate Change in the Upper and Middle Niger River Basin, River Basin Snapshot. May. KFW Entwicklungsbank, BMZ Federal Ministry for Economic Cooperation and Development.

Kheradmand, S., Seidou, O., Konte, D., and Barmou Batourec, M.B., 2018. Evaluation of adaptation options to flood risk in a probabilistic framework. Journal of Hydrology: Regional Studies, 19, 1-16. <http://dx.doi.org/10.1016/j.ejrh.2018.07.001>.

Khokher, A. and Talwar, R., 2012. Content-based Image Retrieval: Feature Extraction Techniques and Applications," in International Conference on Recent Advances and Future Trends in Information Technology, Proceedings Published in International Journal of Computer Applications, PP 9-14.

Kingma, D.P., and Ba, J., 2017. Adam: A Method for Stochastic Optimization. International Conference on Learning Representations, pages 1–13.

Knebl, M.R., Yang, Z.L., Hutchison, K., and Maidment, D.R., 2005. Regional scale flood modeling using NEXRAD rainfall, GIS, and HEC-HMS/RAS: a case study for the San Antonio River Basin summer 2002 storm event. Journal of Environmental Management 75(4 SPEC. ISS.), 325–336. <https://doi.org/10.1016/j.jenvman.2004.11.024>.

Koc San, D., and Turker, M., 2010. Building extraction from high resolution satellite images using Hough transform. International Archives of the Photogrammetry, Remote Sensing and Spatial Information Science, Volume XXXVIII, Part 8, Kyoto Japan.

Kocsis, I., Haidu, I., and Maier, N., 2020. Application of a Hydrological MIKE HYDRO River – UHM Model for Valea Rea River (Romania). Case Study, Flash Flood Event Occurred on August 1st, 2019. 2020 ”Air and Water – Components of the Environment” Conference Proceedings, Cluj-Napoca, Romania, p. 257-272, <10.24193/AWC2020_24>.

Kotzé, H., Kamper, H., and Jordaan, H.W., 2020. Training Neural Networks for Plant Estimation, Control and Disturbance Rejection. IFAC-PapersOnLine 53 (2), 1664-1670.

Kumar, D.G., Padmaja, M., 2012. A novel image processing technique for counting the number of trees in a satellite image "Scholars Research Library, European Journal of Applied Engineering and Scientific Research, 1 (4):151-15.

Kumar, M., Singh, R.K., and Kishnamurthy, Y.V.N., 2014. Road Network Extraction from high resolution Multispectral Satellite Imagery Based on Object Oriented Techniques, Remote Sensing and Spatial Information Sciences, Volume II-8, 2014 ISPRS Technical Commission VIII Symposium, 09 – 12, Hyderabad, India, December 2014.

Kundzewicz, Z.W., Kanae, S., Seneviratne, S.I., Handmer, J., Nicholls, N., and Peduzzi, P., 2013. Flood risk and climate change. Global and regional perspectives. Hydrological Sciences Journal, 59 (1), 1–28. <http://dx.doi.org/10.1080/02626667.2013.857411>.

Lebel, T., and Ali, A., 2009. Recent trends in the Central and Western Sahel rainfall regime (1990–2007), Journal of Hydrology 375(1–2), 52-64. <https://doi.org/10.1016/j.jhydrol.2008.11.030>.

Levy, B.S., Jonathan A. Patz, J.A., 2015. Climate Change, Human Rights, and Social Justice, Annals of Global Health 81 (3), 310–322 .

Lian, J.J., Xu, K., and Ma, C., 2013. Joint impact of rainfall and tidal level on flood risk in a coastal city with a complex river network: a case study of Fuzhou City, China. Hydrology and Earth System Science, 17 (2), 679–689. <https://doi.org/10.5194/hess-17-679-2013>.

Liu, Z., Merwade, V., and Jafarzadegan, K., 2019. Investigating the role of model structure and surface roughness in generating flood inundation extents using one- and two-dimensional hydraulic models. Journal of Flood Risk Management, 12 (1), e12347. <http://dx.doi.org/10.1111/jfr3.12347>.

Mabogunje, A.L., 2014. Niger River. Encyclopedia Britannica. Encyclopaedia Britannica, Inc., Web. <http://www.britannica.com/place/Niger-River>.

Massazza, G., Tamagnone, P., Wilcox, C., Belcore, E., Pezzoli, A., Vischel, T., Panthou, G., Ibrahim, M.H., Tiepolo, M., Tarchiani, V., et al., 2019. Flood Hazard Scenarios of the Sirba River (Niger): Evaluation of the Hazard Thresholds and Flooding Areas. Water, 11, 1018.

Massazza, G., Bacci, M., Descroix, L., Ibrahim, M.H., Fiorillo, E., Katiellou, G.L., Panthou, G., Pezzoli, A., Rosso, M., Sauzedde, E., et al., 2021. Recent Changes in Hydroclimatic Patterns over Medium Niger River Basins at the Origin of the 2020 Flood in Niamey (Niger). Water, 13, 1659. <https://doi.org/10.3390/w13121659>.

Mayomi, I., Dami, A., Maryah, U.M., 2013. GIS based assessment of flood risk and vulnerability of communities in the Benue floodplains, Adamawa State, Nigeria. J. Geography Geol. 5, 148–160. <https://doi.org/10.5539/jgg.v5n4p148>.

Merz, B., Kreibich, H., Schwarze, R., and Thieken, A., 2010. Review article: Assessment of economic flood damage. Nat. Hazards Earth Syst. Sci., 10, 1697–1724.

Mohammadi, S.A., Nazariha, M., and Mehrdadi, N., 2014. Flood damage estimate (Quantity), using HEC-FDA model. Case study: the Neka River. Procedia Engineering, 70, 1173–1182. <https://doi.org/10.1016/j.proeng.2014.02.130>.

Morsy, M.M., Goodall, J.L., O'Neil, G.L., Sadler, J.M., Voce, D., Hassan, G., and Huxley, C., 2018. A cloud-based flood warning system for forecasting impacts to transportation infrastructure systems. Environmental Modelling & Software 107, 231-244. <https://doi.org/10.1016/j.envsoft.2018.05.007>.

Musa, Z.N., Popescu, I., and Mynett, A., 2015. Sensitivity analysis of the 2D SOBEK hydrodynamic model of the Niger River. E-proceedings of the 36th IAHR World Congress, 28 June – 3 July, 2015, The Hague, the Netherlands.

National Geographic Society. <https://www.nationalgeographic.org/encyclopedia/africa-physical-geography/>.

National Research Council, Division on Earth and Life Studies. Alluvial Fan Flooding. Washington, DC: The National Academies Press. <https://doi.org/10.17226/5364, 182 pages>.

National Research Council 2015. Tying Flood Insurance to Flood Risk for Low-Lying Structures in the Floodplain. Washington, DC: The National Academies Press. <https://doi.org/10.17226/21720>.

Neal, J., Keef, C., Bates, P., Beven, K., Leedal, D., 2013. Probabilistic flood risk mapping including spatial dependence. J. Hydrol. Process 27, 1349–1363. <https://doi.org/10.1002/hyp.9572>.

Nka, B.N., Oudin, L., Karambiri, H., Paturel, J.E., Ribstein, P., 2015. Trends in floods in West Africa: Analysis based on 11 catchments in the region. Hydrol. Earth Syst. Sci., 19, 4707–4719.

Nkeki, F.N., Henah, P.J., Ojeh, V.N., 2013. Geospatial techniques for the assessment and analysis of flood risk along the Niger-Benue Basin in Nigeria. J. Geogr. Inform. Syst. 5, 123–135. <https://doi.org/10.4236/jgis.2013.52013>.

Nut, N., and Plermkamon, V., 2015. Floodplain Mapping Using HEC-RAS and GIS in Nam Phong River Basin, Thailand. International Journal of Environmental and Rural Development.

OCHA, Bulletin humanitaire Niger, Juillet 2015, Web. <http://www.unocha.org/niger|https://www.humanitarianresponse.info/operations/niger>.

OCHA, Bulletin humanitaire Niger, Août/Septembre 2015. Web. <http://www.unocha.org/niger|https://www.humanitarianresponse.info/operations/niger>.

OCHA Niger - Flash Update - Inondations, juin 2017. Web.<http://reliefweb.int/sites/reliefweb.int/files/resources/NER_Flash_Inondations_16062017.pdf>.

OCHA Niger - Flash Update # 2: Flood report as of September 7, 2020 in Niger. Web. <https://reliefweb.int/report/niger/ocha-niger-flash-update-2-bilan-des-inondations-au-7-septembre-2020-au-niger-0>.

OCHA, September 2020, Web. <https://reliefweb.int/map/niger/niger-niamey-flood-impact-map-15092020>.

OECD (Organisation for Economic Co-operation and Development) DAC (Development Assistance Committee), 2012. The challenge of capacity development: working towards good practice.

OECD, 2016. Financial Management of Flood Risk, OECD Publishing, Paris. <http://dx.doi.org/10.1787/9789264257689-en>.

Ok, A.O., 2014. A new approach for the extraction of aboveground circular structures from Near-Nadir VHR satellite imagery. Geosciences and Remote Sensing, IEEE Transactions on 52, pp. 3125-3140.

Ongdas, N., Akiyanova, F., Karakulov, Y., Muratbayeva, A., and Zinabdin, N., 2020. Application of HEC-RAS (2D) for Flood Hazard Maps Generation for Yesil (Ishim) River in Kazakhstan. Water 12, 2672. <https://doi.org/10.3390/w12102672>.

Oregon State University, Map of Basins Africa, Web. <https://transboundarywaters.science.oregonstate.edu/database-and-research/galleries/africa-gallery >.

Othman, F., Muhammad Amin, N.F., Mi Fung, L., and Mohamed Elamin, A.E., 2013. Utilizing GIS and Infoworks RS in Modelling the Flooding Events for a Tropical River Basin. In Applied Mechanics and Materials, Vols. 353–356, 2281–2285. Trans Tech Publications, Ltd. <https://doi.org/10.4028/www.scientific.net/amm.353-356.2281>.

Oyinloye, M.A., Olamiju, O.I., Oyetayo, B.S., 2013. Combating flood crisis using GIS: empirical evidences from ala river floodplain, Isikan Area, Akure, Ondo State, Nigeria. Commun. Inform. Sci. Manage. Eng. 3 (9), 439–447.

Pandey, A.K., 2004. Automatic urban road extraction using airborne laser scanning– altimetry and high resolution satellite data (M.Sc. Thesis). ITC.

Paprotny, D., Morales-Nápoles, O., Jonkman, S.N., 2018. HANZE: a pan-European database of exposure to natural hazards and damaging historical floods since 1870. Earth Syst. Sci. Data 10, 565–581. <https://doi.org/10.5194/essd-10-565-2018>.

Peraresi, M. and Benediktsson, A., 2001. A new approach for the morphological segmentation of high-resolution satellite imagery. IEEE Transactions on Geosciences and Remote Sensing, Vol. 39 (2), p.309-320.

Population Stat. Retrieved in July 2021 from <https ://populationstat.com/niger/niamey>.

Prinos, P., 2008. Review on Flood Hazard Mapping. Report Number. T03-07-01. Revision Number. 4_2_P13. Co-ordinator: HR Wallingford, UK.

Public Safety Canada, 2021, National Disaster Mitigation Program (NDMP) - Terms and Conditions. Retrieved from <https://www.publicsafety.gc.ca/cnt/mrgnc-mngmnt/dsstr-prvntn-mtgtn/ndmp/trms-cndtns-en.aspx>.

Purvis, M.J., Bates, P.D., Hayes, C.M., 2008. A probabilistic methodology to estimate future coastal flood risk due to sea level rise. J. Coast. Eng. 55, 1062–1073. <https://doi.org/10.1016/j.coastaleng.2008.04.008>.

Quiroga, V.M., Kure, S., Udo, K., and Mano, A., 2016. Application of 2-D numerical simulation for the analysis of the Febraury 2014 Bolivian Amazonia flood: Application of the new HEC-RAS version 5. RIBAGUA, 3, 25-33. <10.1016/j.riba.2015.12.001>.

Raux, J., Copard, Y., Laignel, B., Fournier, M., Masseï, N., 2011. Classification of worldwide drainage basins through the multivariate analysis of variables controlling their hydrosedimentary response. Global and Planetary Change 76 (3-4), 117–127. <https://doi.org/10.1016/j.gloplacha.2010.12.005>.

Reese, S., and Ramsay., D., 2010. RiskScape: Flood fragility methodology. NIWA Technical Report: WLG2010-45, National Institute of Water & Atmospheric Research Ltd.

Rogelis, M.C., Lam, J.C., Ramirez Cortes, F., 2014. Advances in flood risk assessments for data-limited changing environments. In: Proceedings of the 6th International Conference on Flood Management (ICFM6). Sep. 2014, Sao Paulo, Brazil.

Rubiu, F., 2018. Flood risk assessment in the vicinity of Kartena town using HEC-RAS 1-D-2-D models. (Electronic Thesis or Dissertation). Retrieved from <https://vb.vdu.lt/object/elaba:28564107/index.html>.

Ruiz-Bellet, J.L., Balasch, J.C., Tuset, J., Barriendos, M., Mazon, J., Pino, D., 2015. Historical, hydraulic, hydrological and meteorological reconstruction of 1874 Santa Tecla flash floods in Catalonia (NE Iberian Peninsula). Journal of Hydrology 524, 279–295. <https://doi.org/10.1016/j.jhydrol.2015.02.023>.

Röthlisberger, V., Zischg, A.P., Keiler, M., 2017. Identifying spatial clusters of flood exposure to support decision making in risk management. Sci. Total Environ. 598, 593–603. <https://doi.org/10.1016/j.scitotenv.2017.03.216>.

Salih, N.M., Kadhim, M., Mourshed, M., and Bray, M.T., 2015. Shadow detection from very high-resolution satellite image using grab cut segmentation and ratio-band algorithms. The International Archives of the Photogrammetry, Remote Sensing and Spatial Information Sciences, Volume XL-3/W2, 15+HRIGI15 – Joint ISPRS conference 2015, 25–27, Munich, Germany.

Samela, C., Albano, R., Sole, A., and Manfreda, S., 2018. A GIS tool for cost-effective delineation of flood-prone areas. Journal of Computers, Environment and Urban Systems 70, 43–52. <https://doi.org/10.1016/j.compenvurbsys.2018.01.013>.

Schober, B., Hauer, C., Habersack, H., 2015. A novel assessment of the role of Danube floodplains in flood hazard reduction (FEM Method). Natural Hazards 75 (S1), 33–S50. <https://doi.org/10.1007/s11069-013-0880-y>.

Schumann, A.H., 2011. Flood Risk Assessment and Management: How to Specify Hydrological Loads, Their Consequences and Uncertainties. Book. Springer Science & Business Media, 279 pages.

Sewdien, V.N., Preece, R., Rueda Torres, J.L., Rakhshani, E., and van der Meijden, M., 2020. Assessment of critical parameters for artificial neural networks based short-term wind generation forecasting. Renewable Energy, 161, 878-892. <https://doi.org/10.1016/j.renene.2020.07.117>.

Shackelford, A.K., and Davis, C.H., 2003. A Combined Fuzzy Pixel-Based and Object-Based Approach for Classification of High-Resolution Multispectral Data over Urban Areas. IEEE Transactions on Geosciences and Remote Sensing, Vol. 41.

Shan, J. and D. Scott, L., 2002. Generalization of building polygons extracted from IKONOS imagery. Symposium on Geospatial Theory, Processing and Applications, Working Group IV/3, Ottawa.

Shortridge, J., Aven, T., Guikema, S., 2017. Risk assessment under deep uncertainty: a methodological comparison. J. Reliab. Eng. Syst. Saf. 159, 12–23. <https://doi.org/10.1016/j.ress.2016.10.017>.

Shrivastava, N., and Rai, P.K., 2015. An object-based building extraction method and classification using high resolution remote sensing data"Forum geographic Volume XIV, Issue pp. 14-21(8), 1 June 2015.

Shustikova, I., Domeneghetti, A., Neal, J.C., Bates, P., and Castellarin, A., 2019. Comparing 2-D capabilities of HEC-RAS and LISFLOODFP on complex topography, Hydrological Sciences Journal, 64:14, 1769-1782. <http://dx.doi.org/10.1080/02626667.2019.1671982>.

Sighomnou, D., Ilia, A., Tanimoun, B., 2011. Evenements de Crues de juillet à Septembre 2010 Dans Le Niger Moyen. (Note Technique). Autorité du Bassin du Niger (ABN), pp. 1–8.

Sighomnou, D., Descroix, L., Genthon, P., Mahe, G., Bouzou Moussa, I., Gautier, E., Mamadou, I., Vandervaere, J.P., Bachir, T., Coulibaly, B., Rajot, J.L., Malam Issa, O., Dessay, N., Delaître, E., Maiga, O.F., Diedhiou, A., Panthou, G., Vischel, T., Yacouba, H., Karambiri, H., Paturel, J.E., Diello, P., Mougin, E., Kergoat, L., and Hiernaux, P., 2013. La Crue de 2012 à Niamey: Un Paroxysme Du Paradoxe Du Sahel? Science et Changements Planetaires - Secheresse 24 (1), 3–13. <https://doi.org/10.1684/sec.2013.0370>.

Singh, R.K., Villuri, V.G.K., Pasupuleti, S., and Nune, R., 2020. Hydrodynamic modeling for identifying flood vulnerability zones in lower Damodar river of eastern India. Ain Shams Engineering Journal 11(4), 1035-1046. <https://doi.org/10.1016/j.asej.2020.01.011>.

Smith, J.B., 1996. Development of adaptation measures for water resources. International Journal of Water Resources Development, 12 (2), 151–163. <https://doi.org/10.1080/07900629650041920>.

Suman, A., and Akther, F., 2016. River Flood Modelling Using SOBEK: A Case Study from Ciliwung Catchment, Indonesia. International Journal of Engineering Research 3, 662-668.

Şen, O., Kahya, E., 2017. Determination of flood risk: A case study in the rainiest city of Turkey. Environmental Modelling & Software 93, 296-309, <https://doi.org/10.1016/j.envsoft.2017.03.030>.

Tadesse, Y.B., and Fröhle, P., 2020. Modelling of Flood Inundation due to Levee Breaches: Sensitivity of Flood Inundation against Breach Process Parameters. Water 12(12), 3566, <https://doi:10.3390/w12123566>.

Tang, Z., Yi, S., Wang, C., Xiao, Y., 2018. Incorporating probabilistic approach into local multi-criteria decision analysis for flood susceptibility assessment. J. Stoch. Environ. Res. Risk Assess. 32, 701–714. <https://doi.org/10.1007/s00477-017-1431-y>.

Tarhule, A., 2005. Damaging Rainfall and Flooding: The Other Sahel Hazards. Clim. Chang, 72, 355–377.

Thompson, C.M., and Frazier, T.G., 2014. Deterministic and probabilistic flood modeling for contemporary and future coastal and inland precipitation inundation, Applied Geography 50, 1-14.

Tilford K., Sene K., Khatibi R., 2007. Flood Forecasting Model Selection. In: Begum S., Stive M.J.F., Hall J.W. (eds) Flood Risk Management in Europe. Advances in Natural and Technological Hazards Research, vol 25. Springer, Dordrecht. <https://doi.org/10.1007/978-1-4020-4200-3_21>.

Tompkins, E.L., 2005. Planning for Climate Change in Small Islands: Insights from National Hurricane Preparedness in the Cayman Islands. Global Environmental Change 15(2),139-49.

Tseng, Y-H., and Wang, S., 2003. Semi automated building extraction based on CSG model-image fitting. Photogrammetric Engineering & Remote Sensing 69 (2), 171-180.

UNDRR (United Nations Office for Disaster Risk Reduction), Retrieved in July 2021 from <https://www.undrr.org/terminology/structural-and-non-structural-measures>.

UNDRR, 2019. Global Assessment Report on Disaster Risk Reduction, Geneva, Switzerland, United Nations Office for Disaster Risk Reduction (UNDRR).

UNISDR (United Nations International Strategy for Disaster Reduction), 2009. UNISDR Terminology on Disaster Risk Reduction. The United Nations International Strategy for Disaster Reduction (UNISDR), Geneva, Switzerland.

UNISDR (United Nations International Strategy for Disaster Reduction), 2013. Global Assessment Report on Disaster Risk Reduction 2013.

UNISDR (United Nations International Strategy for Disaster Reduction), 2015. Global Assessment Report on Disaster Risk Reduction 2015.

U.S. Environmental Protection Agency (USEPA), 2014. Risk Assessment Forum White Paper: Probabilistic Risk Assessment Methods and Case Studies. EPA/100/R-09/001A. Washington, D.C.: Risk Assessment Forum, Office of the Science Advisor, USEPA.

United Nations. 2017. People and Oceans [Fact sheet]. The Ocean conference, United Nations, New York, 5-9 June 2017. Retrieved from <https://www.un.org/en/conf/ocean/>.

United Nations (UN), 2021. The Sahel: Land of Opportunities. Retrieved from <https://www.un.org/africarenewal/sahel>.

United States Environmental Protection Agency (EPA), 2021. Exposure Assessment Tools by Tiers and Types - Deterministic and Probabilistic Assessments. Retrieved from <https://www.epa.gov/expobox/exposure-assessment-tools-tiers-and-types-deterministic-and-probabilistic-assessments>.

United States Geological Survey (USGS). Retrieved from the website, 2021, <https://www.usgs.gov/>.

United States, US Army Corps of Engineers (USACE), Institute for Water Resources, Hydrologic Engineering Center. <https://www.hec.usace.army.mil/software/hec-ras/>.

Vienna University of Technology. (2020, July 22). Flood data from 500 years: Rivers and climate change in Europe. ScienceDaily. Retrieved September 7, 2021 from <www.sciencedaily.com/releases/2020/07/200722112655.htm>.

Wang, J., Qin, Q., Chen, L., Ye, X., Qin, X., Wang, J., and Chen, C., 2013. Automatic Building Extraction from very high resolution satellite imagery using line segment detector" Institute of Remote Sensing and Geographic Information System Peking University, Beijing,100871, China.

Wilcox, C., Vischel, T., Panthou, G., Bodian, A., Blanchet, J., Descroix, L., Quantin, G., Cassé, C., Tanimoun, B., Kone, S., 2018. Trends in hydrological extremes in the Senegal and Niger Rivers. Journal of Hydrology, 566, 531-545.

WMO (World Meteorological Organization), 2006. Social Aspects and Stakeholder Involvement in Integrated Flood Management. APFM Technical Document No. 4, Flood Management Policy Series, Geneva, Switzerland: World Meteorological Organization. Web. <http://www.apfm.info/pdf/ifm_social_aspects.pdf>.

WMO (World Meteorological Organization), 2021. WMO Atlas of Mortality and Economic Losses from Weather, Climate and Water Extremes (1970–2019), WMO-No. 1267.

World Bank (2014). High resolution Aerial Imagery of the city of Niamey. Unpublished data.

Wu, L., Zhang, Y., Gao, Y., and Zhang, Y., 2004. Tree Crown Detection and Delineation in High Resolution RS Image, in Institute of Remote Sensing and Geographic Information Systems, 0-7803-8742-2/04/$20.00 (c) IEEE, PP 3841-3844.

Yang, J., Townsend, D., and Daneshfar, B., 2006. Applying the HEC-RAS model and GIS techniques in river network floodplain delineation. Canadian Journal of Civil Engineering 33, 19-28. <doi:10.1139/l05-102>.

Yee, R., 2013. Architectural drawing: a visual compendium of types and methods. John Wiley & Sons, New Jersey, USA.

Zeiler., M.D., 2012. ADADELTA: An Adaptive Learning Rate Method. arXiv preprint arXiv:1212.5701.

Zhang, Z., Yang, L., and Zheng, Y., 2020. Chapter 8 - Multimodal medical volumes translation and segmentation with generative adversarial network, Editor(s): S. Kevin Zhou, Daniel Rueckert, Gabor Fichtinger, In The Elsevier and MICCAI Society Book Series, Handbook of Medical Image Computing and Computer Assisted Intervention, Academic Press, 183-204.